VACANCY LIFETIMES IN PLATINUM STUDIED BY MODULATION METHODS

David Paul Crane

Thesis submitted for the Degree of

Doctor of Philosophy

The City University

1980

Department of Physics

Declaration

This thesis was written by me and, except where otherwise indicated, describes my own work carried out under the supervision of Doctor A.H. Seville in the Department of Applied Physics, The City University, London.

Abstract

A study of vacancy lifetimes in platinum using modulation techniques is described. The theory of producing the sinusoidal temperature oscillations by two related methods and the application to vacancy lifetime measurements using an a.c. bridge technique is given.

An account is briefly given of an experiment measuring the third harmonic voltage generated across an a.c. heated wire sample. The sample was a platinum wire of 50μm diameter whose temperature was modulated at ~40Hz over a mean temperature range of 1400K-1800K. A modified form of de Sauty's Bridge was used to obtain these results. Results for the temperature coefficient of resistivity as a function of temperature were calculated. The agreement with accepted results for the temperature coefficient of resistivity was poor due to difficulties and inaccuracies associated with the use of the a.c. bridge when not implemented as a null detector.

A second experiment is described in which the a.c. bridge was used to determine the equivalent impedance of an a.c. heated platinum wire of 50μm diameter over the temperature range of 1400K - 1800K. The frequency of the heating current was in the range of ~40Hz - ~180Hz. The absolute values and temperature dependence of the temperature coefficient of resistivity calculated from the equivalent impedance results are in agreement with accepted

results of other workers at low modulating frequencies ($\sim$ 40Hz). At higher modulating frequencies a reduction in the temperature coefficient of resistivity at temperatures $>$ 1650K was discerned. These results are discussed and compared with theory : they are interpreted as due to a vacancy lifetime of $\sim$1ms at 1800K.

Contents

Index of Figures

Symbols

The following list contains only the most common symbols used.

Suffixes:

d	relating to defects.
L or l	relating to long wire.
m	melting point value.
M	mean value (except when used with entropy and energy).
S	relating to short wire.
v	relating to vacancies.
o	constant, d.c. value or value at $0^{\circ}C$ depending on context.
1	fundamental value.
2	second harmonic.
3	third harmonic.

Main Symbols

a	lattice constant.
b	Burger's Vector.
C	capacitance or concentration depending on context.
c_p	specific heat at constant pressure.
c_v	specific heat at constant volume.
D_v	diffusion coefficient.
E_M	vacancy activation energy.
f	modulating frequency or number of jumps made by a vacancy in its lifetime.
f_D	Debye frequency.
G	Gibbs free energy.
H	enthalpy.
i	heating current.
j	$\sqrt{-1}$
k	Boltzmann's Constant.
k_T	Isothermal compressability.
l	vacancy source/sink separation or $\frac{1}{2}$ dislocation length.

m	mass.
R	resistance.
r_e	resistance ratio, R_M/R_o
S	formation entropy.
S_M	vacancy activation entropy.
T	absolute temperature.
V	voltage, or volume.
W	power lost.
X	ratio of resistive to capacitative impedances.
Y	admittance.
Z	impedance.
α	temperature coefficient of resistivity.
β	$1/R_M \; dR_M/dT$.
γ	$1/W_M \; dW_M/dT$.
τ	thermal time constant.
τ_v	vacancy lifetime.
λ	coefficient of thermal expansion.
ϕ	heating current/temperature phase lag.
θ	temperature excursion amplitude.
w	angular frequency.

1. Introduction

1.1. Introduction

This is the account of a study to determine the vacancy lifetime in platinum at temperatures in the range 1400K-1800K. Studies of this kind are of interest because of the importance of vacancies in diffusion and their effect on the mechanical properties of materials.

The experimental techniques used to study vacancy lifetimes are usually indirect and not performed under equilibrium conditions. For instance , diffusion studies by means of mechanically stressing a sample and measuring creep give indirect measurements of the lifetime of a supersaturation of vacancies with a non-thermal equilibrium array of sources and sinks.

A modulation method was used in the present study. This is an experimental technique in which a sample is subjected to fluctuating temperature excursions about a mean. The resulting temperature excursions are typically in the region of 0-1K-10K. In the present experiment, the central temperature range was 1400K-1800K and the amplitude of the temperature excursions typically 10K, therefore the experiments were performed under quasi-equilibrium conditions. This is a feature of modulation experiments in general.

Various types of modulation experiment have been used to determine a range of physical parameters, for a review see Kraftmakher (1973 a,b), but have not been used before to determine the effect of vacancy lifetimes directly.

The present investigation used a modulation method to determine the temperature coefficient of resistivity as a function of modulation frequency (in the range 40Hz - 200Hz). As shown later, a reduction in the temperature coefficient of resistivity with modulating frequency was observed implying a vacancy lifetime in platinum of $\sim$1 ms at 1800K.

1.2. Vacancies in Metals

Theoretical considerations predict that under conditions of thermal equilibrium there will be a finite concentration of defects. This is because the entropy term in the expression for the free energy offsets the effect of the work done in creating a defect. This can be seen in the expression for the free energy below:

$$G = H - TS \qquad 1.1$$

where G is the Gibbs free energy, H is the enthalpy, T the absolute temperature and S the formation entropy.

The application of Boltzmann statistics to the problem produces the well known expression for the

concentration of defects at thermal equilibrium:

$$C_d = \exp\left[\frac{S}{k}\right] \exp\left[\frac{-H}{kT}\right] \qquad 1.2$$

where C_d is the atomic concentration of defects and k is Boltzmann's Constant.

The simplest types of defect envisaged in a metal lattice at thermal equilibrium are the vacancy and interstitial. Early theoretical calculations showed that the formation energy of a vacancy was nearly an order of magnitude less than that for an interstitial (e.g. Huntingdon and Seitz (1942) and Huntingdon (1942) calculated 1 - 2eV for a vacancy and 5 - 6eV for an interstitial).

Experiments have confirmed that under equilibrium conditions vacancies are the dominant point defect. For reviews on the subject of vacancy concentration experiments see Seeger (1973), Kovacs and El Sayed (1976) and Siegel (1978). Typically, vacancy atomic concentrations are of the order of 10^{-4} - 10^{-3} at the melting point.

The large difference in the formation energies of vacancies and interstials indicates that vacancies are not created in a perfect crystal lattice under equilibrium conditions, but at certain specific sites. It is a general assumption of vacancy kinetic studies that these sites act as sinks as well as sources for vacancies. As such, it is clear that a vacancy diffusing away from a site at which it has just

been created, must reach a similar site before it can be annihilated. This implies a vacancy lifetime, dependent upon the jump rate and the spacing of the vacancy source/sinks.

Since vacancies are not created or annihilated in a perfect crystal lattice, the formations that can act as vacancy source/sinks are the surface of the test sample, grain boundaries in the sample and dislocations in the bulk of the lattice.

The lifetimes of vacancies should therefore range from about 500ms for surface source/sinks (and dependent, obviously, on the dimensions of the sample, typically ~50μm) to about 1ms for dislocation source/sinks.

1.3. Experimental Studies of Vacancy Lifetimes

The experimental study of vacancy lifetimes has generally taken the form of diffusion or annealing experiments. However, both these methods have their problems : not the least of which is the fact that they are performed under non-equilibrium conditions. For example, different sources and sinks may operate under these conditions making it difficult to apply the results directly in the calculation of vacancy lifetimes, which are defined under near-equilibrium conditions.

The application of a modulation method to the determination of vacancy lifetimes allows their direct measurement under conditions closely approaching equilibrium.

1.3.1. Diffusion Experiments

There are two types of diffusion experiment that are generally performed : those using labeled atoms (self diffusion and chemical diffusion) and those in which a binary system is investigated (the Kirkendall effect).

The diffusion coefficient is given by the following equation

$$D_v = \frac{f_D a^2}{6} \exp\left[\frac{S_M}{k}\right] \exp\left[\frac{-E_M}{kT}\right] \qquad 1.3$$

where f_D is the Debye frequency,
a the lattice constant,
S_M the activation entropy of a vacancy,
E_M the activation energy of a vacancy,
k Boltzmann's constant
and T the absolute temperature.

The vacancy lifetime can be expressed as

$$v = \frac{3l^2}{2f_D a^2} \exp\left[\frac{-S_M}{k}\right] \exp\left[\frac{E_M}{kT}\right] \qquad 1.4$$

where l is the distance between vacancy source/sinks and the lattice is f.c.c.

Obviously, the vacancy lifetime can be expressed in terms of the diffusion coefficient as shown below

$$v = \frac{l^2}{4D_v} \qquad 1.5$$

The structure (dislocation, grain boundary, etc.) specified as vacancy source/sinks will determine the vacancy lifetime deduced in this way.

Diffusion acts in response to a gradient of some kind - the most common type being, obviously, a concentration gradient - and as such is a non-equilibrium process. In addition, dissimilar elements may be diffused, (Kirkendall Effect). In this case there is a mismatch of size and valency of the atoms moving which will also introduce changes of properties.

1.3.2. Annealing Experiments.

Annealing experiments involve the production of a supersaturation of vacancies and its removal by annealing. The various types of annealing experiments differ in the methods of production of the vacancy supersaturation and in the methods of observing the annealing.

Supersaturation of vacancies is obtained by, most commonly, cooling a sample from a temperature at which there is a relative abundance of vacancies to one at which their equilibrium concentration is small (quenching). If a high fraction of vacancies is to be retained the cooling must be at a rate such that the vacancies do not have time to migrate to sinks, (alternatively the rate of quenching can be varied to investigate the above mentioned migration). Annealing of the sample then gives information about the vacancy lifetime.

Another common method of producing vacancies is by plastic deformation, again annealing characteristics can be investigated.

The annealing of experimental samples is typically studied as follows : the physical parameter to be measured (usually resistivity) is determined for the sample at a low temperature. The sample is heated and quenched and the resistance measured as a function of time. The rate of return to the preheating value of the parameter allows calculation of the lifetime of vacancies before destruction at sinks.

There are a number of errors and experimental difficulties that beset this type of study. One is that in the case of quenching vacancies may aggregate to form polyvacancies and other defects. Thus the apparent lifetime may not be characteristic of the material. In the case of plastic deformation, there is the difficulty of a range of defects being formed, not just vacancies, and this will affect the mobility of and sink distribution for vacancies.

1.3.3. Modulation Experiments.

As mentioned above, the temperature excursion used in modulation experiments is 10K. This means that at 1800K the change in vacancy concentration over 10K is fairly small : $\frac{Cv10K}{Cv1800K} \sim 10\%$. Therefore since vacancies are not appreciable at temperatures below $\frac{2}{3}Tm$, the experiments are performed under essentially equilibrium conditions.

In addition, by determining some vacancy dependent parameter (in the present case the temperature coefficient of resistivity) as a function of modulation frequency, a direct measurement of vacancy lifetimes may be obtained.

Related to the advantage of equilibrium conditions is the fact that it is easy to reproduce the experimental conditions to confirm results. Alternatively comparative experiments can be performed on, for example, a pure element and alloys of that element, the confidence in reproducibility would facilitate comparison of vacancy lifetimes in the various samples. This aspect is expanded later in section 1.5.

A modulation method has already been used to investigate the physical properties of a sample near a phase transition temperature; examples are, the Seebeck coefficient at the Curie point of Fe-Au, Kraftmakher and Pinegina (1970), and Co-Pt + 10% Rh, Kraftmakher and Pinegina (1971). also the specific heat at the Curie point of iron, Kraftmakher and Romashina (1965), and of cobalt, Kraftmakher and Romashina (1966). The resistivity at the Curie point of iron has also been investigated by a modulation method, Kraftmakher and Pinegina (1974). Modulation methods are well suited to this owing to the small amplitude of the temperature oscillations. An experiment such as one performed in this study could be used to investigate vacancy lifetimes in different phases of the same element or alloy.

1.4. Modulation Methods.

As mentioned in section 1.1 a modulation method is one in which the temperature of a sample is made to fluctuate about some set value. Temperature oscillations may be measured by a method that depends on the physical parameter under study. Possible parameters include the coefficients of resistivity, thermal expansion and specific heat, the Seebeck Coefficient and the specific heat. For a review of modulation methods see Kraftmakher (1973a, 1973b).

1.4.1. Types of Modulation Method.

Modulation methods can be categorised according to the means used to heat the sample or the means used to find its temperature.

Heating methods include Joule heating, electron bombardment and radiation bombardment : of these, Joule heating is by far the most common. Electron and radiation bombardment have been used only in studies of the Seebeck Coefficient.

The method of heating, of course, has a bearing on the means of temperature measurement. In the case of Joule heating the temperature dependence of the temperature coefficient of resistivity can be used, via resistance measurements, to determine the mean temperature of the sample and its oscillations. This is done wherever possible, but if the temperature coefficient of resistivity is not known, and this is

particularly true at high temperatures, then often emissivity measurements are performed by focussing radiation emitted from the sample onto a photo-multiplier tube. Obviously the emissivity as a function of temperature must be known. Another alternative, little used now, is the measurement of the thermionic emission from the sample : again detailed information of the temperature dependence is required.

If none of the above techniques is available the only alternative is to use a thermocouple. Although in general a most reliable device, it has its own difficulties. The main one is the disturbance of the experimental system by conduction of heat away from the sample. This necessitates a reduction in the modulating frequency to not more than 30Hz. This disadvantage is often acceptable because of the inherent reliability of the method.

1.4.2. Modulation Studies of Vacancies.

The study of vacancies by modulation methods requires measurement of some vacancy sensitive physical property from the temperature dependence of which the vacancy concentration is to be inferred. This has been done by extrapolation data from low and medium temperature ranges to high ($> \frac{2}{3}Tm$) temperature ranges. The differences between experimental and extrapolated results have then been attributed to the effect of vacancies.

This procedure has been used to determine vacancy concentrations and the formation energy of vacancies. The elements that have been studied in this way are listed below :

Gold	Kraftmakher and Strelkov (1966a).
Copper	Kraftmakher (1967a).
Titanium	Sestopal (1965).
Zirconium	Kanel and Kraftmakher (1966).
Niobium	Kraftmakher (1963a).
Molybdenum	Kraftmakher (1964).
Tantalum	Kraftmakher (1963b).
Tungsten	Kraftmakher and Strelkov (1962).
Platinum	Kraftmakher and Lanina (1965).

All the above experiments use direct measurements of the specific heat of the element in question; however, deduction of the concentration and formation energy of vacancies depends on an unjustified extrapolation procedure.

A thermal expansion experiment was performed on platinum by Kraftmakher (1967b) again using the extrapolation method to determine the concentration and formation energy of vacancies.

Finally, a modulation experiment was carried out, again on platinum, by Seville (1974) over a frequency range of 100Hz to 1kHz. This set out to assess any frequency dependence of the high temperature specific heat : there was no measurable frequency dependence over the range stated and the results were in good agreement with Kraftmakher and

Lanina (1965). This has important consequences that will be discussed in section 1.4.3.

All the experiments mentioned above were performed in order to determine the vacancy concentrations : none were used to determine vacancy lifetimes. The present study uses the frequency dependence of the temperature coefficient of resistivity as a means of determining the lifetime of vacancies in platinum.

1.4.3. Interpretation of previous Modulation Studies.

Previous modulation experiments applied to the study of vacancies have been orientated towards the determination of vacancy concentrations and formation energies. As mentioned in section 1.4.2., they involve an extrapolation procedure which provides an estimate of the vacancy concentration and formation energy. This procedure involves extrapolating a property (typically the specific heat) from low temperatures ($< \frac{2}{3}T_m$) linearly to high temperatures. The difference between the extrapolation and the observed result being attributed to the contribution of vacancies.

This technique has been criticised because it does not take into account any anharmonic contributions from the lattice with the result that in some cases, e.g. platinum, the vacancy concentrations appear to be too large.

For instance, comparing X-ray parameter experiments and modulation experiments, the results for gold are 0.07% and 0.4%, and for copper are 0.02% and 0.5%, respectively.

In addition, the comparison of the results of Kraftmakher and Linina (1965) with those of Seville (1974), as mentioned in section 1.4.2., imply that either there was no measurable contribution to the specific heat of platinum at high temperatures or that the lifetime of vacancies was unrealistically short ($\sim 40\mu s$). The former possibility leads to an estimated vacancy concentration of not more than 0.1%.

On a theoretical basis, the linear extrapolation does not take into account anharmonic lattice vibrations or possible unusual electronic structure (as in the case of the Transition Elements).

Justification for the extrapolation has been sought in the results of studies of this type. In particular, the enhancement obtained in this way is an exponential function of $^1/T$ as would be expected according to equation 1.2. However, while a temperature dependence of this kind is common it is not in itself a justification. This is not to say that this method is in all cases incorrect, but it cannot be considered a general technique as proposed by (Kraftmakher and Strelkov (1966b)).

1.5. Choice of Modulation Method and Experimental Material.

On the basis of a vacancy concentration of 0.1% in platinum at high temperatures, Seville (1975) has estimated the percentage contribution of vacancies to the specific heat, coefficient of thermal expansion and the temperature coefficient of resistivity as 1%, 6% and 23% respectively. For this reason, it was decided to measure the frequency dependence of the temperature coefficient of resistivity. The modulation method chosen for this experiment was to heat the sample, in wire form, by Joule heating and to estimate the temperature oscillations by means of resistance measurements. There are three ways of doing this : supplementary current, third harmonic voltage and equivalent impedance methods. These are discussed, along with the choice of material, in this section.

1.5.1. Supplementary Current.

In its basic form, this method depends upon the presence of a d.c. voltage across an a.c. heated sample when a supplementary a.c. current at twice the frequency of the heating current is applied. The d.c. voltage varies as the inverse of the heating current frequency.

A modified form of this method was used by Kraftmakher and Tonaevskii (1972). For this a supplementary current of frequency close to that of the temperature oscillations was used. The result was

a low frequency a.c. voltage (rather than a d.c.) whose amplitude depended only on the amplitude of the resistance oscillations. The advantage of this modification is that a high degree of noise immunity is possible.

1.5.2. Third Harmonic Voltage.

Heating a sample by means of an a.c. current will give rise to resistance oscillations of frequency twice that of the heating current. Interaction of the heating current with the resistance oscillations therefore gives rise to a voltage across the sample whose frequency is three times that of the heating current : the third harmonic voltage.

An expression for the third harmonic voltage in terms of the temperature coefficient of resistivity is possible and this method was considered in some detail. It is discussed in Chapter 2.

1.5.3. Equivalent Impedance.

This method exploits the phase lag of the resistance behind the temperature oscillations. The lag, though small, can be resolved into components in phase and in quadrature with the temperature oscillations. It is a simple matter to consider this as a reactive, RC circuit. This suggests a technique which is ideal for use in an a.c. bridge for the capacitative component, though typically 0.1% of the resistive, can be measured using a phase sensitive detector.

Because, in principle, this method is simple and well known techniques could be applied to it (i.e. a.c. bridge measurement) it was chosen as the modulation method to be used. It is considered in more detail in Chapter 2.

1.5.4. Choice of Material.

The material chosen was platinum for the following reasons :

1. It is one of the group of F.C.C. metals whose vacancy properties in general are fairly well known. In addition it is known not to have any phase transitions.

2. It is an industrial standard and samples of high purity can be obtained.

3. It is available in a convenient form : wire samples of 50μm diameter.

4. The specific heat is known up to 1850K (this is necessary to determine the mean temperature and the temperature coefficient of resistivity).

5. It was considered at the start of the study to have a measurable vacancy contribution to the temperature coefficient of resistivity.

6. Other modulation experiments have been performed on platinum (see section 1.4) and this enables comparisons to be made of results (temperature coefficient of resistivity and vacancy lifetime) and the procedure for analysis of results.

7. Platinum is of use in high temperature engineering structures, e.g. chemical reactors, because of its chemical inertness. The solution to the problem of creep induced by stress at high temperatures in these applications is to alloy the platinum with rhodium. It would be of interest to perform studies to compare vacancy kinetics in pure platinum and rhodium-platinum alloys of varying proportions, therefore the present study using pure platinum left scope for further work.

The disadvantage of using platinum is that it has an unusual electronic structure which gives rise to an unusual temperature coefficient of resistivity. This will be discussed in section 1.6. where it is shown that the resistivity of vacancies in platinum is similar to that of other common metals.

1.6. The Electronic Structure of Platinum

Platinum is a member of the Transition Elements : a group that as a whole are well known for their variability of valency. Broadly, this is due to an overlap of the s and d electron bands.

The band structure and Fermi surface of platinum have been known for a number of years, studies generally taking the form of a combination of theoretical calculation and experiment. For instance, recently Nemmonov (1976) compared theoretical calculations with X-ray analysis of the 3d, 4d and 5d Transition

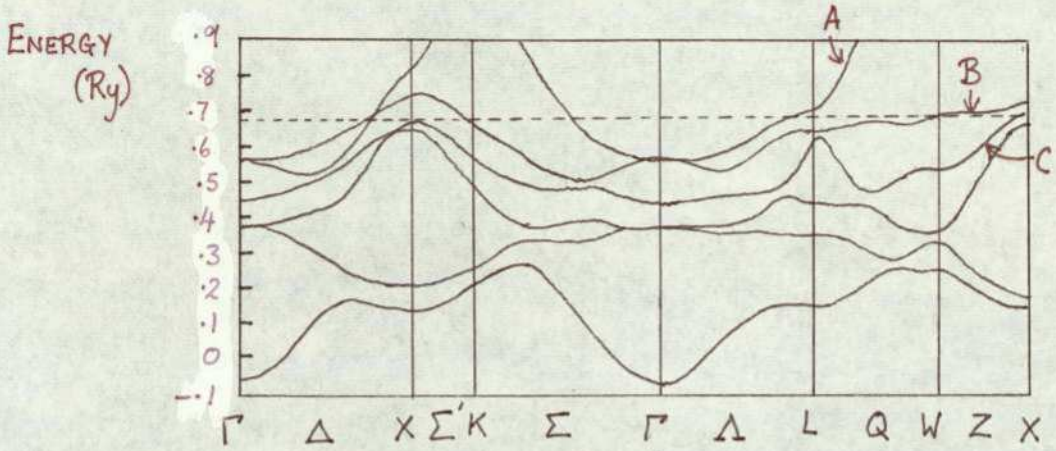

Fig.1.1. Calculated band structure of platinum

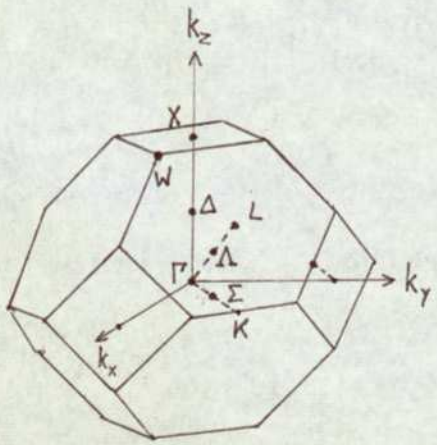

Fig.1.2. Brillouin Zone for an F.C.C. lattice showing the points of symmetry.

Elements, whilst Dye, Ketterson and Crabtree (1978) combined a theoretical analysis with a de Haas-van Alphen experiment to examine the Fermi surface of platinum.

An idea of the Fermi surface of platinum can be obtained by observing the relationship of the band structure, as calculated by Mackintosh (1966), with the Fermi energy. This is shown in Fig.1.1. and it can be seen that the Fermi level cuts three bands and this gives rise to a complicated Fermi surface made up of three components. (Fig. 1.2. shows the Brillouin Zone and symmetry points for an F.C.C. lattice).

The first surface is produced by cutting the band in Fig. 1.1. marked "A" and is shown in Fig. 1.3.; it is a closed electron surface.

Fig. 1.4. shows the second surface formed by cutting band "B" : the surface shown is that of holes and for clarity only the symmetry points, not the Brillouin Zone, are shown.

Similarly Fig. 1.5. shows the effect of cutting band "C" by the Fermi level and is again a hole surface.

An increase in temperature will lead to the occupancy of states whose energy is kT according to a Boltzman distribution. In the present case, at ~1500K, kT is ~1% of the Fermi energy.

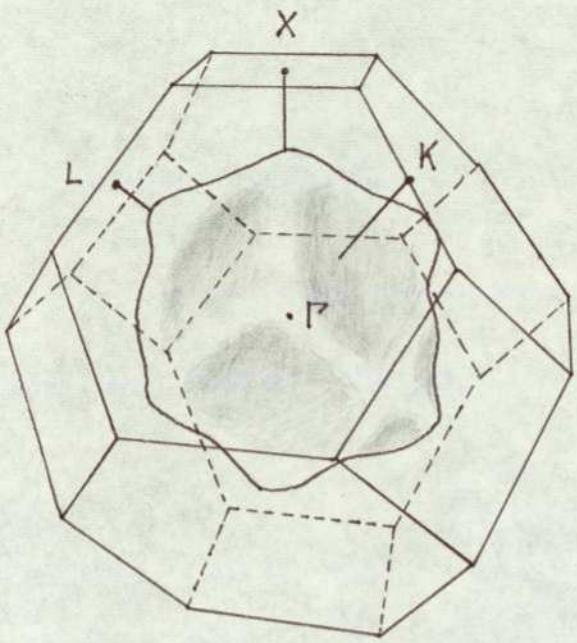

Fig.1.3. Closed electron surface of platinum

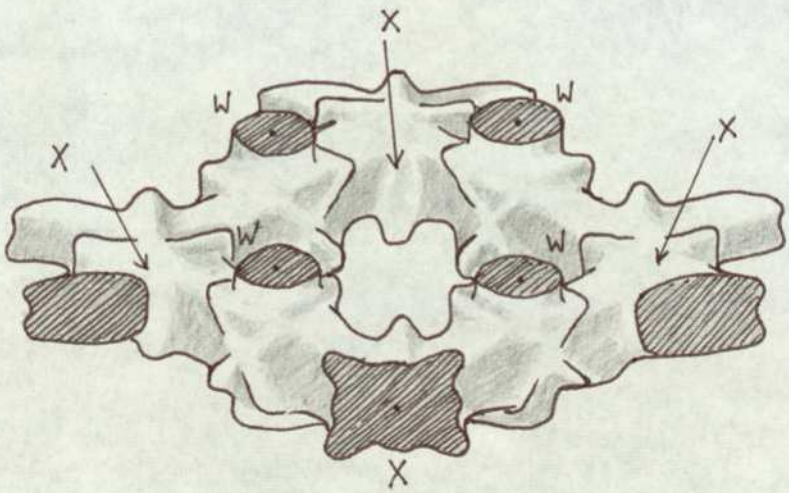

Fig.1.4. Open hole surface of platinum

Since the states occupied at temperatures above OK are due to thermal electrons their occupancy is essentially random and fluctuating. It could be said, therefore, that the Fermi level has been smeared out and has resulted in an expanding of the Fermi surface towards the Brillouin Zone edge. In the case of platinum at ~1500K, this will severely reduce or remove completely the pockets of holes shown in Fig. 1.5. and similarly reduce the hole volume shown in Fig. 1.4. There will be an increase in the area of the electron surface. As mentioned above, these surfaces are due to d band electrons; as such they are localised and do not directly contribute to conduction. However, they do provide states to which electrons can be scattered, thereby contributing to the resistivity of the element. The change in Fermi surface with temperature indicated above will therefore markedly affect the temperature dependence of the resistivity.

Referring to Fig. 1.1. again, it is clear that there is some overlapping of the s and d bands and a band structure way of looking at the electrical structure can lead to a useful, simple model for understanding the electrical properties of platinum.

Fig. 1.6. shows the density of states as a function of energy and the position of the Fermi level. In common with other Transition Elements, the density of states is to a large extent due to d band, localised, states (i.e. there are far fewer conduction, s band,

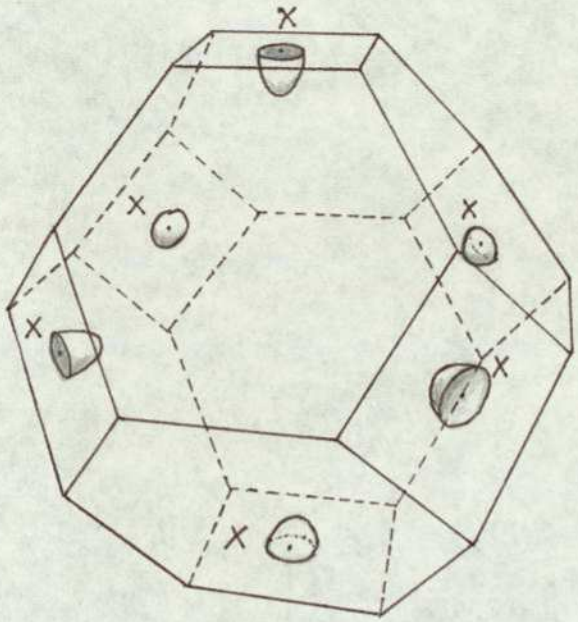

Fig.1.5. Closed hole pockets of platinum

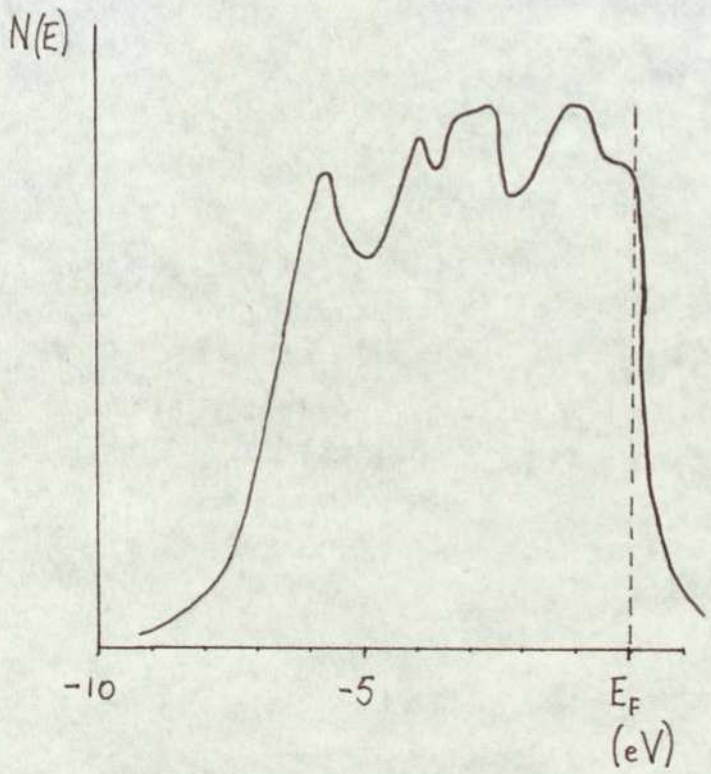

Fig.1.6. Density of states as a function of energy for platinum showing the Fermi energy.

states than localised d band, states : see Fig. 1.7.). The result of this inequality is a high probability of conduction electrons being scattered into states which do not contribute to conduction. But, more importantly from a temperature dependence point of view, the Fermi Energy coincides with the energy at which a sharp decrease in the density of states begins and it will move to higher energies with increasing temperature, (i.e. by ~1% at ~1500K) to a region of lower state density. Since these states are predominantly localised d band there will be fewer states to which conduction electrons can be scattered, leading to a decrease in resistivity as compared with that of a normal metal. This accounts for the decrease observed in the temperature coefficient of resistivity of platinum with increasing temperature in the temperature range below about $\frac{2}{3}T_m$.

A theoretical study of energy bands in 4d Transition Elements has been performed by Pettifor (1978) in which it was shown that the removal of an atom to create a vacancy will result in s electrons spilling into the space. The study proposes that this is due to the intrinsic property in Transition Elements of d band electrons to be cohesive and s band electrons to be repulsive. This means that the resistivity of vacancies in the Transition Elements is due to inter s band transitions : the complications presented by the immobile d band are no longer applicable. Therefore, the resistivity of vacancies in platinum should be similar to that in any common metal.

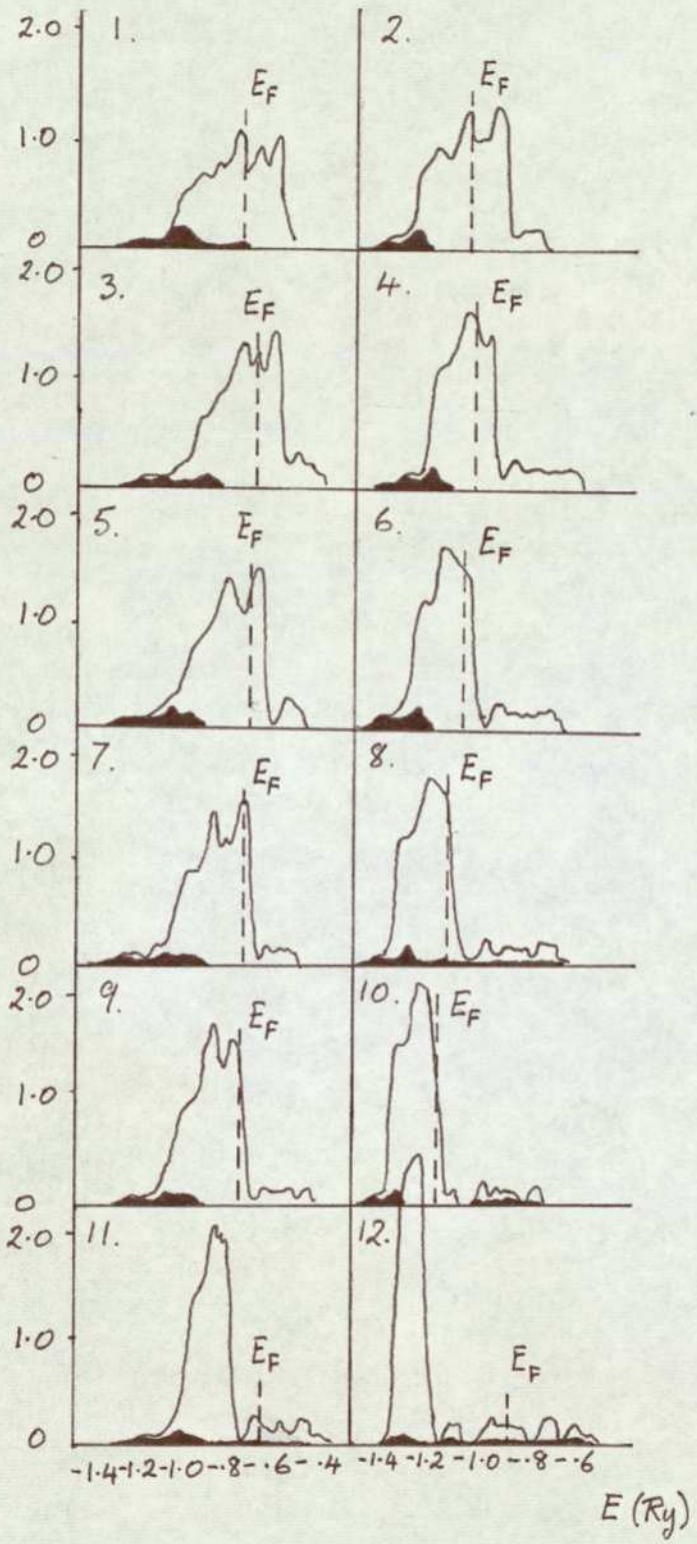

Fig.1.7. Density of states as a function of energy for a series of Transition Elements showing the Fermi energies

Key to Fig.1.7.

1.	Chromium	$3d^5 4s^1$
2.	Chromium	$3d^4 4s^2$
3.	Manganese	$3d^6 4s$
4.	Manganese	$3d^5 4s^2$
5.	Iron	$3d^7 4s^1$
6.	Iron	$3d^6 4s^2$
7.	Cobalt	$3d^8 4s^1$
8.	Cobalt	$3d^7 4s^2$
9.	Nickel	$3d^9 4s^1$
10.	Nickel	$3d^8 4s^2$
11.	Copper	$3d^{10} 4s$
12.	Copper	$3d^9 4s^2$

The density of states curves comprise of two parts : the outline areas are the d-like portions, the four smaller, filled in areas are the s-like portions.

1.7. Summary

This chapter has briefly reviewed the accepted understanding of vacancies in metals and presented the idea that vacancies will have a lifetime depending upon the nature of the sources and sinks operating.

This was followed by a section on the various experimental techniques of studying vacancies. The parameter usually estimated is the concentration of vacancies in the sample. It was pointed out that the present modulation method is unusual in that it gives estimates of the vacancy lifetime at high temperatures.

A short account was given of the various types of modulation method and of their application to the study of vacancy properties. Previous vacancy studies using modulation methods were examined.

The choice of modulation method depends on the physical property to be measured; calculations have shown that the vacancy contribution to the temperature coefficient of resistivity would be 23%. Methods suitable for measurement of this property were the supplementary current, third harmonic voltage and equivalent impedance methods, the latter being chosen because well known techniques could be applied to it.

The choice of platinum as the experimental material was justified on the basis mainly of purity and availability in a convenient form.

Finally, the electronic structure of platinum in particular and certain aspects of the Transition Elements in general were discussed in order to explain the unusual shape of the temperature coefficient of resistivity at high temperatures. The assumption of normal resistivity for vacancies in platinum was briefly discussed.

2. THEORY

2.1. Introduction

A number of workers have analysed the temperature variation of wires heated with a.c. only and wires heated with a.c. superimposed on d.c.

In this chapter, sections 2.2. and 2.3. are concerned with the analysis of a.c. only and a.c. + d.c. heated wires respectively; the analyses result in expressions for the impedances of these wires and the model them as a resistance/ capacitance equivalent parallel circuits. Expressions for the third harmonic voltages that are generated are briefly considered.

In section 2.4. the theory of measuring the impedances and third harmonic voltages resulting from these heated wires using an a.c. bridge is considered.

Finally, the frequency dependence of the temperature coefficient of resistivity due to the relaxation of vacancies is considered.

2.2. a.c. Heating Only

The most detailed analysis of an a.c. only heated wire is by Holland and Smith (1966) who developed equations for the magnitude and phase of temperature harmonics. Smith and Holland (1966) obtained an expression for the third harmonic voltage generated across an a.c. heated germanium whisker. Similarly

Van den Sype (1965) developed an expression for the third harmonic voltage generated across an a.c. heated wire. Kraftmakher and Tonaevskii's (1972) analysis used a non-linear power balance equation to obtain an expression for the temperature coefficient of specific heat. Both Holland (1963) and Kraftmakher (1973a) developed identical expressions giving the specific heat from measurement of the third harmonic voltage generated; the derivation of Holland (1963) being the more detailed. Rosenthal (1961, 1965) obtained an expression that gave the heat capacity, heat loss factor or thermal time constant from the measurement of the third harmonic voltage.

2.2.1. Heated Wire Analysis.

The power balance equation is

$$mc_p \frac{dT}{dt} + W = i_1^2 R \qquad 2.1.$$

where the a.c. heating current, i_1, is given by $i \cos \omega t$,

mc_p is the thermal capacity of the wire,

$T = T_M + \theta$, T_M being the constant, absolute temperature and θ the temperature fluctuation.

W is the power lost and in a linear approximation $W = W_M(1 + \gamma\theta)$,

and R is the resistance of the wire, again in a linear approximation $R = R_M(1+\beta\theta)$.

R_M and W_M are the values at the constant temperature, T_M, and the linear approximation being valid only if $\theta \ll T_M$ (say $\sim 1\%$).

So the linear approximation of the power balance equation is

$$mc_p \frac{d\theta}{dt} + W_M (1+\gamma\theta) = \frac{i^2 R_M}{2} (1+\cos 2wt)(1+\beta\theta) \qquad 2.2.$$

The temperature excursions will obviously vary at twice the frequency of those of the current, the phase relationship at present being unknown. Let $\theta = \theta_2 e^{j(2wt-\phi)}$, then equation 2.2. becomes

$$j2wmc_p\theta_2 e^{j(2wt-\phi)} + W_M(1+\gamma\theta_2 e^{j(2wt-\phi)}) =$$

$$\frac{i^2 R_M}{2} (1+e^{j2wt})(1+\beta\theta_2 e^{j(2wt-\phi)}) \qquad 2.3.$$

Taking constant terms

$$W_M = \frac{i^2 R_M}{2} \qquad 2.4.$$

i.e. at steady state, the power output equals the power input.

Taking second harmonic terms

$$j2wmc_p\theta_2 e^{-j\phi} + W_M\gamma\theta_2 e^{-j\phi} = \frac{i^2 R_M}{2} (1+\beta\theta_2 e^{-j\phi}) \qquad 2.5.$$

N.B. there is an unbalanced 4w term in 2.3. because only temperature fluctuations at 2w were considered.

An expression for $\theta_2 e^{-j\phi}$ can be derived from 2.5. giving as follows

$$\theta_2 e^{-j\phi} = \frac{i^2 R_M}{j4wmc_p + 2W_M\gamma - i^2 R_M\beta} \qquad 2.6.$$

Where the phase lag is represented by $e^{-j\phi}$

$$\text{Let} \quad \hat{\theta} = \frac{i^2 R_M}{2W_M\gamma - i^2 R_M \beta} \qquad 2.7.$$

$$\text{and} \quad \tau = \frac{2mc_p}{2W_M\gamma - i^2 R_M \beta} \qquad 2.8.$$

Where τ is the thermal time constant and $\hat{\theta}$ is the value of θ_2 in the limit $\tau \to 0$

Equation 2.6. now becomes

$$\theta_2 \, e^{-j\phi} = \frac{\hat{\theta}}{j2w\tau + 1} \qquad 2.9.$$

Using the Binomial Expansion

$$\theta_2 \, e^{-j\phi} = \frac{\hat{\theta}}{j2w\tau} \left(1 - \frac{1}{j2w\tau} + \ldots\right) \qquad 2.10.$$

Typically $\tau \sim 0.1$ s and $w \sim 240$ rads$^{-1} \to$ 1,200 rads^{-1} so the value of $2w\tau$ ranges from 48 $\to$ 240. So equation 2.10. simplifies down to

$$\theta_2 e^{-j\phi} \approx \frac{\hat{\theta}}{j2w\tau} \qquad 2.11.$$

The accuracy of equation 2.11. is determined by the value of w and therefore $\phi = -90^\circ$ to an accuracy of 2% at w = 240 rad s^{-1} and 0.4% at w = 1200 rad s^{-1}.

Typically, $i^2R \sim 6$W, $m \sim 5 \times 10^{-6}$kg, $C_p \sim$ 165 J kg^{-1} K^{-1}, $w > 240$ rad s^{-1}. So $\theta_2 \sim 8$K at w = 240 rad s^{-1} and the working temperatures are

> 1400K thus the linear approximation of the power balance equation is justified.

2.2.2. Equivalent Impedance Derivation.

Using equation 2.11. the resistance fluctuations about a mean value, R_M, can be seen to be

$$R = R_M (1-\beta\theta_2 \sin 2wt). \qquad 2.12.$$

As stated above, the heating current is i cos wt, so the voltage generated across the wire is given by

$$V = iR_M(\cos wt - \frac{\beta\theta_2}{2} (\sin wt+\sin 3wt)) \qquad 2.13.$$

Equation 2.13. shows two terms at the fundamental frequency; one in phase, the other 90^o out of phase, and one term at the third harmonic of the quadrature voltage.

If this last term could be filtered out, the result could be used in an equivalent impedance method. Consider Fig. 2.1.

Let the same current be flowing between A and B as was heating the wire, then the voltage generated across A and B will be

$$V_{RC} = \frac{i \cos wt}{Y} \qquad 2.14.$$

where $$Y = \frac{1}{R_M} + jwC \qquad 2.15.$$

and is the admittance of the circuit. Substituting equation 2.15. in equation 2.14

$$V_{RC} = \frac{iR_M \cos wt}{1 + jwCR_M} \qquad 2.16.$$

At low frequencies used ($\sim$40Hz) the product wCR is a maximum. Typical values under these conditions are $w \sim 240$ rad s^{-1}, $C \sim 200nF$ and $R \sim 20\Omega$ therefore $wCR \sim 4 \times 10^{-3}$. So in general $wCR \ll 1$, the Binomial Expansion may be used giving as the voltage

$$V_{RC} = iR_M(\cos wt - wCR_M \sin wt) \qquad 2.17.$$

Comparing equations 2.13. and 2.17. gives

$$wCR_M = \frac{\beta\theta_2}{2} \qquad 2.18.$$

Substituting for θ_2 from equations 2.7., 2.8. and 2.11. leads to

$$wCR_M = \frac{\beta i^2 R_M}{8wmc_p} \qquad 2.19.$$

(taking the modulus of θ_2).

To get an expression for the temperature coefficient of resistivity, that for β from equation 2.19. must be multiplied by the resistance ratio $r_e = R_M/R_o$

$$\alpha = \frac{8w^2 mc_p r_e C}{i^2} \qquad 2.20.$$

So by using a suitable a.c. bridge all the quantities except c_p can be measured; c_p having been tabulated previously for high temperatures using a modulation technique by Seville (1974).

This work showed that the contribution to the specific heat of vacancies was $\lesssim 1\%$. This is important because, as was pointed out by Van den Sype (1965), error can occur due to relaxation effects of vacancies. Seville (1975) has calculated the relaxation effect on the temperature coefficient of resistivity and shown that the decrease at temperatures of ~ 1800K can be $\sim 23\%$ at a frequency depending on the source/sinks operating and their efficiency. The frequency variation of the temperature coefficient of resistivity, therefore, will give information of the sources/sinks and their efficiency.

Alternatively the third harmonic voltage in equation 2.13. can be measured directly and so give a value for α

$$\alpha = \frac{8wmc_p r_e V_3}{i^3 R_M^2} \qquad 2.21.$$

where V_3 is the measured third harmonic voltage. This is the same expression as obtained by Holland (1963).

2.3. a.c. + d.c. Heating.

Kraftmakher (1962) analysed a.c. + d.c. heated wires and after making simplifying assumptions, obtained expressions for the specific heat by modelling the impedance of the wire by an inductive or capacitative circuit. Seville (1972) analysed a.c. + d.c. heated wires to a greater accuracy.

The following analysis improves on that of Seville (1972) by the inclusion of a non-negligible second term in the expression for the second harmonic temperature oscillations which is consequently more accurate.

2.3.1. Heated Wire Analysis

In this case, if the heating current is $(i_o + i_1 \cos \omega t)$, the power balance equation becomes

$$mc_p \frac{d\theta}{dt} + W_M (1+\gamma\theta) =$$

$$R_M ((i_o^2+\tfrac{1}{2}i_1^2)+2i_1 i_o \cos \omega t + \tfrac{1}{2}i_1^2 \cos 2\omega t)(1+\beta\theta) \qquad 2.22.$$

It is apparent that now the temperature excursion, θ, is made up of $\theta_1 \cos(\omega t-\phi_1)+\theta_2\cos(2\omega t-\phi_2)$.

Adopting exponential notation again, 2.22. becomes

$$j\omega mc_p (\theta_1 e^{j(\omega t-\phi_1)} + 2\theta_2 e^{j(2\omega t-\phi_2)}) + W_M(1+\gamma(\theta_1 e^{j(\omega t-\phi_1)} + \theta_2 e^{j(2\omega t-\phi_2)}) =$$

$$R_M ((i_o^2+\tfrac{1}{2}i_1^2)+2i_1 i_o e^{j\omega t} + \tfrac{1}{2}i_1^2 e^{j2\omega t})(1+\beta(\theta_1 e^{j(\omega t-\phi_1)} + \theta_2 e^{j(2\omega t-\phi_2)})) \qquad 2.23.$$

Taking constant terms

$$W_M = R_M(i_o^2 + \tfrac{1}{2}i_1^2) \qquad 2.24.$$

First harmonic terms

$$jwmc_p\theta_1 e^{-j\phi_1} + \gamma W_M \theta_1 e^{-j\phi_1} = R_M((i_o^2+\tfrac{1}{2}i_1^2)\beta\theta_1 e^{-j\phi_1} + 2i_1 i_o) \qquad 2.25.$$

Second harmonic terms

$$j2wmc_p\theta_2 e^{-j\phi_2} + \gamma W_M \theta_2 e^{-j\phi_2} = R_M((i_o^2+\tfrac{1}{2}i_1^2)\beta\theta_2 e^{-j\phi_2} + 2i_1 i_o \theta_1 e^{-j\phi_1} + \tfrac{1}{2}i_1^2) \qquad 2.26.$$

Manipulating 2.25. for an expression for θ_1 gives

$$\theta_1 e^{-j\phi_1} = \frac{2i_1 i_o R_M}{jwmc_p + \gamma W_M - R_M\beta(i_o^2+\tfrac{1}{2}i_1^2)} \qquad 2.27.$$

As in subsection 2.2.1. let

$$\hat{\theta}_1 = \frac{2i_1 i_o R_M}{\gamma W_M - R_M\beta(i_o^2+\tfrac{1}{2}i_1^2)} \qquad 2.28.$$

and

$$\tau = \frac{mc_p}{\gamma W_M - R_M\beta(i_o^2+\tfrac{1}{2}i_1^2)} \qquad 2.29.$$

Then using 2.28. and 2.29., 2.27 becomes

$$\theta_1 e^{-j\phi_1} = \frac{\hat{\theta}_1}{jw\tau+1} \qquad 2.30.$$

From the discussion in subsection 2.2.1.

$$\theta_1 e^{-j\phi} \approx \frac{\hat{\theta}_1}{jw\tau} = \frac{2i_1 i_o R_M}{jwmc_p} \qquad 2.31.$$

However, at w = 240 rad s^{-1} the approximation of 2.31. is accurate only to 4%; this is worse than the approximation of 2.11. because the temperature fluctuations are at the fundamental frequency.

Again, rearranging 2.26 gives

$$\theta_2 e^{-j\phi_2} = \frac{\frac{1}{2}i_1^2 R_M + 2i_1 i_o \theta_1 R_M \beta}{j2wmc_p + \gamma W_M - R_M \beta (i_o^2 + \frac{1}{2}i_1^2)} \qquad 2.32.$$

Up to this point the analysis has been from Seville (1972), but he has failed to include the second term in equation 2.32.

Let

$$\hat{\theta}_2 = \frac{\frac{1}{2}i^2 R_M}{\gamma W_M - R_M \beta (i_o^2 + \frac{1}{2}i_1^2)} \qquad 2.33.$$

Then, using equations 2.28., 2.29 and 2.33, equation 2.32. becomes

$$\theta_2 e^{-j\phi_2} = \frac{\hat{\theta}_2 + \beta \theta_1 \hat{\theta}_1}{j2w\tau + 1} \qquad 2.34.$$

From above and to the same accuracy as equation 2.11.

$$\theta_2 e^{-j\phi} \approx \frac{\hat{\theta}_2 + \theta_1 \hat{\theta}_1}{j2w\tau} \qquad 2.35.$$

Substitute in for $\hat{\theta}_2$, $\hat{\theta}_1$ and τ from the appropriate equations

$$\theta_2 = \frac{\frac{1}{2}i_1^2 R_M + jwmc_p (2i_1 i_o R_M / jwmc_p)^2 \beta}{j2wmc_p}$$

$$= \frac{i^2 R_M}{j4wmc_p} - \frac{\beta(2i_1 i_o R_M)^2}{2(wmc_p)^2} \qquad 2.36.$$

Typically $\beta \sim 5\times10^{-4} K^{-1}$, $i_o^2 R_M \sim 6W$, $w \sim 240 \rightarrow 1200$ rad s^{-1}, $m \sim 5\times10^{-6}$ kg and $c_p \sim 165$ J $kg^{-1}K^{-1}$, so the ratio of the first to the second term is $\sim 8:1$ at $w = 240$ rad s^{-1} to $\sim 40:1$ at $w = 1200$ rad s^{-1}.

Also since $i \sim \frac{1}{4} i_o$ typically, $\theta_1 \sim 8K$ and $\theta_2 \sim 2K$ at $w = 240$ rad s^{-1}. Again the linear approximation of the power balance equation is justified.

2.3.2. Equivalent Impedance Derivation.

Equations 2.31. and 2.35. show a 90^o phase lag of θ_1 and θ_2, so the equation for the resistance fluctuations is

$$R = R_M(1+\beta(\theta_1 \sin wt + \theta_2 \sin 2wt)) \qquad 2.37.$$

The voltage now becomes

$$V = (i_o + i_1 \cos wt) R_M (1+\beta(\theta_1 \sin wt + \theta_2 \sin 2wt)) \qquad 2.38.$$

Separating into the component harmonics

$$V = i_o R_M + i_1 R_M \cos wt + (i_o R_M \beta\theta + \tfrac{1}{2} i_1 R_M \beta\theta_2) \sin wt$$

$$+ (\tfrac{1}{2} i_1 R_M \beta\theta_1 + i_o R_M \beta\theta_2) \sin 2wt + \tfrac{1}{2} i_1 R_M \beta\theta_2 \sin 3wt \qquad 2.39.$$

Therefore the voltage generated across a wire so heated is made up of, apart from constant

and in phase components, quadrature first, second and third harmonics.

If an equivalent impedance method is used, from equation 2.15. the voltage across an RC circuit, when a current $i_o+i_1\cos wt$ is passed through it, is

$$V_{RC} = i_o R_M + i_1 R_M \cos wt + i_1 wCR_M^2 \sin wt \qquad 2.40.$$

bearing in mind that the d.c. component will not pass through the capacitor.

Comparing 2.39 and 2.40 gives

$$i_1 wCR_M^2 = i_o R_M \beta\theta_1 + \tfrac{1}{2} i_1 R_M \beta\theta_2 \qquad 2.41.$$

Substituting for θ_1 from 2.31. and for θ_2 from 2.36., but neglecting the second term, we obtain

$$i_1 wC = \frac{2i_1 i_o^2 \beta}{wmc_p} + \frac{\tfrac{1}{4} i_1^3 \beta}{2wmc_p} \qquad 2.42.$$

Typically $i_1 \sim \tfrac{1}{4} i_o$ and so the ratio of the two terms in equation 2.42. is

$$2i_o^2 : \tfrac{1}{8} i_1^2 \sim 250 : 1 \qquad 2.43.$$

Hence neglecting the second term of 2.36. in the substitution has negligible effect (0.4%). The temperature coefficient of resistivity is therefore given by

$$\alpha = \frac{w^2 mc_p r_e C}{2i_o^2} \qquad 2.44.$$

The similarity with equation 2.20. is apparent.

Though equation 2.44. is clearly the same as that derived by Kraftmakher (1973a) the approximation of $i_1 \ll i_o$ has not been made, the expression for α depending only on the first harmonic temperature fluctuations to an accuracy of 1% if $i_1 \sim \frac{1}{2} i_o$ and even if $i_1 = i_o$ the accuracy is $\sim 6\%$. So a small decrease in i_1 compared with i_o will cause a large increase in the accuracy of equation 2.44.

Again, as in the a.c. only heated wire, all the parameters in 2.44. are known or measurable.

2.3.3. Third Harmonic Voltage Derivation.

An expression for the third harmonic voltage can be found as follows. Let the components of equation 2.36. be labelled :

$$\theta_2^{\,1} = \frac{i_1^2 R_M}{4wmc_p} \quad \text{and} \quad \theta_2^{\,11} = \frac{\beta(2i_1 i_o R_M)^2}{2(wmc_p)^2}$$

Then equation 2.37 becomes

$$R = R_M(1+\beta(\theta_1 \sin wt + \theta_2^1 \sin 2wt - \theta_2^{11} \cos 2wt)) \quad 2.45.$$

The voltage now becomes

$$V = (i_o + i_1 \cos wt) R_M (1+\beta(\theta_1 \sin wt + \theta_2^1 \sin 2wt - \theta_2^{11} \cos 2wt)). \quad 2.46.$$

Multiplying out gives

$$V = R_M(i_o + \beta i_o(\theta_1 \sin wt + \theta_2^1 \sin 2wt - \theta_2^{11} \cos 2wt) + i_1 \cos wt + \beta \frac{i_1 \theta_1}{2} \sin 2wt + \beta \frac{i_1 \theta_2^1}{2} \sin 3wt - \beta \frac{i_1 \theta_2^{11}}{2} (\cos wt + \cos 3wt)). \quad 2.47.$$

An attempt to use the third harmonic voltage is not as straight forward as in the a.c. only method. The voltage is given by

$$V_3 = \frac{\beta i_1 \theta_2^1 R_M}{2} \sin 3wt - \frac{\beta i_1 \theta_2^{11} R_M}{2} \cos 3wt. \qquad 2.48.$$

Substituting for θ_2^1 and θ_2^{11} gives

$$V_3 = \frac{\beta i_1^3 R_M^2}{8wmc_p} (\sin 3wt - \frac{8\beta i_o^2 R_M}{wmc_p} \cos 3wt). \qquad 2.49.$$

Notice that this expression is now a quadratic expression in β. The ratio of the two terms is the same as that of the equation 2.36.

Therefore if the second term is neglected the maximum error (at $w \sim 240 \text{rads}^{-1}$) is $\sim 13\%$ and the resulting expression is

$$\beta = \frac{8V_3 mc_p w}{i_1^3 R_M^2} \qquad 2.50.$$

The accuracy of the value of β obtained can be increased by successive approximations.

2.4. Bridge Theory

In this section the voltage generated by a small resistive and/or capacitative imbalance is considered, together with the resolution of the a.c. bridge with reference to the capacitative voltage component as a function of frequency. The solution to the problem of end effects is dealt with in the context of a.c. bridge measurements. Finally, the

problems of using an a.c. bridge in the measurement of the third harmonic voltage generated by a heated wire are considered.

2.4.1. Impedance Measurement.

As mentioned in subsection 2.2.2. above, the a.c. heated wire can be modelled as a resistance/capacitance parallel circuit, the capacitative component being important for measuring the temperature coefficient of resistivity. To perform this measurement an a.c. bridge was used, the rough circuit diagram with the wire replaced by a resistance/capacitance parallel circuit, is shown in Fig. 2.2. As can be seen, it is a parallel resistance modification of de Sauty's Bridge.

At balance the amplitude and phase of the signal at point A is the same as that at point B. However the effect of a change in resistance and/or capacitance on this signal difference is important.

The signal difference between points A and B is V_{A-B}, the applied voltage, V, having a frequency f, $w = 2\pi f$.

$$\text{Now } Z_1 = \frac{R_1}{1+jwC_1R_1}, \quad Z_2 = \frac{R_2}{1+jwC_2R_2} \quad \text{and}$$

$$V_{A-B} = V\left(\frac{R_3}{R_3+Z_1} - \frac{R_4}{R_4+Z_2}\right)$$

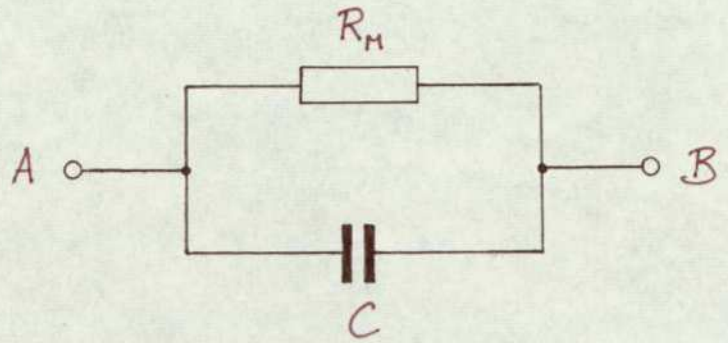

Fig.2.1.

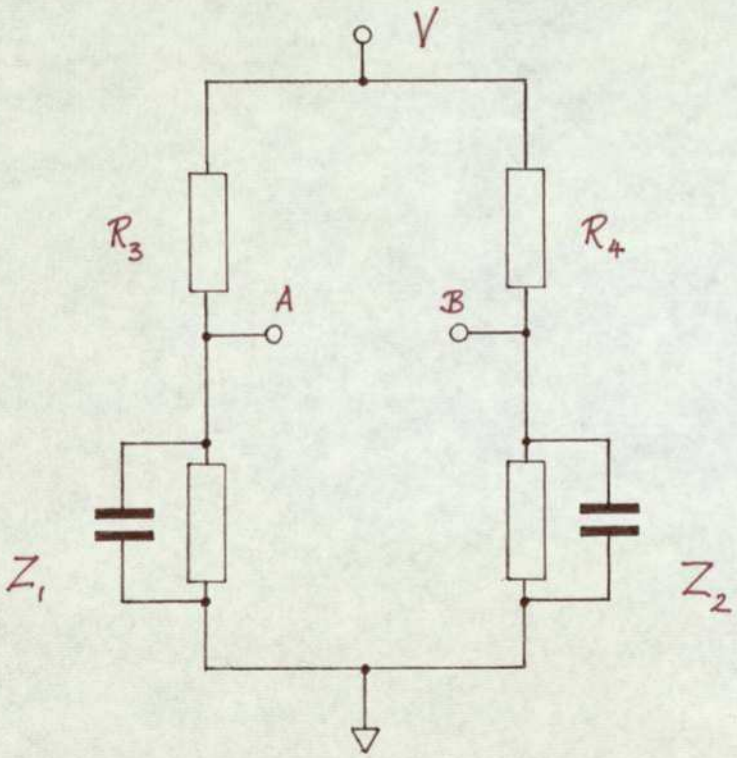

Fig.2.2. de Sauty's Bridge

Substituting in for Z_1 and Z_2 gives

$$V_{A-B} = V\left[\underbrace{\frac{R_3(1+jwC_1R_1)}{R_1+R_3(1+jwC_1R_1)}}_{I} - \underbrace{\frac{R_4(1+jwC_2R_2)}{R_2+R_4(1+jwC_2R_2)}}_{II}\right] \qquad 2.51.$$

Dealing with parts I and II separately :

$$I = \frac{R_3(R_1+R_3)+(wC_1R_1R_3)^2}{(R_1+R_3)^2+(wC_1R_1R_3)^2} + j\,\frac{wC_1R_1^2R_3}{(R_1+R_3)^2+(wC_1R_1R_3)^2}$$

$$II = \frac{R_4(R_2+R_4)+(wC_2R_2R_4)^2}{(R_2+R_4)^2+(wC_2R_2R_4)^2} + j\,\frac{wC_2R_2^2R_4}{(R_2+R_4)^2+(wC_2R_2R_4)^2}$$

Typical values are $R_3=R_4=5\Omega$, $R_1\sim R_2\sim 30\Omega$, $w\sim 1200$ rads^{-1} and $C < 10^{-6}$F. Using these values the terms containing w^2 can be neglected causing $\sim .001\%$ error.

Equation 2.51. then becomes

$$V_{A-B} = V\left(\frac{R_3}{(R_1+R_3)} - \frac{R_4}{(R_2+R_4)} + jw\left(\frac{C_1R_1^2R_3}{(R_1+R_3)^2} - \frac{C_2R_2^2R_4}{(R_2+R_4)^2}\right)\right) \qquad 2.52.$$

If $R_3 = R_4$, $R_1 = R_2$ and $C_1 = C_2$ then both real and imaginary components go to zero as should happen. However, it is important to know the result of a small resistive or capacitative imbalance.

1. Resistive imbalance.

Let $R_3 = R_4 = R$, $C_1 = C_2 = C$, $R_1 = R_1 + \delta r$ and $R_2 = R_1$. Real component of 2.52. then becomes

$$V\left(\frac{R}{(R+R_1+\delta r)} - \frac{R}{(R_1+R)}\right) \qquad 2.53.$$

Imaginary component

$$wV\left(\frac{C_1R(R_1+\delta r)^2}{(R+R_1+\delta r)^2} - \frac{CR_1^2R}{(R+R_1)^2}\right) \qquad 2.54.$$

Now let δr be small enough to allow terms of δr^2 and higher to be ignored. Equation 2.54. then becomes

$$wV\left(\frac{CR(R_1^2+2R_1\delta r)}{(R^2+R_1^2+2RR_1+2\delta r(R_1+R)} - \frac{CR_1^2R}{(R+R_1)^2}\right) \qquad 2.55.$$

2. Capacitative imbalance.

Let $R_3 = R_4 = R$, $C_1 = C+\delta C$, $C_2 = C$, $R_1 = R_2 = R_1$.

Obviously the real component of equation 2.52. will be zero. The imaginary component becomes

$$wV\left(\frac{R_1^2R(C+\delta C)}{(R_1+R)^2} - \frac{R_1^2RC}{(R_1+R)^2}\right)$$

which in turn simplifies down to

$$\frac{wVR_1^2R\delta C}{(R_1+R)^2} \qquad 2.56.$$

Therefore, although a small capacitative imbalance causes only a capacitative signal, a similar, small resistive imbalance causes not only a resistive signal, but also a capacitative one as well.

The size of this capacitative component can be estimated by substituting typical values into equations 2.55. and 2.56 : $R = 5\Omega$, $R_1 = 30\Omega$ and $w = 600$ rads^{-1}. At this frequency the capacitance to be measured is small ~ 30nF, so let $\delta C = 30$nF. Let $\delta r = 0.1\Omega$, although the balance can be obtained to a greater accuracy than this in practice.

Using these values, the capacitative signal due to a resistive imbalance is ~ 6 x 10^{-8} V, whilst that due to a purely capacitative one is ~ 6 x 10^{-5} V. Therefore under the worst conditions the error in the capacitative signal is $\sim 0.1\%$.

2.4.2. Bridge Resolution.

It is important to realize that according to equations 2.20. and 2.44., the capacitance being measured will vary as the inverse of the length of the wire (due to the mass term), and also as the inverse of the square of the modulating frequency.

However, the method of measuring the capacitance is by balancing voltages on an a.c. bridge and the significant property is how the ratio of the resistive and capacitative impedances vary with modulating frequency and wire length.

The ratio of the resistive and the capacitative components of the impedance of the circuit in Fig.2.1 is wCR_M.

Putting $wCR_M = X$, this depends only on the inverse of the frequency and wire length.

where for a.c. only, $X = \frac{\alpha i^2 R_M}{8wmc_p r_e}$

and for a.c. & d.c., $X = \frac{2\alpha i_o^2 R_M}{wmc_p r_e}$

So, although the capacitance being measured will vary as the inverse of the square of the frequency, the resolution only varies as the inverse of the frequency.

For a.c. only, $X \sim 3 \times 10^{-3} \rightarrow 1.5 \times 10^{-4}$ when $w \sim 240$ rads$^{-1} \rightarrow 1200$ rads^{-1}.

For a.c. + d.c., $X \sim 4 \times 10^{-2} \rightarrow 2 \times 10^{-3}$ when $w \sim 240$ rads$^{-1} \rightarrow 1200$ rads^{-1}.

Note, however, that this is a comparison at constant temperature : over the temperature range 1400K - 1800K experimentally the impedance ratio increases by a factor of < 3 (at constant frequency and wire length).

2.4.3. End effects.

As is to be expected there are end effects due to the wire supports acting as heat sinks. However, if the temperature is high enough and the wire long enough there is a central portion whose temperature is sensibly constant. This has been studied

in some detail by Jain and Krishnan (1954 a,b,c). All measurements should, obviously, be obtained under conditions that ensure that the central portion is at a constant temperature. Then the capacitance of an end effect free wire whose length is the difference of the lengths of two test wires can be calculated from the measured capacitances of the test wires.

It was thought at first that instead of measuring each wire separately against an RC parallel circuit, both wires could be measured at the same time by having a wire on opposite sides of the bridge as shown in Fig.2.3. This, it was thought, would automatically remove the end effects and result in the measurement of the capacitance of a wire whose length was the difference of the lengths of the two test wires.

Referring to Fig.2.3: at balance, assuming the ratio resistors are equal, the current flowing in each arm is the same, therefore the end effects of the wires should cancel out.

Bearing in mind the model of a resistance/capacitance parallel circuit, let the components of the short wire be R_s and C_s and those of the long one R_L and C_L.

Using equations 2.13. and 2.17. then, for an a.c. only heated wire, the following relationship is true

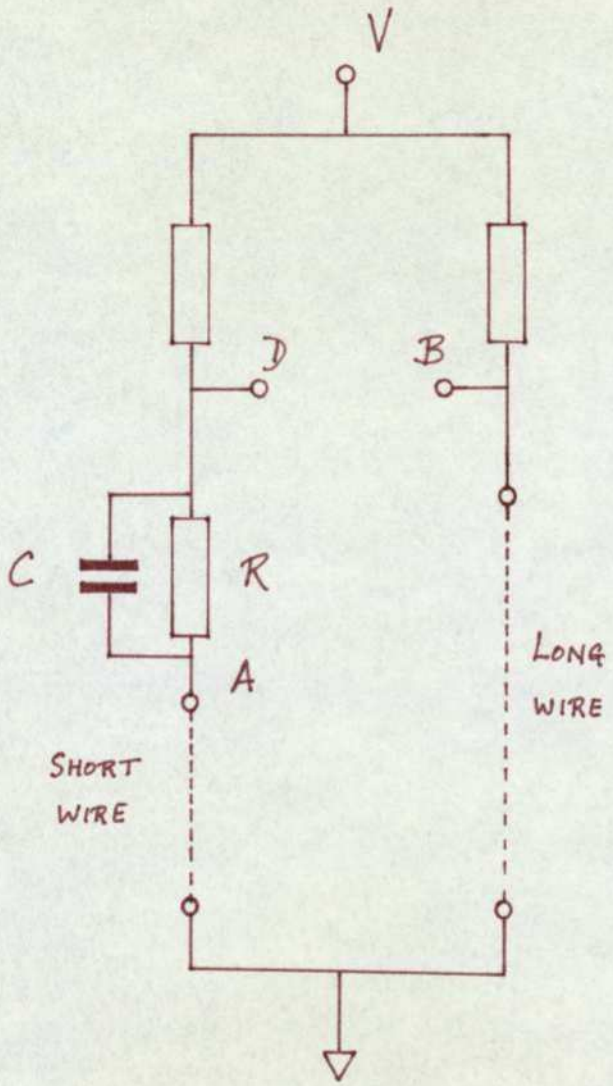

Fig.2.3. Bridge circuit proposed to remove the end effects of the heated wires

$$iR(\cos wt - wCR \sin wt) + iR_s(\cos wt - \frac{\beta\theta_s}{2}(\sin wt + \sin 3wt)) =$$

$$iR_L(\cos wt - \frac{\beta\theta_L}{2}(\sin wt + \sin 3wt)) \qquad 2.57.$$

In equation 2.57 above the assumption has been made that the phase shift of the heating current when passing through the CR circuit is small enough to be neglected. Typically, it is of the order of $\tan \phi \sim 10^{-3}$.

Substituting for θ_s, θ_L and neglecting the third harmonic term as being filtered out, the voltage across the RC circuit, AD becomes

$$i(R_L - R_s)\cos wt - \frac{i^3\beta}{8wc_p}\left(\frac{R_L^2}{m_L} - \frac{R_s^2}{m_s}\right)\sin wt =$$

$$iR(\cos wt - wCR\sin wt) \qquad 2.58.$$

As a result, the expression for the temperature coefficient of resistivity becomes

$$\alpha = \frac{8w^2 c_p r_e CR^2 m_L m_s}{i^2(m_s R_L^2 - m_L R_s^2)} \qquad 2.59.$$

This should be compared with the expression obtained when measuring each wire separately. From equation 2.20.

$$\frac{1}{C_L} - \frac{1}{C_s} = \frac{8w^2 c_p r_e}{i^2 \alpha}(m_L - m_s) \qquad 2.60.$$

So the result corresponding to 2.59. is

$$\alpha = \frac{8w^2 c_p r_e C_L C_s (m_L - m_s)}{i^2 (C_s - C_L)} \qquad 2.61.$$

It is apparent that there are more quantities to be determined for equation 2.59. than for 2.61. In addition, when both wires are measured at the same time, it is not possible just to measure R and C, R_s and R_L must also be found and that is not possible using the circuit shown in Fig.2.3. It was therefore decided that the wires should be measured independently, rather than using the simultaneous measurement of two wires as shown in Fig.2.3.

2.4.4. Third Harmonic Voltage Measurement.

There is another possible measurement; this is the determination of the third harmonic voltage, the fundamental having been balanced out by means of an RC circuit.

Here the problem is different; consider first the single wire circuit shown in Fig.2.4. where R_{st} is a standard resistance for current sensing and Z_p is the impedance of the power supply.

Effectively the wire is acting as a third harmonic voltage source of output impedance R, at fundamental balance. Now for the detector to measure the third harmonic voltage generated, the impedances of the balancing side of the bridge and

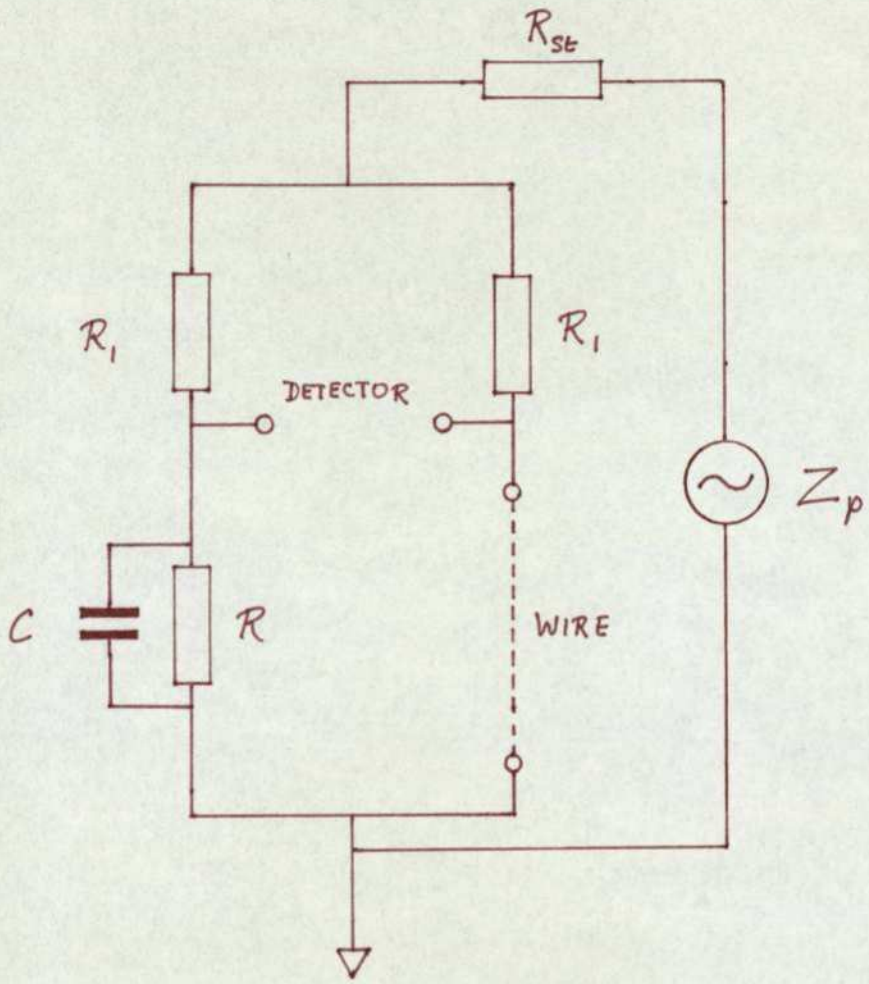

Fig.2.4. Circuit diagram relevant to a third harmonic voltage generated by an a.c. heated wire

the power supply circuit must each be, ideally, infinite. This will not be the case.

If $Z = \frac{R(1-jwCR)}{1+(wCR)^2}$, let $Z_1 = R_1 + Z$ and $Z_2 = R_{st} + Z_p$.

Then the total third harmonic current is given by

$$I_3 = \frac{V_3 Z_1 Z_2}{(Z_1+Z_2)+Z_1 Z_2 (R_1+R_2)} \qquad 2.62.$$

While that flowing in the balancing side is

$$I_{3B} = \frac{V_3 Z_1 Z_2}{((Z_1+Z_2)+Z_1 Z_2 (R_1+R_2))} \cdot \frac{Z_1}{(Z_1+Z_2)} \qquad 2.63.$$

Therefore the voltage across the detector is

$$V_{A-B} = V_3 \left[1 - \frac{Z_1^2 Z_2 Z}{((Z_1+Z_2)+Z_1 Z_2 (R_1+R_2))(Z_1+Z_2)} \right] \qquad 2.64.$$

Typical values for the above quantities are: $Z_1 \sim 35\Omega$, $Z_2 \sim 200\Omega$, $Z \sim 30\Omega$, $R \sim 30\Omega$ and $R_1 = 5\Omega$. If these values are used, then $V_{A-B} \sim 0.9\ V_3$ depending on the exact values.

Due to the complexity of the analysis of the results and the inaccuracies introduced, particularly by the impedance of heating source, this circuit is not suited to third harmonic voltage measurement. Obviously the situation is not improved when both wires are in circuit as in Fig.2.3.

This problem is not present when measuring the equivalent capacitance because a null technique is being used, i.e. the voltage generated by the wire is, at balance, modelled by the voltage generated by the RC circuit. Therefore any leakage to earth through the power circuit or other side of the bridge is exactly the same for both sides.

2.5. Frequency Dependence of the Temperature Coefficient of Resistivity

Van den Sype (1970) pointed out that the vacancy contribution to the specific heat and temperature coefficient of resistivity will be frequency dependent. Seville (1972) elaborated upon the point and produced a detailed derivation of the lattice and vacancy contributions to the specific heat and temperature coefficient of resistivity assuming linear vacancy kinetics.

For the temperature coefficient of resistivity, the expression is

$$\alpha(w) = \sqrt{\frac{\alpha_L^2 + (\alpha_L+\alpha_v)^2 w^2 \tau_v^2}{1+w^2\tau_v^2}} \qquad 2.65.$$

where τ_v is the vacancy lifetime,

α_L the lattice temperature coefficient,

α_v the vacancy contribution at w = 0.

Experimentally, the component of the temperature coefficient of resistivity that is measured is that in phase with the temperature

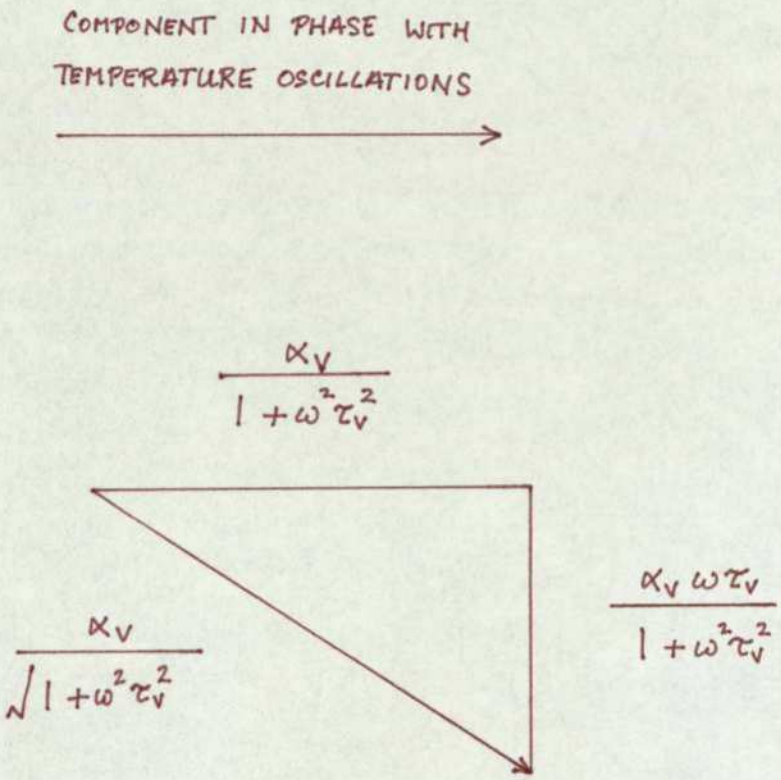

Fig.2.5. Components of the vacancy contribution to α

fluctuations. Fig.2.5. shows this component clearly and it is obvious that the temperature coefficient of resistivity will decrease with frequency according to

$$\frac{\Delta\alpha_v}{\alpha_v} = \left(\frac{w^2\tau_v^2}{1+w^2\tau_v^2} \right) \qquad 2.66.$$

where $\Delta\alpha_v$ is the reduction in the vacancy contribution.

Typically, α_v is of the order of 10% of the total temperature coefficient of resistivity $(\alpha_L + \alpha_v)$. Therefore a 1% decrease in the total temperature coefficient of resistivity, as can be seen in Fig.5.22. at ~60Hz, would lead to an estimation of the vacancy lifetime according to

$$\tau_v = \frac{1}{3w} \qquad 2.67.$$

In general equation 2.67. is only valid for a frequency which gives a 10% decrease in α_v. As shown in Chapter 5 and discussed in Chapter 6, the experimental and theoretical curves are in good agreement. Therefore the theoretical value for α_v can be used to deduce the 10% drop.

2.6. Summary

Wires heated with a.c. only and those heated with a.c. superimposed on d.c. were analysed; the results showed that their impedances could be modelled as a resistance/capacitance parallel circuit.

The expressions for the temperature coefficient of resistivity for wires heated by a.c. only and those heated by both a.c. and d.c. are respectively :

$$\alpha = \frac{8w^2 c_p r_e mC}{i^2} \qquad 2.20.$$

and

$$\alpha = \frac{w^2 c_p r_e mC}{2i_o^2} \qquad 2.44.$$

Typically 2.44. is accurate to at worst 0.4% due to neglected terms; there is no error in 2.20. from this source. However, an approximation is present in both expressions due to inaccuracies in the 90^o phase lag of the respective temperature fluctuations. At $w = 240$ rads^{-1} this error is 2% and 4% in a.c. heated wires and a.c. superimposed on d.c. heated wires respectively : leading to ~2% error in 2.20. and ~4% in 2.44. For this reason, for low frequency measurements, it is advisable to use wires heated by a.c. only.

Expressions for the third harmonic voltage generated across heated wires were developed.

In section 2.4.2. the measurement of resistance/capacitance parallel impedances using a form of de Sauty's Bridge was considered. The effect of small resistive imbalances were shown to produce a capacitative signal but one small enough to be ignored (~0.1% of the capacitative signal).

The treatment of end effects by the simultaneous measurement of two unequal wires was considered and the expression needed to calculate the temperature coefficient of resistivity by this method was shown to be

$$\alpha = \frac{8w^2 c_p r_e C R^2 m_L m_s}{i^2 (m_s R_L^2 - m_L R_s^2)} \qquad 2.59.$$

The corresponding expression for the separate measurement of the wires is

$$\alpha = \frac{8w^2 c_p r_e C_L C_s (m_L - m_s)}{i^2 (C_s - C_L)} \qquad 2.61.$$

Because 2.61. has fewer variables it was decided to measure the capacitance of the wires separately.

The use of the bridge to measure the third harmonic voltage was considered and shown to be impractical because the bridge is a null detector and not suited to measuring unbalanced voltages.

Finally, the frequence dependence of the temperature coefficient of resistivity due to the vacancy contribution is discussed. The expression used to determine the vacancy lifetime from the decrease in temperature coefficient of resistivity as a function of frequency is shown to be

$$\tau_v = \frac{1}{3w} \qquad 2.67.$$

3. TEMPERATURE MEASUREMENT

3.1. Introduction

It is obviously necessary to know the temperature of the wire sample, the choice of method being one of the following : thermocouple, optical pyrometry, thermionic emission, thermal noise or resistance ratio measurements.

The use of a thermocouple is out of the question since the wire samples used are 50μm diameter platinum and the size of the thermocouple needed to restrict the conduction of heat is too small to be practical.

Optical pyrometry is of an approximate nature, the accuracy not being sufficiently high for the requirements of this experiment ($\sim \pm$10K). Also there is a lack of accurate published material for high temperature measurements : calibration experiments would have to be performed, determining the temperature by optical pyrometry and an independent method simultaneously.

Similarly thermionic emission (the ionic "vapour pressure" of the material) and thermal (Johnson) noise measurements have to be calibrated against some independent method. In the case of platinum, this independent method tends to be the resistance ratio as a function of temperature. This measurement has been performed by Kraftmakher and Sushakova (1974)

up to 1830K.

In view of this, temperature determination from resistance ratio measurements was the chosen method.

The basic principle is in using published values of the temperature coefficient of resistivity to find the resistance ratio as a function of temperature. This is used in conjunction with an experimental determination of the resistance ratio as a function of heating current to obtain a calibration graph of temperature versus heating current.

3.2. Temperature Coefficient of Resistivity of Platinum

Reliable results for the resistivity are necessary for the determination of the mean temperature. These are readily available up to ~1500K, beyond this there are only a few results.

Roeser and Wensel (1941) measured the resistivity up to 1773K and the work of Jain, Goel and Narayan (1968), determining the temperature variation of the resistivity, supports their results up to 1700K.

Kraftmakher and Lanina (1965) have determined the specific heat of platinum at high temperatures (1000-2000K). To do this it was necessary to know the temperature coefficient of resistivity and this was done by measuring the resistance directly. The temperature was determined from the radiated power, using

published values for the emittance, and in addition between 1000-1500K the temperature was determined using the quadratic temperature dependence of the resistance. The temperature coefficient of resistivity was then calculated yielding results in agreement with Roeser and Wensel (1941) up to 1500K. However, above 1500K, as was pointed out by Seville (1972), there is some doubt as to the emittance values used by Kraftmakher and Lanina (1965) and this casts some doubt in turn on the temperature coefficient of resistivity obtained.

Kraftmakher and Sushakova (1974) measured the temperature coefficient of resistivity of platinum over the temperature range 1050-1850K directly by a low frequency (period 15s) modulation method. The samples used were in the form of tubes and in this case the temperature was determined using a platinum-platinum/rhodium thermocouple, (possible because the samples were relatively massive : 0.6 mm diameter, 0.07mm wall thickness). This method was therefore superior to that of Kraftmakher and Lanina (1965) because the use of doubtful emittance values is avoided.

There is a discrepancy between the temperature coefficient of resistivity obtained by Kraftmakher and Lanina (1965) and that by Kraftmakher and Sushakova (1974) above ~1500K due to the erroneous emittance values used by Kraftmakher and Lanina (1965). This can be seen in Fig.3.1.

Fig.3.1. α versus temperature from Kraftmakher & Sushakova and Kraftmakher & Lanina.

3.3. End Effects

The work of Jain and Krishnan (1954a,b,c) has shown that if a wire is sufficiently long the central portion is of constant temperature for a given heating current and that if the temperature profiles of 2 wires of different lengths (each being long enough for the central portion to be at constant temperature) are compared, then the end effects are virtually identical and the constant temperature portions are of different lengths.

Therefore if the resistance as a function of temperature is found for two wires of different lengths then, if the wires are sufficiently long to have central portions at identical temperatures, the end effects may be removed by simply subtracting the resistances. The result is the resistance as a function of temperature for an end effect free wire whose length is the difference of the test wires.

To ensure that the wires used were long enough to have central portions of constant temperature, three were heated until they melted : these wires were $\sim$4cm long (i.e. shorter than those used in the experiment) and all melted at a point away from the centre (where the melting would occur if there was no constant temperature central portion).

Checks were made to ensure that end effects were indeed eliminated : the resistance ratios for long,

short and end effect free wires at, for instance, 1670K are $r_{el} = 5.232$, $r_{es} = 5.193$ and $r_e = 5.406$. The amount by which r_{eL} and r_{es} differ from r_e can be considered a measure of the effect of heat conduction by the end supports. As a check, the following relationship should be true

$$\frac{r_e - r_{eL}}{r_e - r_{es}} = \frac{Rs}{R_L} \qquad 3.1.$$

where $r_e - r_{eL}$ is the resistance ratio of the end of the long wire.

$r_e - r_{es}$ the resistance ratio of the end of the short wire.

R_s the resistance of the short wire

and R_L that of the long wire.

Using the values at 1670K above, the left hand side of equation 3.1. becomes

$$\frac{5.406-5.232}{5.406-5.193} = 0.813$$

The resistance values at 1670K are $R_s = 17.39\Omega$ and $R_L = 21.52\Omega$, therefore the right hand side of equation 3.1. becomes 0.808.

This is an agreement of $\sim$1% indicating that this method of removing the effects of conduction to the supports is accurate to 1%. As has been shown by Jain and Krishnan (1954a,b,c) the temperature profile of the end is exponential in shape it is therefore reasonable to state that a 1% error in the

elimination causes approximately a 1% error in the deduced temperature. This assumes that the non-linearity of the resistance ratio v. temperature and heating current v. resistance graphs is insignificant. This is justified by a comparison of these graphs with an exponential curve.

The 1% agreement operates over the temperature range of interest, i.e. 1400K-1850K.

Therefore this method of obtaining results for an end effect free wire is valid provided the shortest wire is long enough to have the centre at the same temperature as that of the long wire. As an example of what happens when this condition is not met the values below are at 1760K and the short wire is too short :

$$r_e = 5.485,\ r_{eL} = 5.223 \text{ and } r_{es} = 5.011.$$

The corresponding resistances being $R_L = 21.33\Omega$ and $R_s = 11.22\Omega$ so

$$\frac{r_e - r_{eL}}{r_e - r_{es}} = \frac{0.262}{0.474} = 0.553$$

and

$$\frac{R_s}{R_L} = \frac{11.22}{21.33} = 0.526$$

The discrepancy here is ~5% compared with ~1% in the previous example and if these results are used to calibrate the heating current significant errors are naturally introduced.

3.4. Resistance Ratio Measurement

3.4.1. Apparatus.

The apparatus used for the ice point and high temperature resistance measurements were in the most part the same : the test wires were mounted by soldering to varnished copper wires that were also the current carrying leads. The potential leads were soldered at the same point and were platinum wires which were in turn soldered to copper wires connected to the potential measuring circuit. All the copper wires were fixed to a central brass rod support screwed into a brass plate which was in turn fixed to a die-cast aluminium box.

At high temperatures the wires were kept under vacuum of $<$.02 Torr. To do this a 5 cm diameter Pyrex tube fitted with brass end pieces and "O" ring seals was placed over the test wire arrangement and screwed into the brass baseplate fixed to the aluminium die-cast box. The vacuum chamber arrangement is shown in Fig. 3.2. The chamber was evacuated by means of a two stage rotary pump.

The circuit diagram for the high temperature resistance measurements is shown in Fig.3.3.

The potential divider was necessary when measuring the voltage across the wire because the voltage was too large for the potentiometer. The potential divider was made up of two Sullivan non-

Fig.3.2. Vacuum chamber arrangement

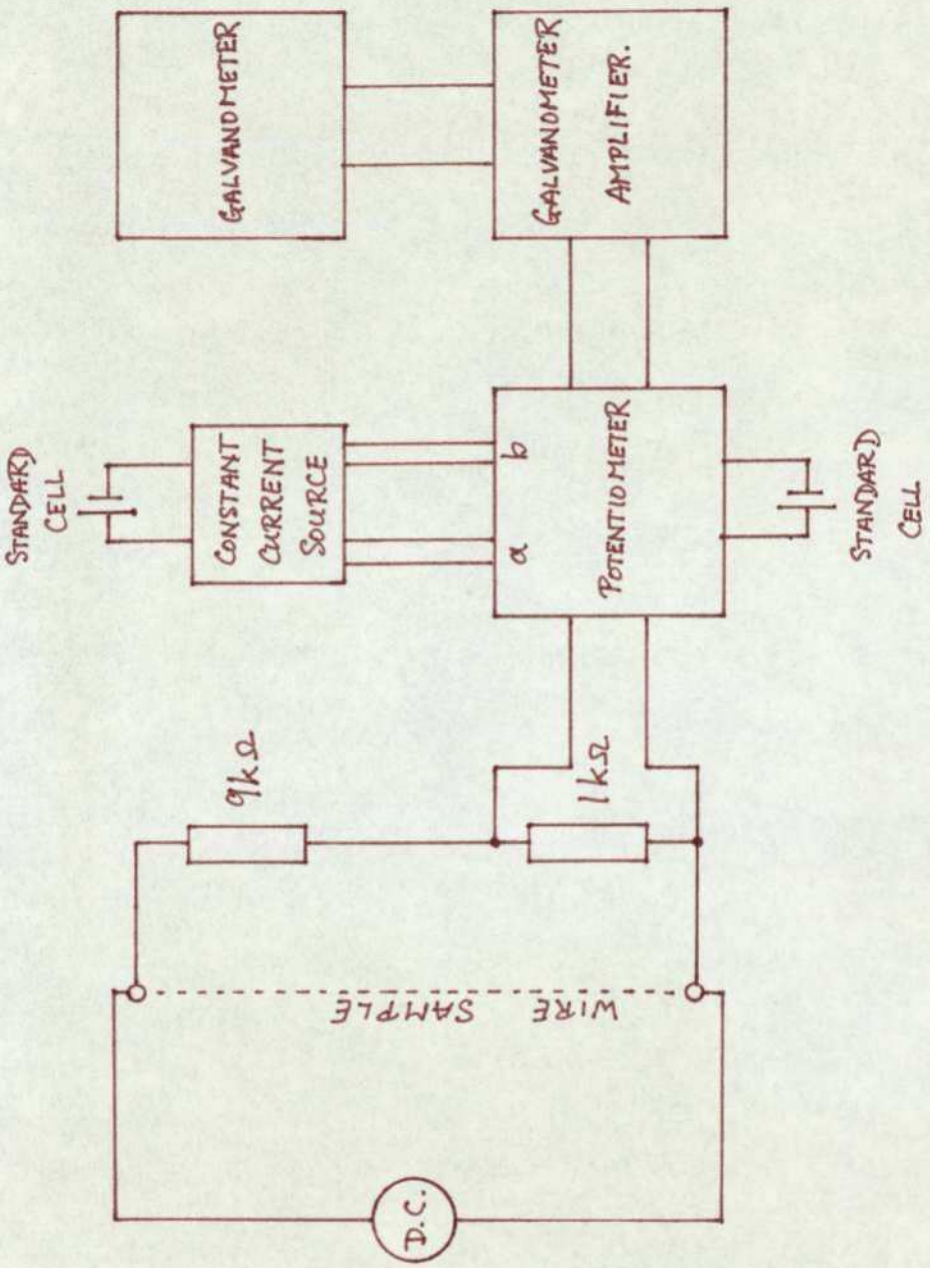

Fig.3.3. High temperature resistance measurement circuit

reactive 0.05% grade resistance boxes set at a ratio of 9:1. Results were taken with the resistance boxes set to 1,000Ω and 9,000Ω (see subsection 3.4.3).

All measurements were taken using a Tinsley Vernier Potentiometer 5590B supplied by a Tinsley Current Controller 5750. Weston Standard Cells 1268 were used throughout. The potentiometer output was to a Tinsley Photocell Galvanometer Amplifier 5588 in series with a Tinsley Galvanometer M.S.2 45E. The amplifier setting was by trial and error, the whole set-up being capable of resolving 1μV.

The power supply was a Solartron P.S.U. AS1412 d.c. source used in its constant voltage mode and in series between the source and the test wire was a Tinsley Grade 1-AC-DC 1Ω standard resistor used as a current sensor.

The circuit for room temperature resistance measurements is shown in Fig.3.4. and is basically the same as that for high temperature measurements. There are two differences : firstly that the lower voltages being measured do not necessitate the potential divider and secondly a Sullivan non-reactive 0.05% grade resistance box set to 1kΩ was connected in series with the Solartron source to act as a current controller.

3.4.2. Ice point resistance determination.

The test wires used were 50μm, 99.999% pure, platinum wires supplied by Johnson Matthey and Co.Ltd.

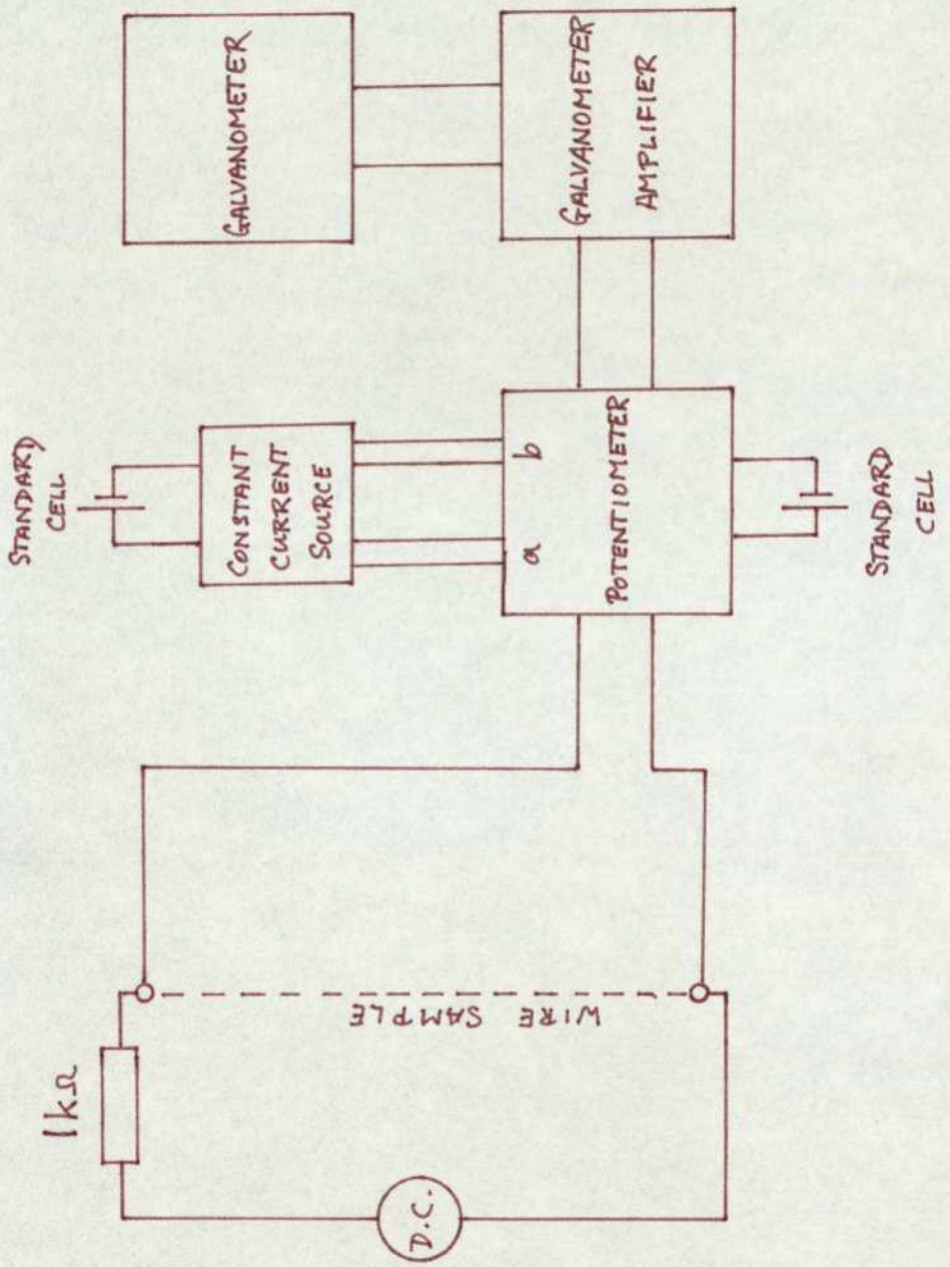

Fig.3.4. Room temperature resistance measurement circuit

The accuracy of the stated diameter was determined by weighing a measured length and was found to be within $\pm 1\%$.

The resistance of the test wires at room temperature was measured, the ice point resistance being determined from equation 3.2. which is known to be accurate up to 650°C

$$R_o = R_T (1 + AT + BT^2) \qquad 3.2.$$

where R_o is the ice point resistance,

R_T the resistance at temperature T ($0°C < T < 650°C$).

A and B are constants from Johnson Matthey Co. Ltd. (1952).

$A = 3.98 \times 10^{-3}\ °C^{-1}$ and

$B = -5.85 \times 10^{-7}\ °C^{-2}$.

To measure the room temperature resistance, the wires were opened to the atmosphere, while the chamber was still in place to prevent air currents causing local cooling and disturbing the resistance measurement. The temperature of the wire was found by placing a mercury-in-glass thermometer in the region of the centre of the test wire. The thermometer used could be read to an accuracy of 0.1°C.

The current passed through the wire had to be small enough to cause no appreciable heating and the maximum allowable value was determined by passing a series of different currents and determining the ice

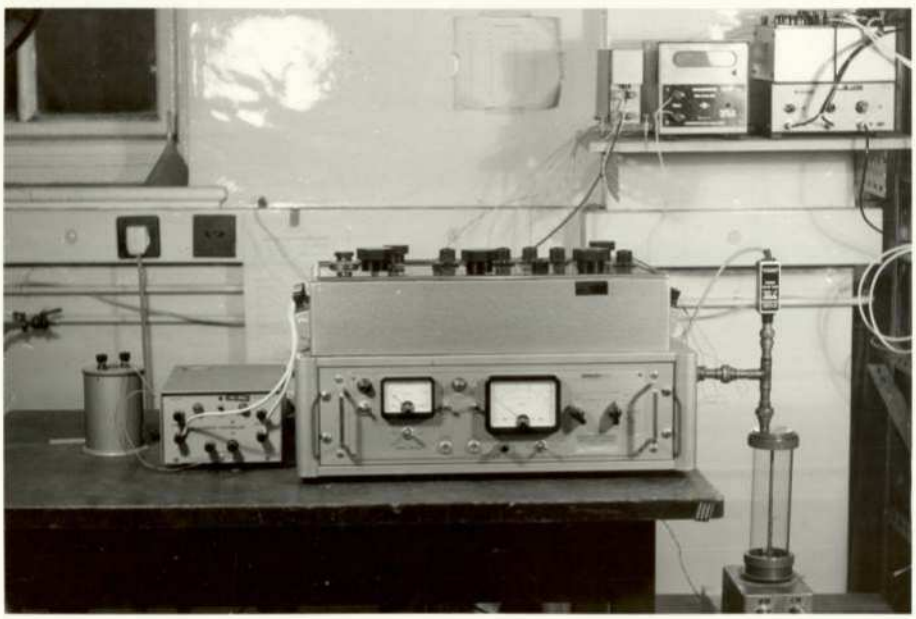

Fig.3.5. General view of the resistance measurement circuitry

point resistances for each current passed. For currents of negligible heating effect, all the ice point resistances should be the same. As an example, the worst results obtained are shown in table 1.

2.1.

Table 2.1.

Current used (mA)	Ice point resistance (Ω)
3.977	4.112
4.974	4.113
5.971	4.113
6.963	4.114

The heating effect is obviously negligible, the ice point being found to better than 3 parts in 10,000. As a consequence all the ice point resistances were measured using currents between 4 - 7 mA.

The ice point resistances determined in this way were found to be consistent with the lengths of 50μm diameter platinum wire used.

As a check, ice point resistances were determined before and after the high temperature measurements. It was found that to ensure good reproducibility (within the limits mentioned above) the test wires had to be heated in vacuo for about an hour at ~1700K. This is in agreement with Seville (1972).

3.4.3. High temperature resistance measurements.

These measurements were performed under a vacuum of <.02 Torr, this pressure was considered adequately low in view of the work of Fryburg (1965)

who determined that the formation of PtO_2 was confined to high temperature platinum in an atmosphere containing a high partial pressure of oxygen.

As mentioned above a potential divider was necessary to enable the measurement by the potentiometer of the voltage across the test wire. The ratio of the resistance boxes making up the potential divider was 9:1, however, the actual values of the resistance boxes were determined by trial and error.

The values of 9kΩ : 1kΩ were used : this leads to a resistance of 10kΩ in parallel with the wire resistance of ~ 30Ω. The current taken by the potential divider network is < .3% that of the test wire and causes a negligible error. The sensitivity of this potential divider network was more than adequate for the measurements required.

To check the reproducibility of the resistances obtained, both a long and short wire were heated from cold to the maximum temperature to be used experimentally twice. The results for the long wire are shown in Fig.3.6. and are typical for the short wire also. There is good reproducibility to about 1 part in 1,000.

3.4.4. Resistance ratio determination

The resistance as a function of heating current was plotted for two lengths of wire and the resistances for each wire were read off at convenient

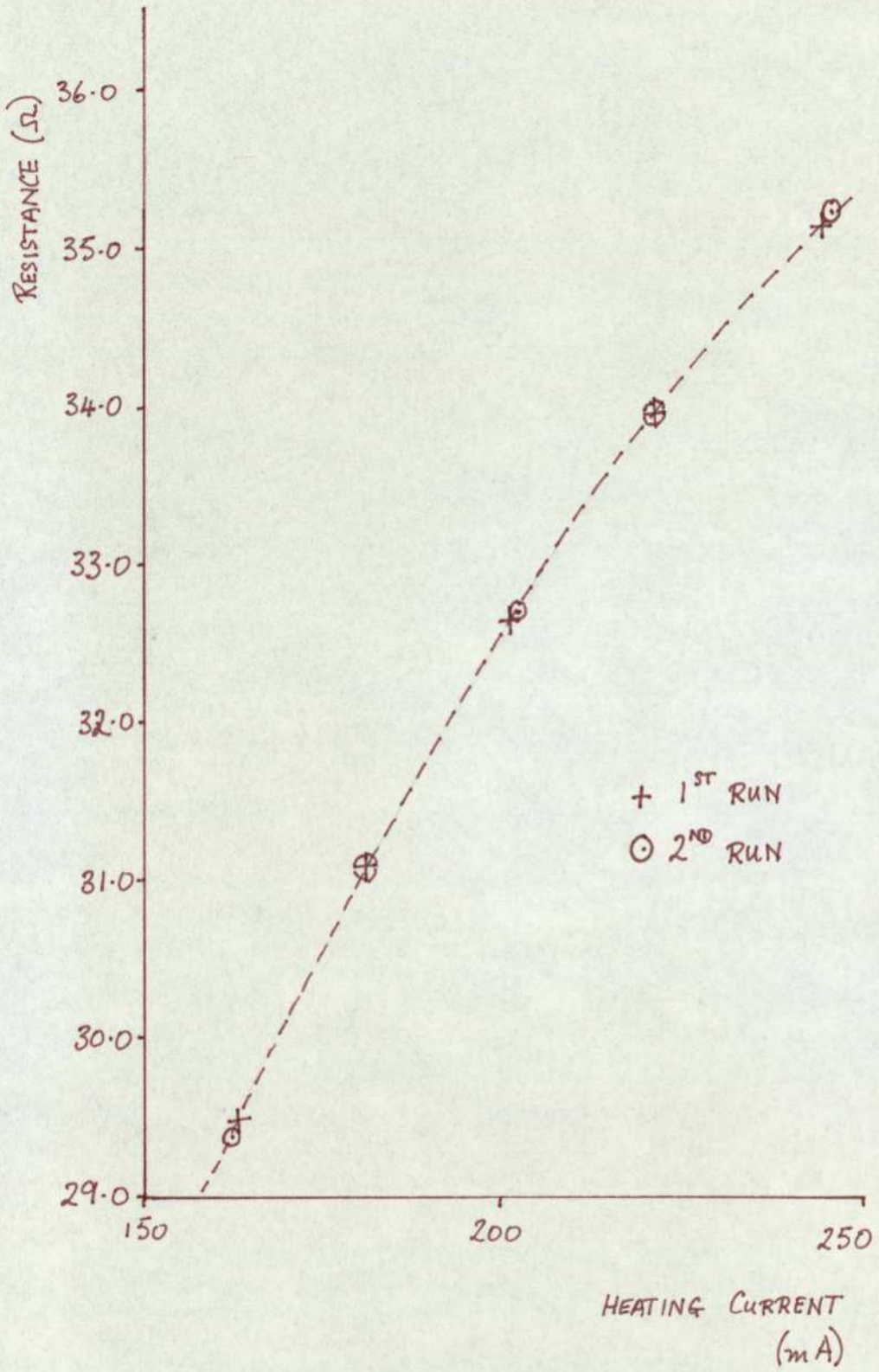

Fig.3.6. Resistance reproducibility for a long wire

current values (e.g. every 10mA). These resistances were subtracted and the resulting resistance of an end effect free wire as a function of heating current was plotted.

The resistance so obtained was divided by the difference of the ice point resistances to give the resistance ratio as a function of heating current, see Fig.3.7.

3.5. Heating Current Calibration

It was necessary to know the resistance ratio as a function of temperature and to calculate this, the temperature coefficient of resistivity as a function of temperature was used. This quantity has been measured by Kraftmakher and Sushakova (1973) and is shown on Fig. 3.1.

The calculation of the resistance ratio as a function of temperature can be performed by making use of the fact that over a small temperature range it is possible to fit a parabolic curve to the graph of temperature coefficient of resistivity against temperature. If the parabola is centred at some temperature T, then the resistance ratio at some temperature $T + \theta$, where $\theta \ll T$, is given by

$$r_e(T+\theta) = r_e(T)+A(T)[\theta]+B(T)[\theta]^2 \qquad 3.3.$$

Now by definition

$$\alpha(T+\theta)=\frac{dr_e}{dT}(T+\theta) \qquad 3.4.$$

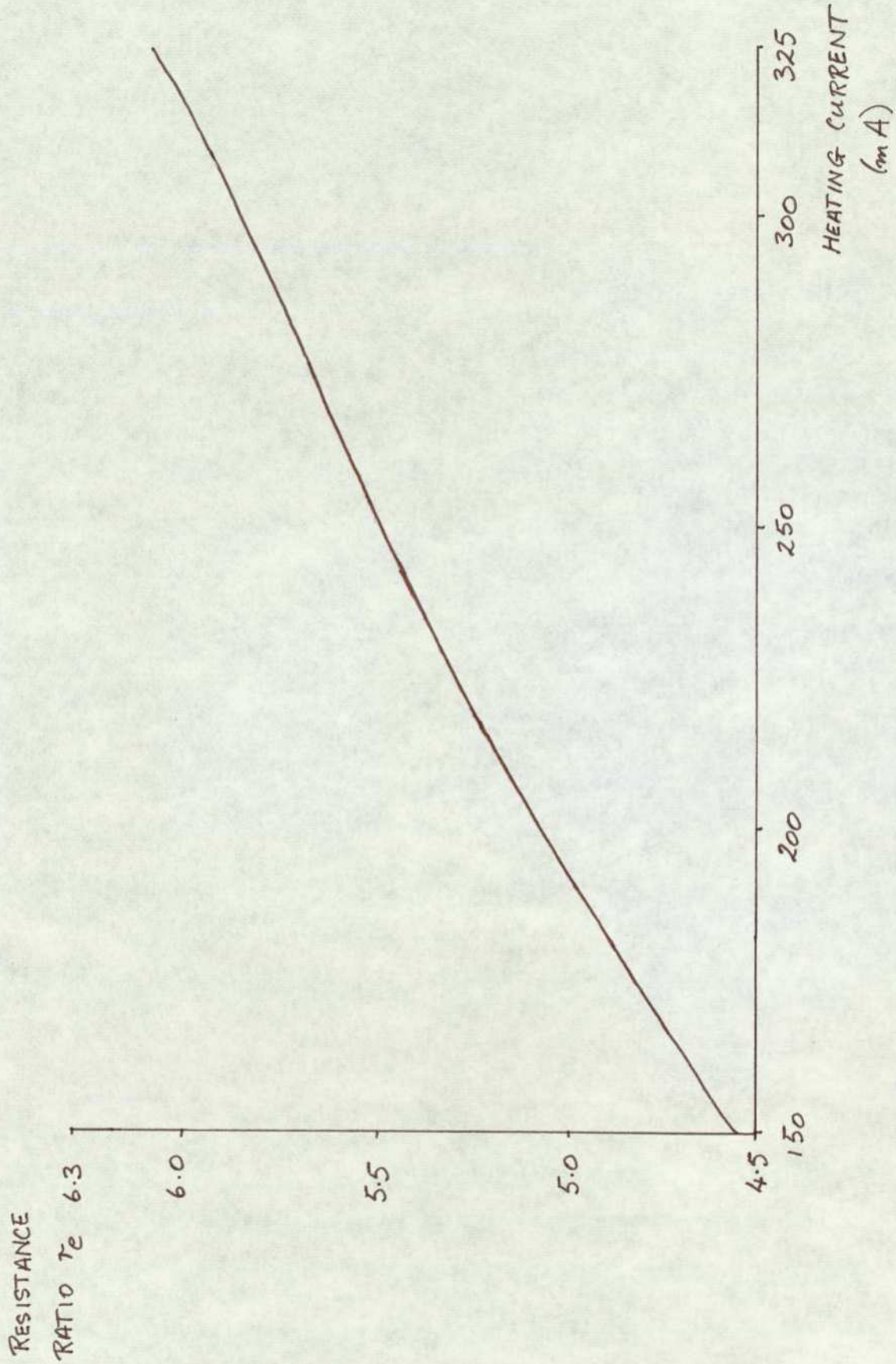

Fig.3.7. Resistance ratio versus heating current

So for small $\pm\theta$,

$$\alpha(T\pm\theta) = \alpha(T)\pm A(T) \qquad 3.5.$$

Similarly the resistance ratio at T-θ is given by

$$r_e(T-\theta) = r_e(T)+A(T)[\theta]+B(T)[\theta]^2 \qquad 3.6.$$

Subtracting equation 3.6. from equation 3.3. gives

$$\frac{r_e(T+\theta)-r_e(T-\theta)}{2\theta} = A(T) \qquad 3.7.$$

Substituting in for A(T) in equation 3.7. from equation 3.5. gives

$$\frac{r_e(T+\theta)-r_e(T-\theta)}{2\theta} = \alpha(T+\theta)-\alpha(T) \qquad 3.8.$$

So to determine the resistance ratio as a function of temperature, an initial resistance ratio value is needed. This can be found by using the results of Kraftmakher and Lanina (1965) for temperatures below 140OK. The temperature coefficient of resistivity was found by Kraftmakher and Lanina (1965) by measuring the resistance ratio and using a technique similar to that shown above. Below 140OK their results for the temperature coefficient of resistivity are in close agreement with those of Kraftmakher and Sushakova (1973) as can be seen from Fig.3.1. Therefore, the resistance ratio value was taken from the published values of Kraftmakher and Lanina (1965) at a temperature

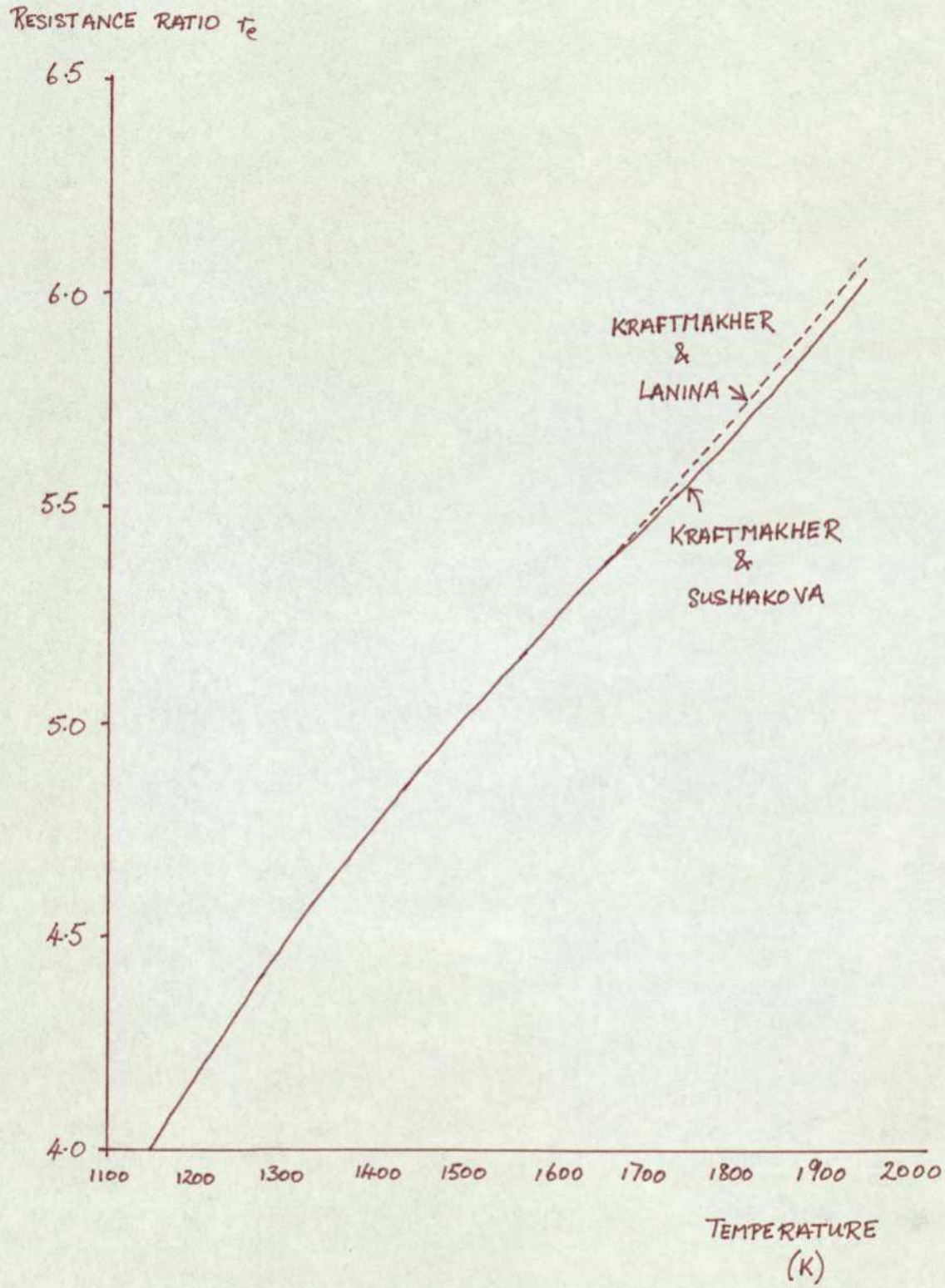

Fig.3.8. Resistance ratio versus temperature from Kraftmakher & Sushakova and Kraftmakher & Lanina

just under 1400K. The temperature coefficient of resistivity values however came from Kraftmakher and Sushakova (1973) at all times.

The value of Θ used was 25K, the graph of the resistance ratio against temperature is shown on Fig.3.8. For comparison, the resistance ratio values derived from Kraftmakher and Sushakova's (1973) results are shown along with those from Kraftmakher and Lanina's (1965).

The heating current calibration was performed by reading the resistance ratio for a given heating current from Fig.3.7. The corresponding temperature at that resistance ratio value was found from Fig.3.8. Thus Fig.3.7. was combined with Fig.3.8. to give a graph of heating current against temperature, see Fig.3.9.

3.6. Comparison with previous results

The other detailed account of temperature measurement by this method is by Seville (1972). The results of Kraftmakher and Sushakova (1973) for the temperature coefficient of resistivity as a function of temperature were not available then and his measurement uses the results of Kraftmakher and Lanina (1965). The resulting difference in the temperature calibration is small and the results are compared in Fig.3.10.

As a check, the emissivity was calculated and compared with results taken by Jain, Goel and Narayan (1968) and Seville (1972). It can be seen in Fig.3.11. that the present results are consistent with those of other workers, especially in view of

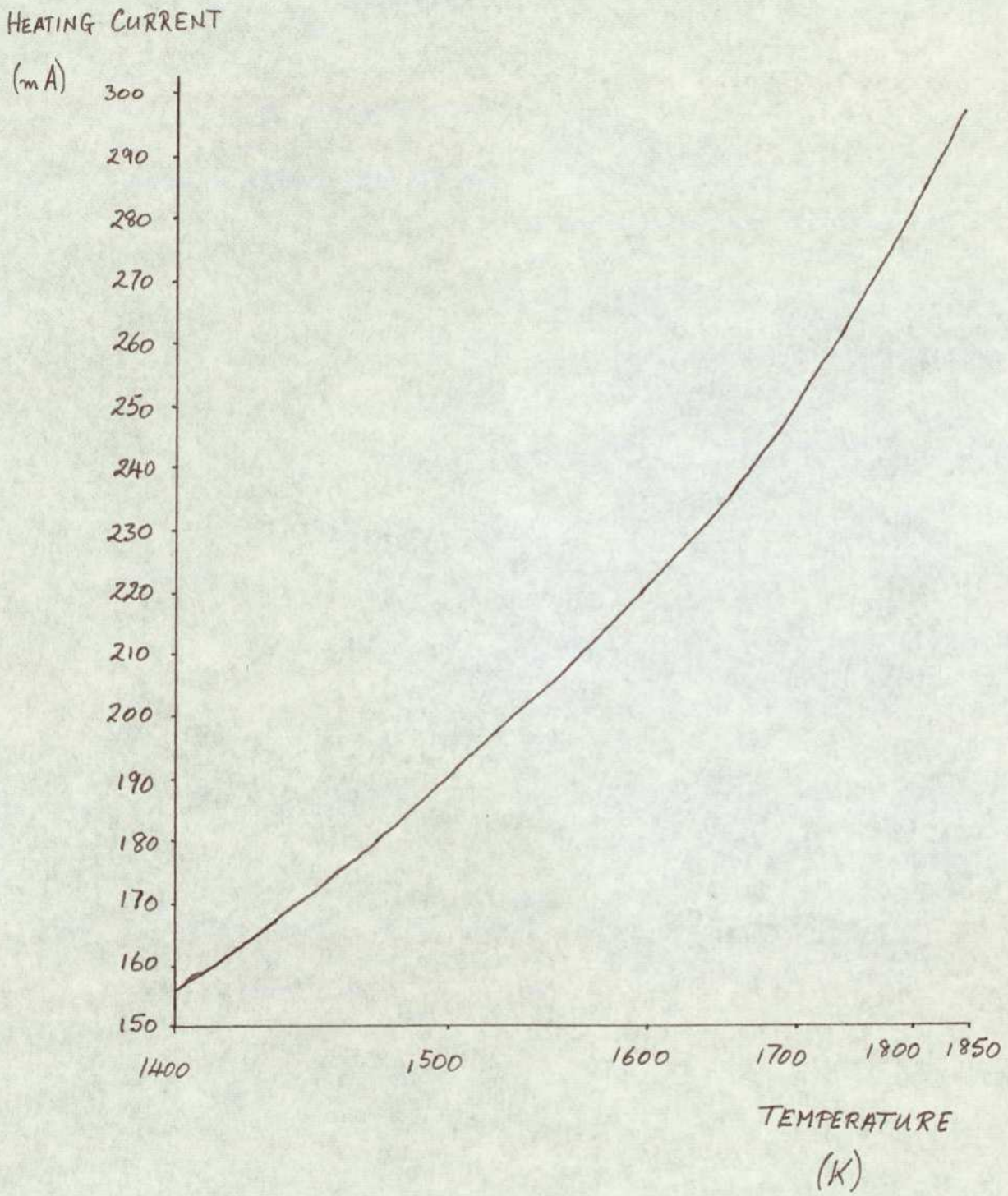

Fig.3.9. Heating current versus temperature

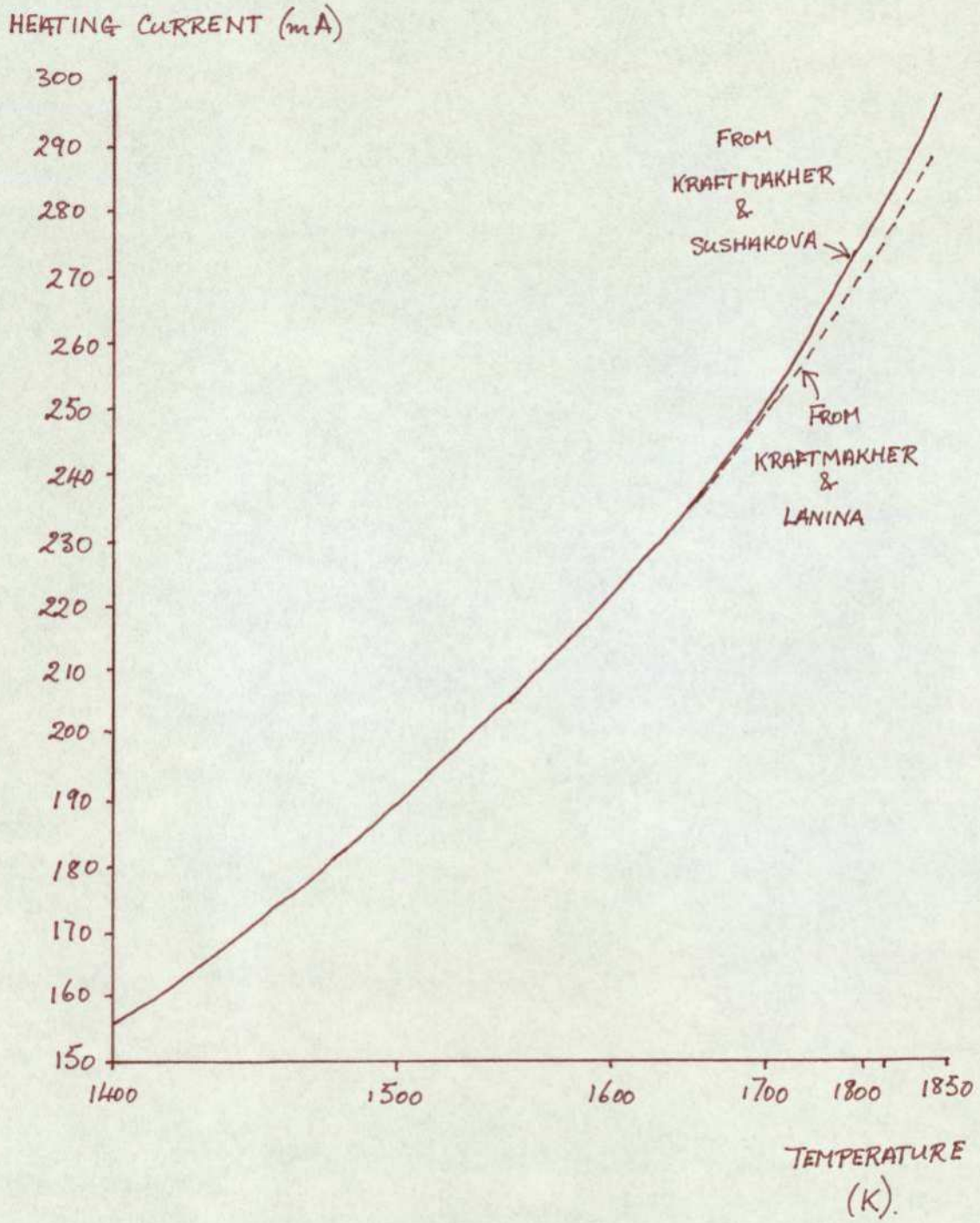

Fig.3.10. Heating current versus temperature from Kraftmakher & Sushakova and Kraftmakher & Lanina

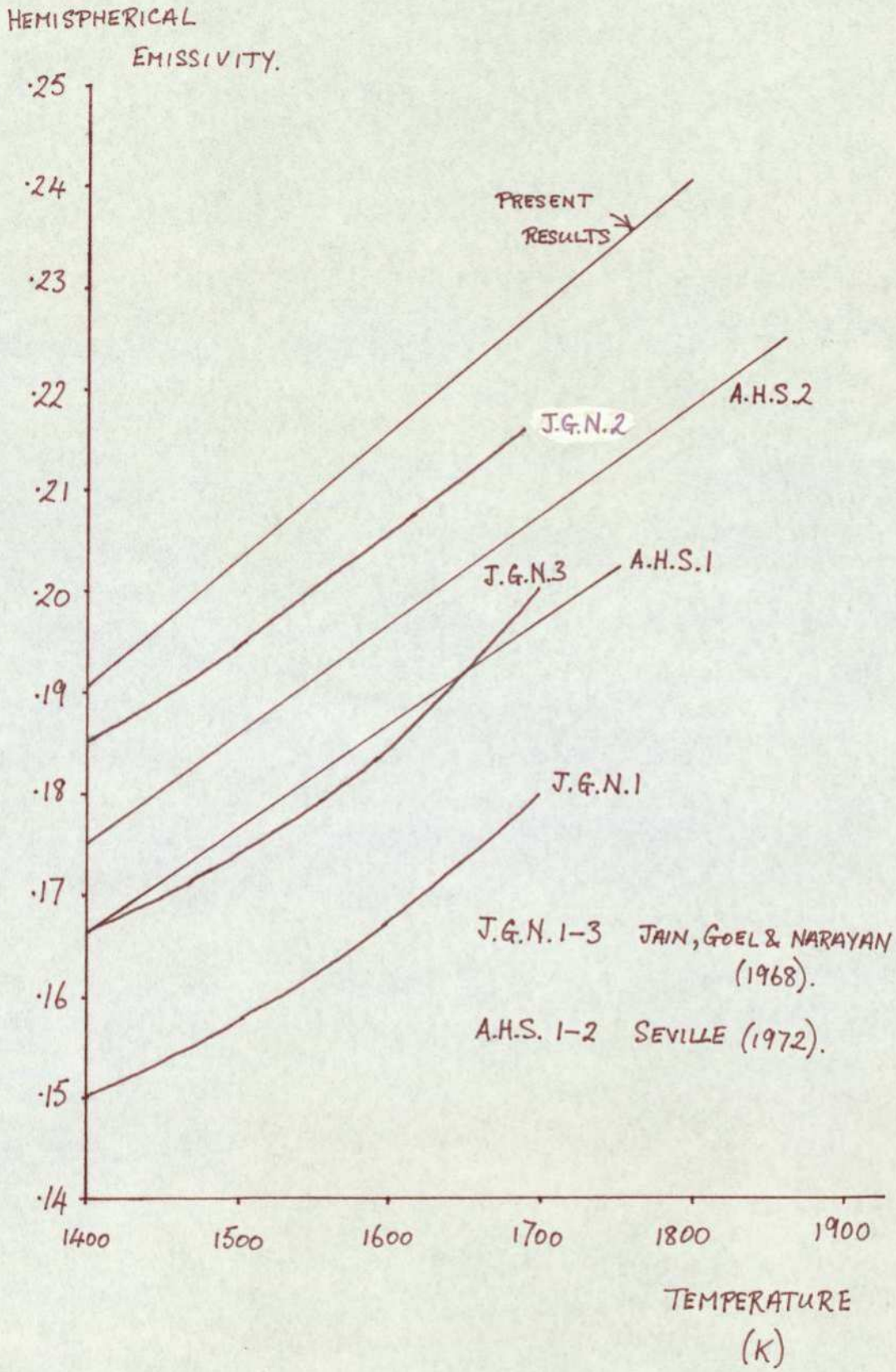

Fig.3.11. Comparison of emissivity results from various workers

the 20% variation in emissivities quoted by Jain, Goel and Narayan (1968).

3.7. Summary

The resistance ratio as a function of heating current was determined and used in conjunction with published results of the resistance ratio as a function of temperature to give a calibration curve of heating current against temperature. The present results were compared with those of other workers and shown to be consistent.

4. INSTRUMENTATION AND PROCEDURE

4.1. Introduction

In measuring the temperature coefficient of resistivity an equivalent impedance technique was primarily considered because a null method could be applied to its measurement and also because phase sensitive detection equipment allowed the accurate measurement of a capacitative voltage in the presence of a much larger (1000:1) resistive voltage. The equations that permit the calculation of the temperature coefficient of resistivity are, for a.c. heating only, equation 2.20 and, for a.c. superimposed on d.c., equation 2.44. Both methods were attempted but due to the larger error in the assumed 90^{o} phase difference between the temperature fluctuations and the heating current for the a.c. superimposed on d.c. method (see section 2.3.1.) the a.c. heating only method was chosen.

The measurement of the third harmonic voltage generated during a.c. heating only was attempted but was not successful due to the reasons given in section 2.4.4. The corresponding measurement for a.c. superimposed on d.c. was not attempted because the equation relating the temperature coefficient of resistivity (α/r_e) to the third harmonic voltage is a quadratic in α/r_e (see equation 2.49) and thus awkward to use. In addition, the third harmonic voltage generated under these conditions is also considerably smaller than that generated during

a.c. only heating.

4.2. Common Instrumentation

4.2.1. Individual instruments

All the experiments mentioned in section 4.1. used the same general circuit diagram which is shown in Fig.4.1. As is mentioned below in sections 4.3. and 4.4., the a.c. only experiments (equivalent impedance and third harmonic voltage) required the use of a filter and potential divider, unlike the a.c. superimposed on d.c. heating experiment. For this reason these instruments are shown cross-hatched in Fig.4.1. The vacuum chamber arrangement is as shown in Fig.3.3. and the connections to the bridge are by means of two B.N.C. sockets (one for each wire) fixed in the die-cast aluminium box, the leads to the test wires were passed through the brass base plate. As before, the pressure in the chamber was $< .02$ Torr.

As shown in Fig.4.1., provision was made to allow a resistance/capacitance parallel circuit to be switched into the bridge instead of the test wire. This allowed ease of calibration. The resistance part of the parallel circuit was in turn made up of a parallel circuit of two resistance boxes. The four resistances boxes used were each Sullivan dual dial non-reactive 0.05% grade resistance boxes and the two capacitances were Muirhead three decade capacitance boxes having a range from 1nF to 1μF. The ratio resistors were 5Ω non-reactive type made by Alma

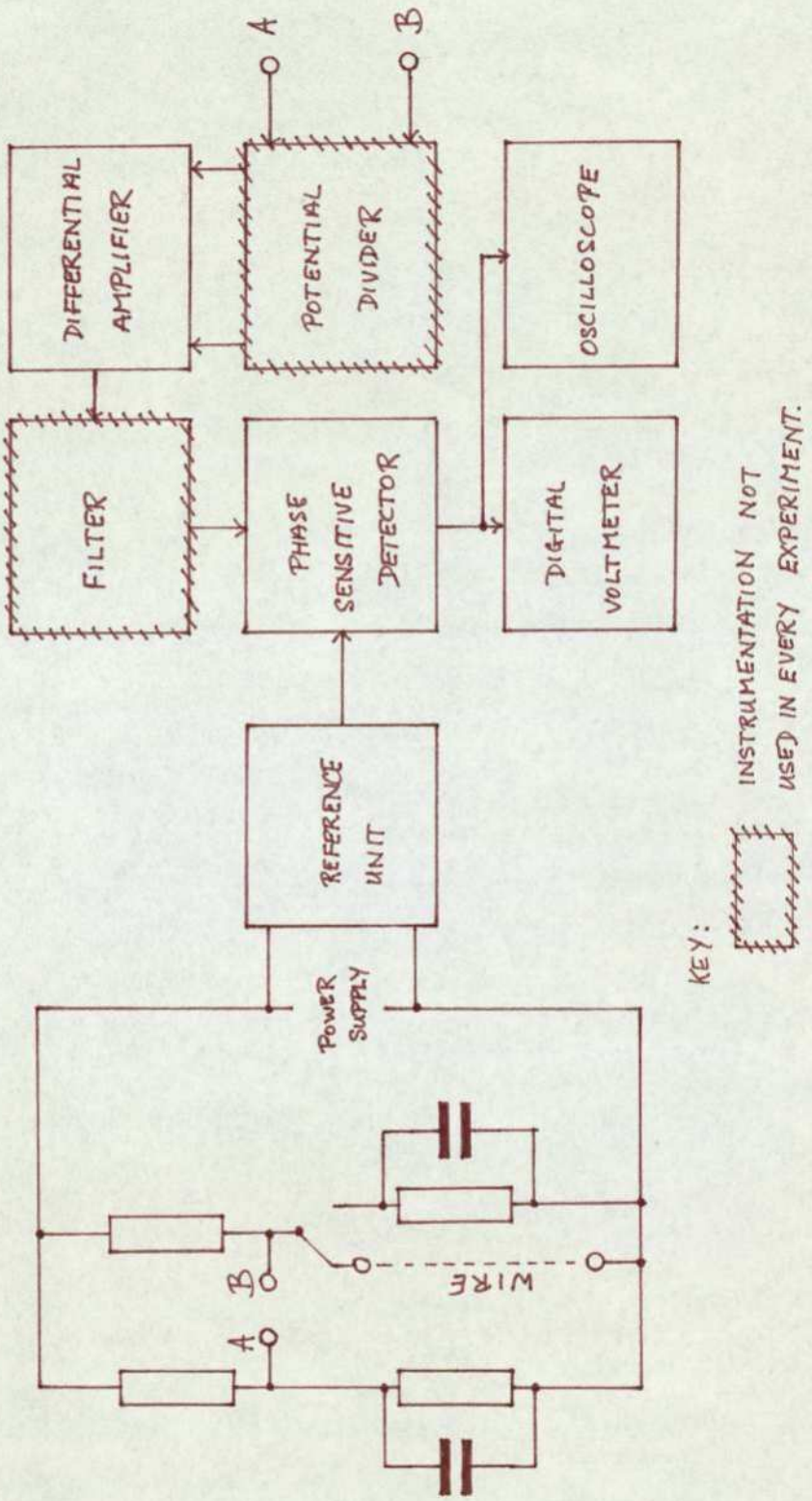

Fig.4.1. Basic diagram of experiments

Components and were in an aluminium die-cast box for shielding. As before the current sensing resistor was a Tinsley 1-AC-DC standard resistor.

The output from the bridge formed, directly or indirectly, see sections 4.3. and 4.4., the input to a Brookdeal differential a.c. amplifier 9454. The differential amplifier was always used on a gain setting of 70dB and at this setting the rejection ratio was 100dB, sufficient for the purposes of the experiment (see subsection 4.2.3.).

The differential amplifier output formed, again directly or indirectly, sections 4.3. and 4.4., the input to a Brookdeal phase sensitive detector 411 which gave a maximum output voltage of 10 Vd.c. for 1 Vr.m.s. input and rejected non reference frequency signals by 80 dB except odd harmonics : third harmonics being reduced by $\frac{2}{3}$, fifth harmonics by $^4/_5$ etc. Used in conjunction with the phase sensitive detector was a Brookdeal reference unit 9422 that provided two reference square waves in quadrature.

This set-up resulted in, during calibration, the capacitance set on one side of the bridge being measured on the other over the current, frequency and resistance ranges of interest. The calibration results are shown in subsection 4.2.5.

The output from the phase sensitive detector was connected to a Tektronix Type 545B oscilloscope with

a Type 1A1 dual-trace plug-in unit and used to obtain rough balance of the bridge, particularly the resistive component. For detailed measurements a Dynamco digital voltmeter Type DM2022S was used. This instrument also had two plug-in units : RMS detector module B1 and LF amplifier module A1, these were used in conjunction with the DM2022S to allow the measurement of a.c. signals, in particular the voltage across the current sensing standard resistor.

D.c. and a.c. voltages measured by means of the DM2022S were accurate to better than $\pm$0.1%. In addition, the r.m.s. mode of measurement of the a.c. voltage ensured that any harmonic voltages were reduced to negligible proportions.

The frequency of the a.c. generator was measured by a SM200 Mk 3 Timer Counter accurate to $\pm$0.1Hz.

The voltage generation circuit varies for the a.c. only and the d.c. with superimposed a.c. methods, however in each case the same a.c. generator was used : a NF low distortion function oscillator Model E-1011. The stated distortion was 0.1% over the frequency range of interest (40Hz-200Hz).

4.2.2. Shielding and earthing.

The 5Ω bridge ratio resistors were mounted in an earthed aluminium die-cast box for shielding and all leads in the bridge were of coaxial cable. The

coaxial cable shield was earthed at the power supply earth; it being necessary to use the shielding as a return line for the balancing arms of the bridge. The calibration results of subsections 4.2.6. and 5.3.1. are attributed to the use of the shielding as the return line, however, since the results were reproducible it was considered satisfactory.

4.2.3. Reference unit phase setting

In each case the basis of the experimental procedure is the compensation of the capacitative fundamental voltage in the presence of a resistive fundamental voltage which is typically 70dB greater for a.c. only and 45dB for a.c. with d.c.

In general it was possible to balance the resistive voltages from each side of the bridge to 1 part in 1000 and the use of the differential amplifier with a rejection of 100dB allowed the resistive signal to be reduced to the same order as the capacitative. The capacitative voltage was then measured by means of the phase sensitive detector/reference unit combination to an accuracy dependent upon the phase setting of the reference unit.

The phase setting of the reference unit was performed as follows : a signal directly from the voltage source was applied to the measurement system immediately after the differential amplifier of such an amplitude that the overload neon of the phase sensitive

detector just started to glow. This ensured that the phase sensitive detector output was at a maximum of ~10V, then the phase of the reference unit was adjusted until an output on the capacitative channel was as close to zero as possible. The two quadrature outputs of the reference unit facilitated checking the resistive and capacitative channels.

The accuracy of the zero obtained by the method described above was determined by the need to obtain capacitative voltages to an accuracy of 1% in the presence of a resistive voltage of the same order of magnitude. This accuracy varied between a.c. only and a.c. superimposed on d.c. methods and it also depends upon the frequency of the a.c. component and the mean temperature.

Consider first the a.c. only : from equation 2.13. the ratio of the resistive and capacitative voltages is given by

$$1 \; : \; \frac{\beta \theta_2}{2} \qquad 4.1.$$

Substituting for θ_2 using equations 2.7., 2.8. and 2.11., the ratio becomes

$$1 \; : \; \frac{i^2 \alpha R_M}{8 m w c_p r_e} \qquad 4.2.$$

where $\alpha = r_e \beta$.

Below is given a table of typical values at extremes of the temperature range of interest.

Table 4.1.

Temperature (K).	i(A).	$\alpha(K^{-1})$.	$R_M(\Omega)$.	$c_p(Jkg^{-1}K^{-1})$	r_e	Ratio
1400	.28	$2.7x10^{-3}$	15	165	4.7	~1:$8x10^{-4}$
1800	.39	$2.5x10^{-3}$	20	180	5.7	~1:$1.6x10^{-3}$

m = 3mg and w = 240 $rads^{-1}$

As can be seen from equation 4.2. the ratio is dependent upon the inverse of the modulating frequency.

It was mentioned above that resistance voltages from each side of the bridge were balanced to 1 part in 1000, therefore the ratio at 1400K and 1800K at the differential amplifier output will be 1:.8 and 1:1.6 respectively. To ensure 1% accuracy, the phase setting of the reference unit must be such that the resistive signal at w = 240 $rads^{-1}$ (~40Hz) is reduced by 125 at 1400K and 62 at 1800K. At w = 1200 $rads^{-1}$ (~200 Hz) the reduction must be by 675 and 338 respectively.

Therefore, when setting the phase of the reference unit by the method described above, if the phase sensitive detector output is 10V, then the phase must be set to such a value that the capacitative voltage (at w = 240 $rads^{-1}$) must be 0 ± 80mV at 1400K and 0 ± 160mV at 1800K. At w = 1200 $rads^{-1}$ capacitative voltages must be 0 ± 16mV and 0 ± 32mV.

Fig.4.2. shows the maximum permissible error in the zero capacitative voltage to ensure 1% accuracy in the experimental capacitative voltage measurement.

The same analysis leads to a corresponding graph for the a.c. superimposed on d.c. method.

The ratio of the resistive and capacitative voltages can be found from equation 2.39, giving

$$1 \; : \; \frac{i_o \beta \theta_1}{i_1} \qquad 4.3.$$

Neglecting the second term in the capacitative voltage term resulting in an error of 0.4%.

Substituting for θ_1 from equation 2.31 gives

$$1 \; : \; \frac{2 i_o^2 \alpha R_M}{w m c_p r_e} \qquad 4.4.$$

Typically $i_1 \sim \frac{1}{3} i_o$ and so $i^2 \approx i_o^2$, i.e. the heating effect of the superimposed a.c. voltage can be neglected to a first approximation. Therefore the ratio of the capacitative voltages using the a.c. only and the a.c.superimposed on d.c. methods can be found from equations 4.2. and 4.4. to be 1:16.

Fig.4.3. shows the maximum permissible error in the zero capacitative voltage for the a.c. superimposed on d.c. method.

In practice, for both methods it was found that the best zero it was possible to obtain when

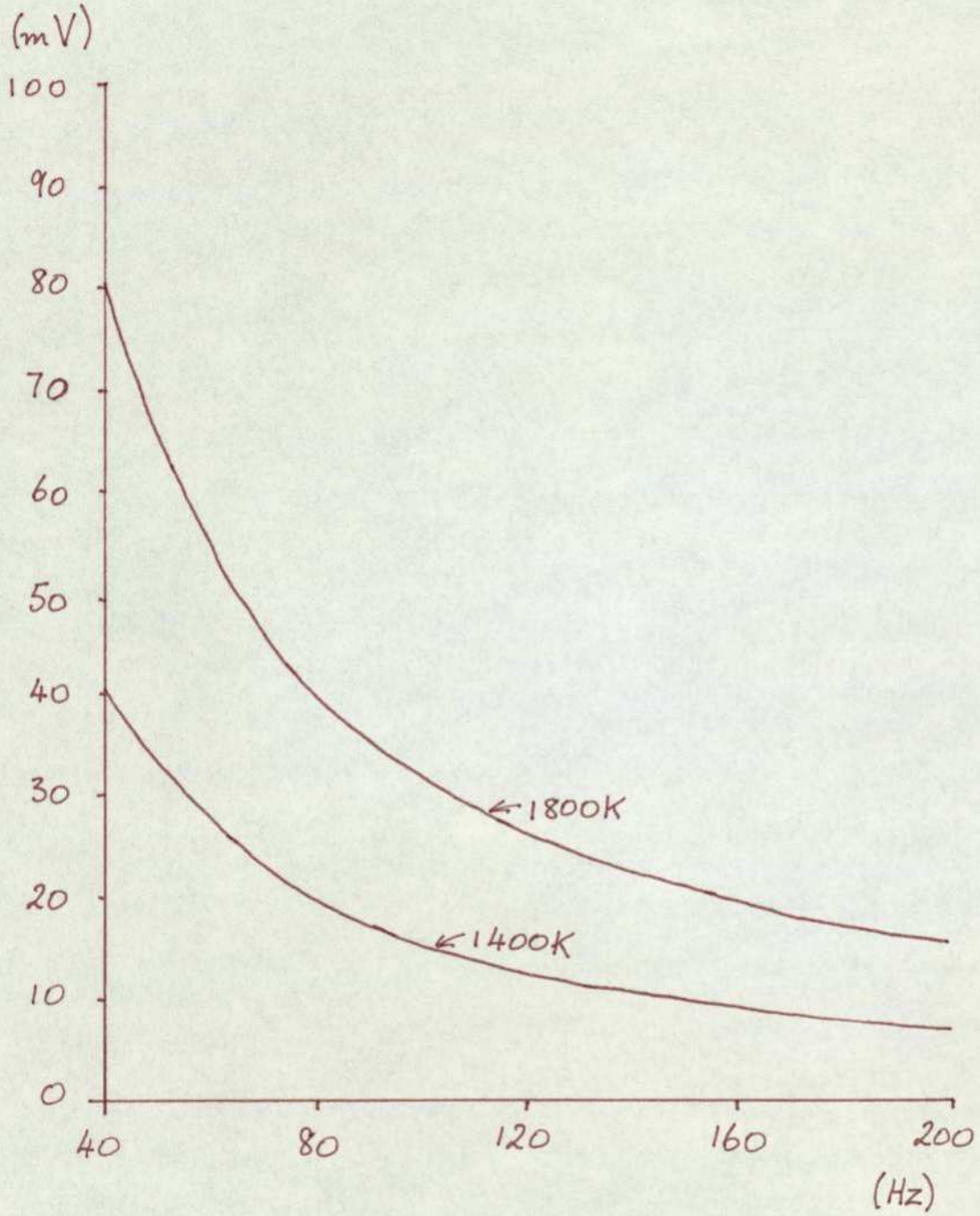

Fig.4.2. Inaccuracy in zeroing capacitative voltage to ensure 1% accuracy of experimental measurement (a.c. only method).

setting the phase of the reference unit was $\pm$20mV. This imposes a limit on the accuracy to which results can be taken at higher frequencies when using the a.c. heating only method.

4.2.4. Phase sensitive detector input requirements.

The effect of out of phase signals referred to full scale output (10V) is 0.01%. Therefore the problem arose that if the capacitative signal input to the phase sensitive detector was too small, the imperfect noise rejection polluted the capacitative channel causing an error in the measured capacitance.

It was found that below a differential amplifier gain of 60 or 70dB there was a discrepancy between the values of the capacitance on each side of the bridge. A graph of capacitance discrepancy against differential amplifier gain is shown in Fig.4.4.

It was decided to use a differential amplifier gain of 70dB to remove the capacitance discrepancy.

4.2.5. Procedure for balancing the capacitative signal.

In each experimental technique, be it equivalent impedance or third harmonic voltage measurement, it was necessary to balance out the capacitative signal, either to measure it or to measure the smaller third harmonic signal.

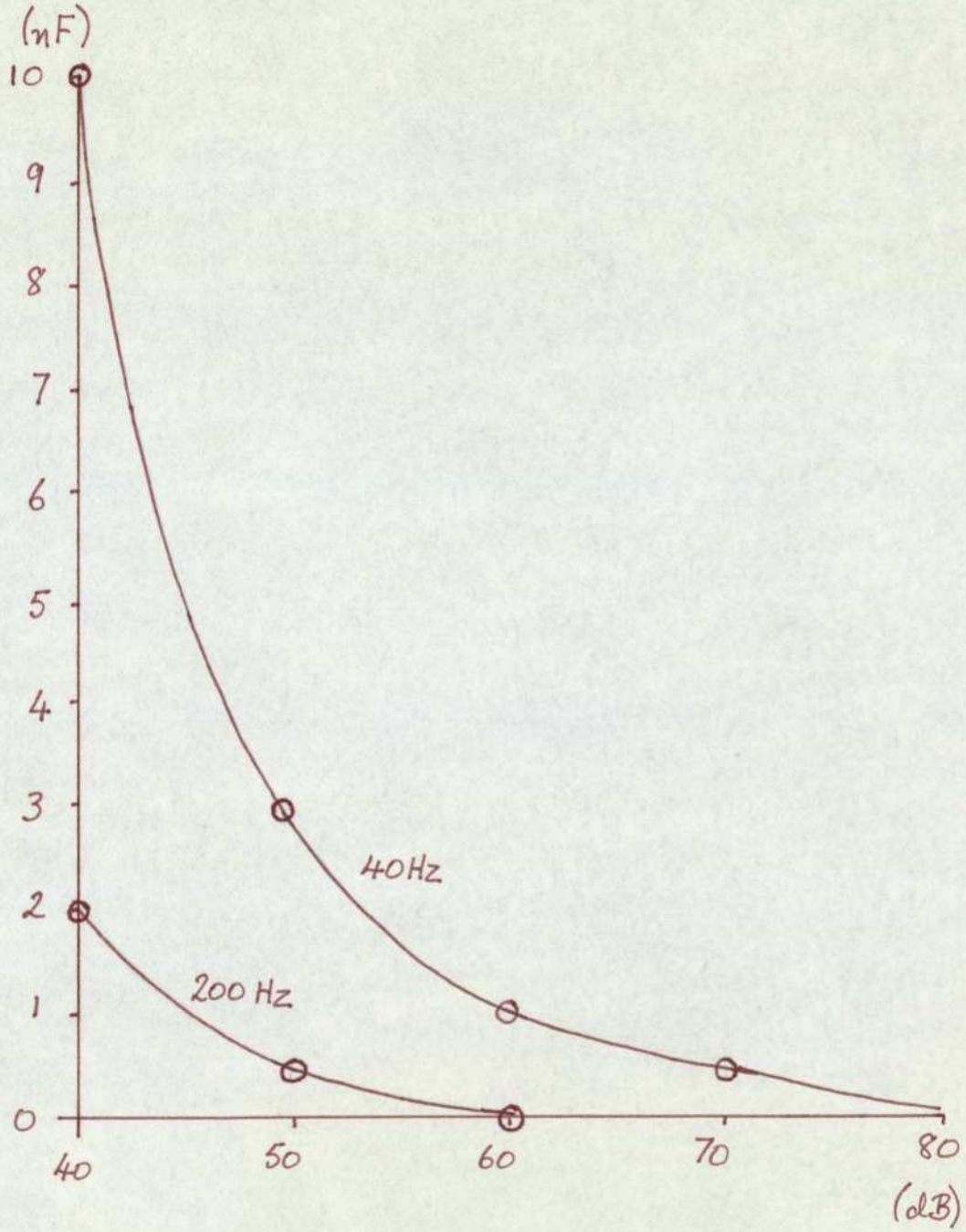

Fig.4.4. Capacitance discrepancy v. differential amplifier gain setting.

Before each experiment all the items of equipment were left to warm up for about half an hour. Then the measurement instruments were checked, and where necessary zeroed, in the following order : digital voltmeter, phase sensitive detector (zero output for zero input $\pm$2mV) and differential amplifier (zero output for the same voltage applied to each input over the range 0V to 3Vpeak-peak $\pm$40mV at a gain of 70dB). The phase of the reference unit was set as described in subsection 4.2.3.

For equivalent impedance measurements the capacitative voltage was recorded as the balancing capacitance was increased. This gave a series of results which when plotted as a graph of capacitance against capacitative voltage gave a straight line graph and allowed the effective capacitance of the wire to be read off at the point where the line intersected the capacitance axis. This method increased the accuracy to which the capacitance could be measured, especially for long wires at high frequencies and low temperatures where the capacitance to be measured was $\sim$5nF and the smallest increment on the capacitance box was 1nF. A typical example of the graphs obtained is shown in Fig.4.5.

An attempt was made to measure the third harmonic voltage using the a.c. only method. At first a balance of the capacitative voltage was performed using the oscilloscope, the digital voltmeter reading being attributed to one third of the third harmonic voltage (the phase sensitive detector rejecting two thirds - see subsection 4.2.1.). This was found to be

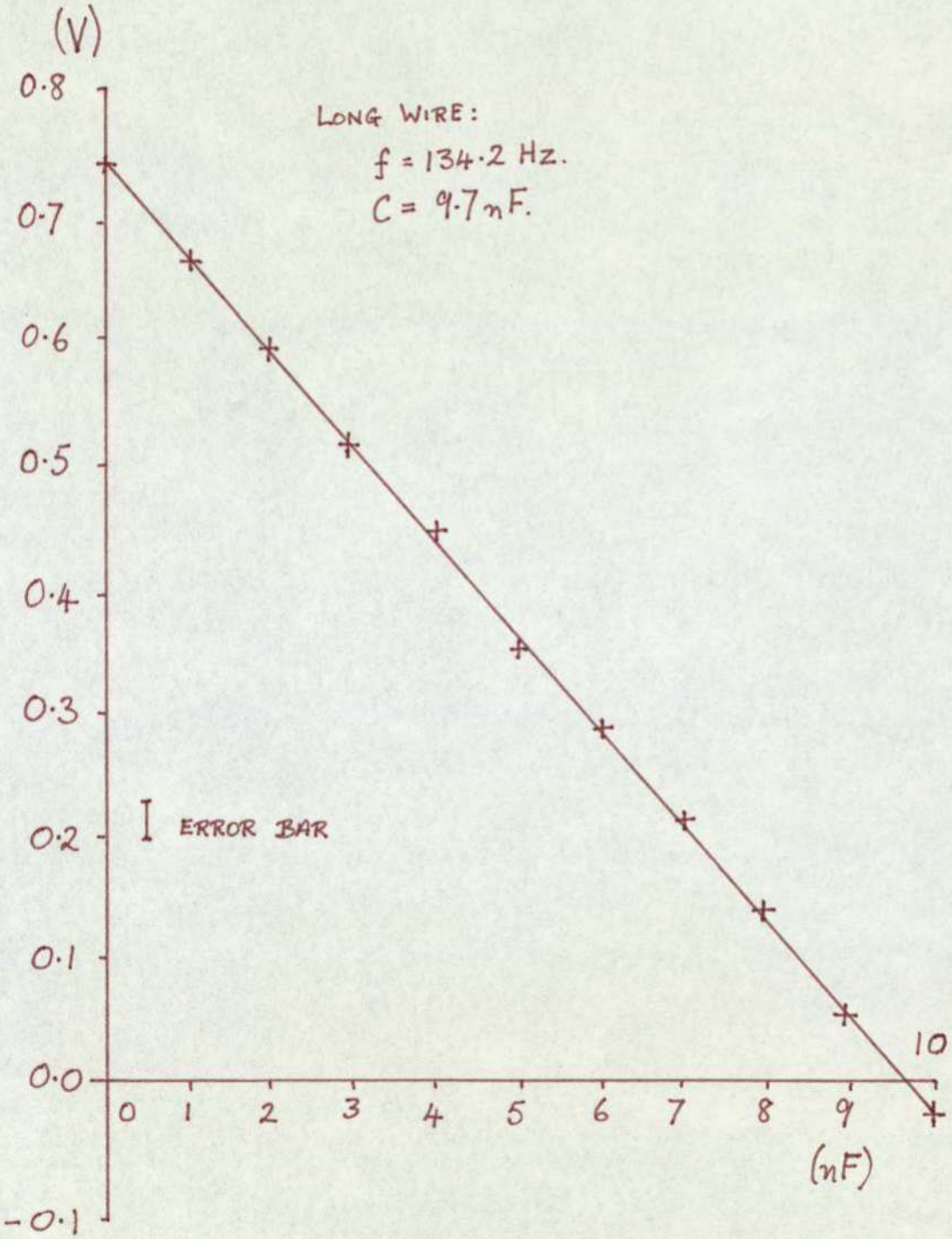

Fig.4.5. Typical voltage v. capacitance graph

too inaccurate and a filter was used to remove the fundamental capacitative voltage that remained after the partial balance using the oscilloscope.

4.2.6. Calibration of the Experiment

This was done by setting a capacitance and resistance combination on one side of the bridge and measuring it using the capacitance/resistance network on the other side. This was done for a number of capacitance and resistance values and also for a variety of frequency and current values. The result was a variation of capacitance discrepancy between the two sides of the bridge as a function resistance mainly but also, to a lesser extent, frequency. This discrepancy is attributed to the use of the shielding as the return line as mentioned in subsection 4.2.2.

The calibration results are presented in subsection 5.3.1.

4.3. d.c. with superimposed a.c. method

The primary d.c. heating current was provided by a Solartron P.S.U. A.S.1412 used in its constant voltage mode and this was modulated by the low distortion oscillator mentioned in subsection 4.2.1. The d.c. and a.c. were mixed using a circuit designed to allow the superposition of the a.c. on the d.c. without the a.c. signal affecting the constant voltage source. The circuit diagram is shown in Fig.4.6.

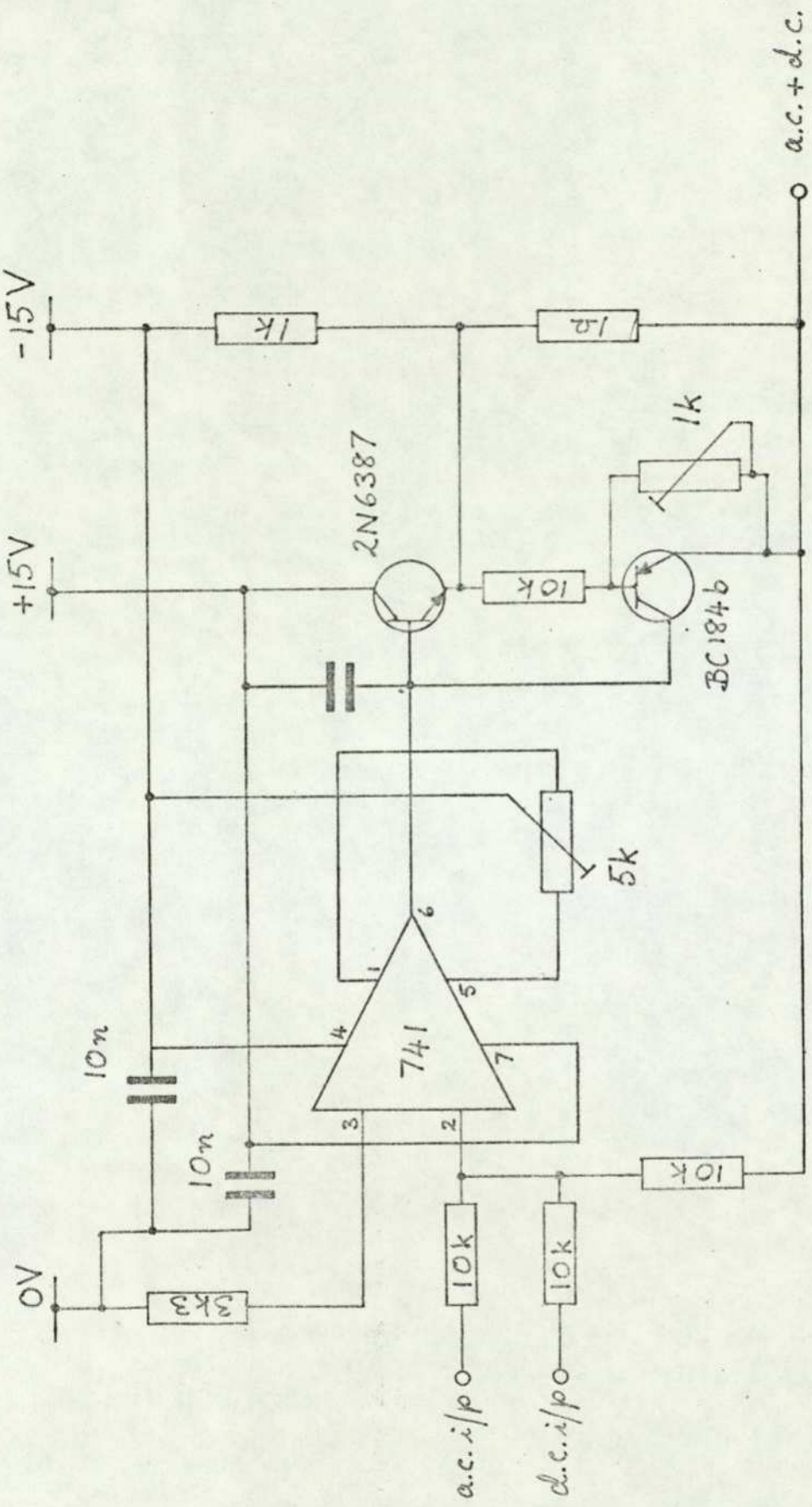

Fig.4.6. Circuit diagram of the a.c. + d.c. summing power amplifier.

The differential amplifier was a.c. coupled, consequently the d.c. heating voltage did not cause an overload (overload at 3Vpeak-peak).

4.3.1. Equivalent impedance method.

The5 The measurements were attempted using the instrumentation and method described above.

From subsection 4.2.3. the ratio of resistive to capacitative voltages is in the range 1 : $1.2\text{x}10^{-2}$ tp 1 : $2\text{x}10^{-2}$ at w = 240 rads^{-1} and five times smaller at w = 1200 rads^{-1}. As was mentioned in subsection 4.2.3. it is possible to set the phase of the reference unit to the required accuracy to measure these relatively large capacitative voltages. However, the inaccuracy of the heating current/temperature quadrature phase relationship made impossible the reproduction of accepted temperature coefficient of resistivity values.

4.3.2. Third harmonic method

This was not attempted, firstly because of the smallness of the third harmonic voltage compared with the fundamental capacitative voltage as can be seen by comparing the relevant terms in equation 2.49. The ratio of the fundamental to third harmonic voltage terms is given below

$$(i_o R_M \theta_1 + \tfrac{1}{2} i_1 R_M \theta_2) : \tfrac{1}{2} i_1 R_M \theta_2 \qquad 4.5.$$

As mentioned above the second term of the fundamental voltage can be neglected. Equation 4.5. then becomes

$$2i_o\theta_1 : i_1\theta_2 \qquad 4.6.$$

Substituting for θ_1 and θ_2 from equations 2.31. and 2.36. respectively (N.B. the second term of equation 2.36. is neglected increasing θ_2 by ~10% at low frequencies).

$$8i_o : i_1 \qquad 4.7.$$

Typically $i_1 \sim \frac{1}{3}i_o$ and so the ratio becomes 24 : 1 which is worsened by the partial rejection of the phase sensitive detector to 72 : 1.

This, in conjunction with the fact that the equation relating the third harmonic voltage to the temperature coefficient of resistivity (equation 2.49) is cumbersome to use, led to the decision not to perform third harmonic voltage measurements with the d.c. superimposed with a.c. method.

4.4. a.c. only method.

The primary heating and modulation current was provided by a single a.c. voltage source. This consisted of the low distortion oscillator and a Class A a.f. amplifier built especially for the purpose, the circuit diagram is shown in Fig.4.7. The larger a.c. heating voltages (up to ~15Vpeak-peak) used necessitated protection for the differential amplifier. This took the form of a voltage divider network made up of two Muirhead D-943-C resistance ratio boxes. The resistance ratios were accurate to better than 0.05% of the ratio set on the box and the resistance ratio selected was 3:1. A total resistance of 4KΩ was chosen because the

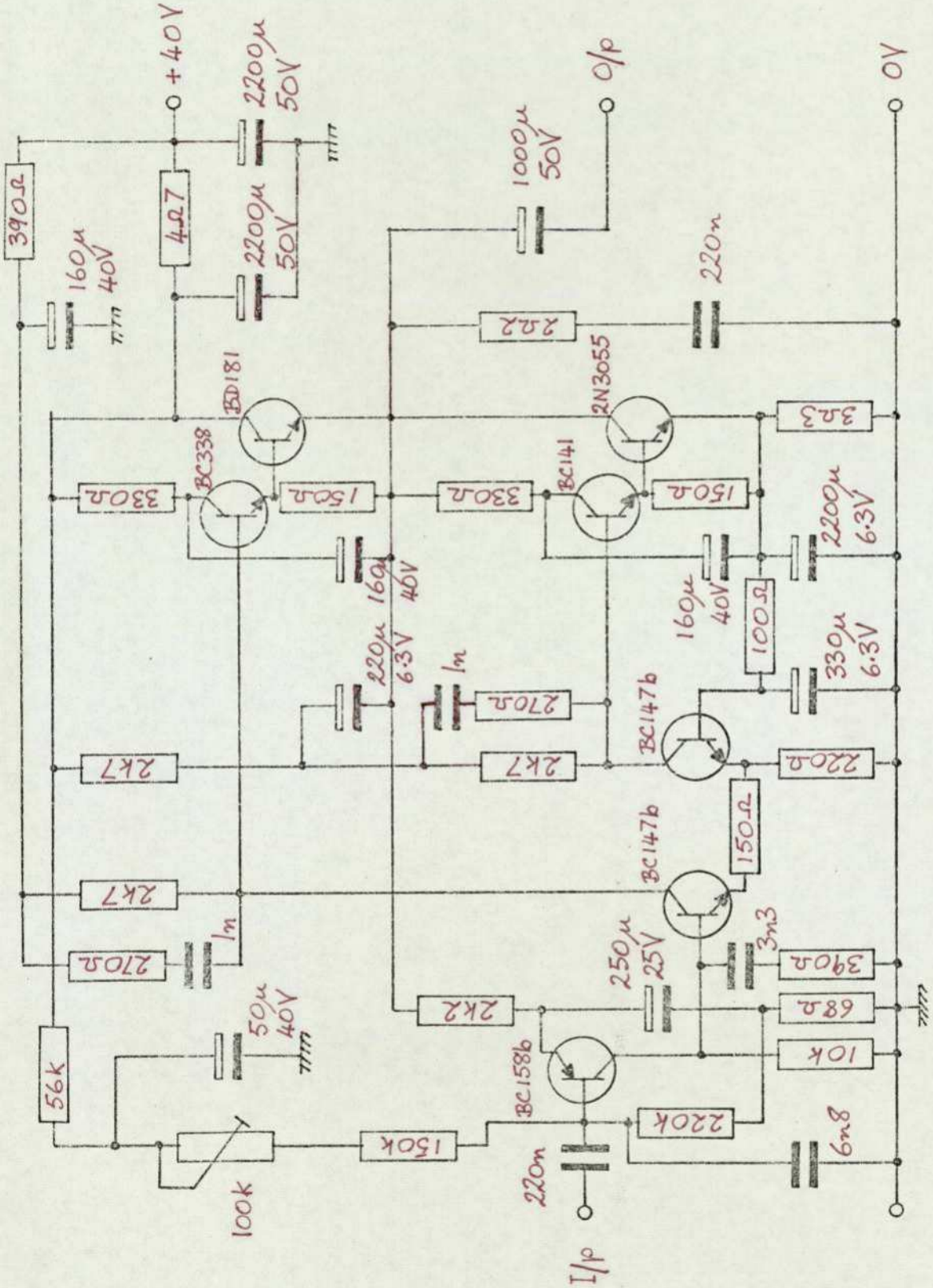

Fig.4.7. Circuit diagram of the Class A, audio frequency power amplifier.

measurement arms of the bridge were typically ~ 20Ω and so the resistance ratio shunted ~1% of the heating current causing a negligible error in measuring the current. Fig. 4.8. is a general view of the set-up, Fig.4.9. showing the measurement circuitry in more detail.

As was mentioned in subsection 4.2.3. it was possible to balance the resistive voltages to 1 part in 1000 and also to set the phase of the reference unit such that this caused ~1% error in the capacitance measurement. Therefore a maximum discrepancy of 0.1% in the resistance ratio causes a maximum resistive voltage discrepancy of the order of that due to imperfect balancing of the bridge. In practice the discrepancy due to the unequal resistance ratios was ~0.02% thereby reducing the error to negligible proportions except at high frequencies when the phase setting of the reference unit is not sufficient to ensure a 1% accuracy measurement of the capacitative voltage (see subsection 4.2.3). This has the effect of reducing the maximum frequency of the a.c. only method but as shall be shown in subsection 4.4.1. there is a more important factor reducing the maximum practical frequency.

As was noted in Chapter 2, and can be seen from equation 2.13., the capacitative fundamental and third harmonic voltages are the same size, the phase sensitive detector rejecting only two thirds of the third harmonic voltage. That this causes erroneous results has been explained elsewhere (subsection 2.4.4.) and is elaborated upon below. The simple solution of using

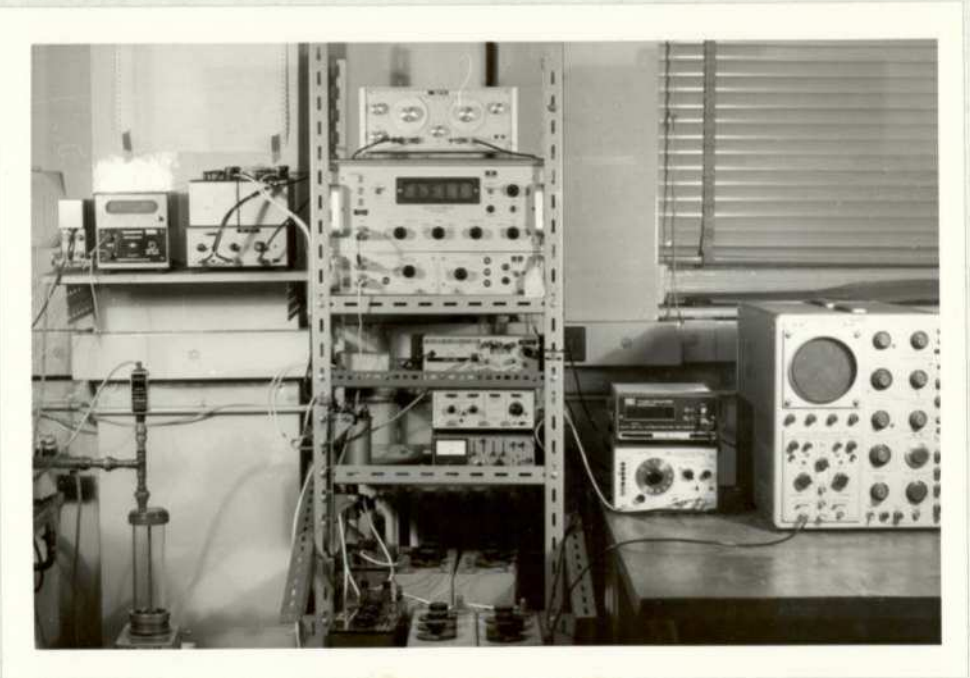

Fig.4.8. General view of the experimental arrangement for a.c. only measurements

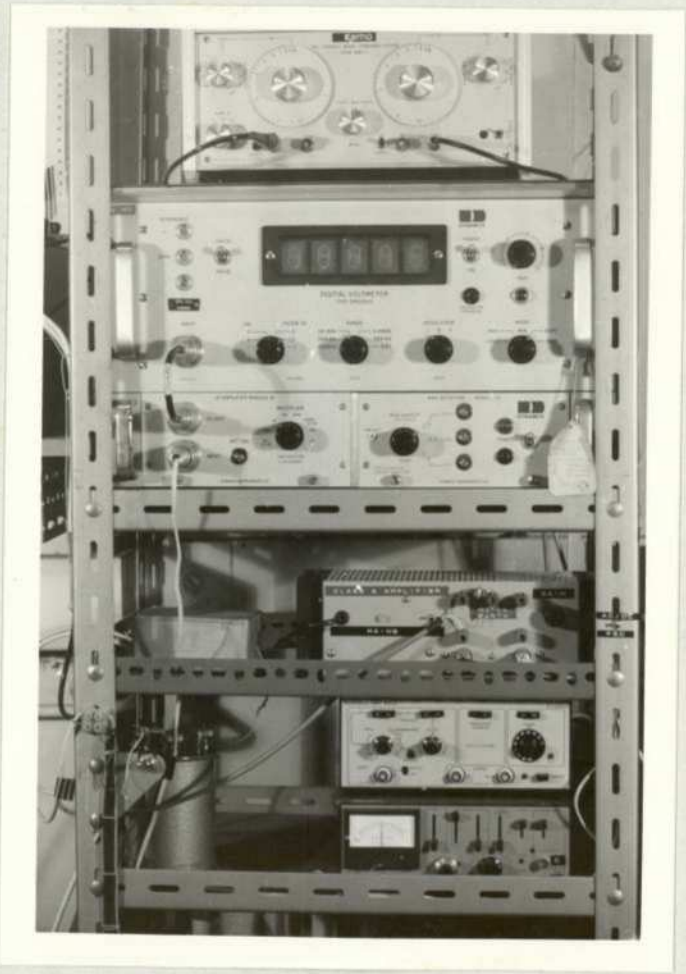

Fig.4.9. Detailed view of the measurement circuitry.

a filter to remove the third harmonic voltage during the equivalent impedance method and to remove the fundamental voltage during the third harmonic method was employed. The filter was a Kemo 1Hz-1kHz dual variable filter Type VBF/1 with attenuation of 48dB/octave outside the selected frequency range.

4.4.1. Equivalent impedance method

As mentioned above, a voltage divider network was necessary to avoid overloading the differential amplifier. It was discovered that there was a phase shift of ~1% across each resistance ratio box. At high frequencies especially it was necessary to correct the phase setting of the reference unit to allow for this extra phase shift. This could only be done to a limited accuracy for the following reasons : the maximum common-mode voltage that can be applied to the differential amplifier is ~1 Vrms therefore this is the maximum voltage from the resistance ratio boxes. However, there is an error in the resistance ratios of ~0.02% so a signal of ~0.2 mVrms is amplified by 70dB by the differential amplifier and the digital voltmeter reading is ~6V. Therefore the reference unit phase must be corrected using a maximum resistive voltage of only 6V instead of the usual 10V (see subsection 4.2.3.).

In practice, as mentioned before, the best capacitative zero was $\pm$20mV. This is in conjunction

with the zero setting error of the CMRR of the differential amplifier of $\pm$40mV. Therefore if the maximum resistive (in phase) voltage is only 6V, then the phase of the reference unit can only be set to 60mV in 6V, i.e. 1%.

The result of this limitation on the accuracy of the capacitative signal measurement can be seen in the table below.

Frequency (Hz)	Temperature (K)	Signal ratio A	B	C	Capacitance accuracy.
40	1400	8×10^{-4}	0.8	80	1.2%
40	1800	16×10^{-4}	1.6	160	0.6%
200	1400	1.6×10^{-4}	0.16	16	7%
200	1800	3.2×10^{-4}	0.32	32	3%

Note : A before differential amplifier.
B after differential amplifier.
C after phase sensitive detector.

Therefore, when there was an inaccuracy in the phase setting, the results tended to be displaced to higher values of α.

Note that these inaccuracies are maximum values, but this does not preclude the possibility of a fortuitous phase setting resulting in little or no displacement.

It was therefore considered acceptable to displace the graphs obtained down towards the 40Hz values (allowing for the variation of displacements

with temperature). The maximum calculated permissible displacements were not exceeded.

Both the experimental and offset values are shown in Chapter 5.

As mentioned above, a filter was used to remove the third harmonic voltage. At first it might be considered that a filter is unnecessary and that the capacitance needed to balance the bridge could be reduced by a quarter to obtain the measurement that would result if no third harmonic voltage were present. However, when the phase sensitive detector output is zero the bridge is "balanced" with a fundamental voltage $^4/_3 V$ on one side of the bridge against a fundamental voltage V and third harmonic voltage V_3. This is not using the bridge at its most sensitive as a null detector and to deduce the "true" capacitance considerations such as those in subsection 2.4.4. must be taken into account.

When setting the phase of the reference unit, the output from the a.f. amplifier was applied to the input of the filter to allow for the phase shift through it. The phase had to be set for each frequency.

4.4.2. Third harmonic method.

The fundamental and third harmonic voltages generated across a wire sample are the same size, however the phase sensitive detector reduces the third

harmonic voltage by two thirds. Even so, the third harmonic voltage is of measurable size and the equation relating the temperature coefficient of resistivity to the third harmonic voltage (equation 2.21) is unambiguous and does not depend upon significant simplifying assumptions. The equation from which the temperature coefficient of resistivity can be found is shown below

$$V_3 = \frac{i^3 \alpha R_M^2}{8wmc_p r_e} \qquad 4.8.$$

However, as was discussed in subsection 2.4.4., the a.c. bridge circuit used to determine the equivalent capacitance was not suited to measuring the third harmonic voltage.

An attempt was, however, made to take third harmonic voltage measurements. The resistive and capacitative balance was roughly obtained by means of an oscilloscope, the filter was used to remove the fundamental voltage, only the third harmonic voltage being measured.

There was the additional problem of errors introduced by the necessity to know the differential amplifier gain, attenuation or gain of the third harmonic voltage by the filter, etc.

4.5. Summary

The instrumentation and circuitry necessary to determine the equivalent capacitance was described

for a.c. only and a.c. superimposed on d.c. heating currents. Various ways possible for measuring the temperature coefficient of resistivity were considered, these consisting of the equivalent impedance and third harmonic voltage measurements for each heating method. Due to experimental difficulties the equivalent impedance method with a.c. only heating was the technique finally chosen to determine the temperature coefficient of resistivity over a range of frequencies.

5. RESULTS

5.1. Introduction

The results obtained by measuring the third harmonic voltage generated across the wire sample and by determining the effective capacitance of an a.c. heated wire are presented in this chapter.

The measurement of the third harmonic voltage was not successful in determining the temperature coefficient of resistivity for the reasons described in Chapter 2 i.e. the bridge was not being used as a null detector.

Results were obtained for the temperature coefficient of resistivity from measurement of the effective capacitance. These results are of the same order and showed the same temperature dependence at low frequencies as those obtained by Kraftmakher and Lanina (1965) and Kraftmakher and Sushakova (1974). A decrease in the measured temperature coefficient of resistivity was found at high temperatures ($>$1600K) and high modulating frequencies ($>$100Hz). The percentage drop in the temperature coefficient of resistivity as a function of frequency and temperature is compared with theory.

Finally the sources of the errors contributing to the overall accuracy of the temperature coefficient of resistivity are considered.

5.2. Third harmonic voltage measurement

The third harmonic voltage for an a.c. only heated wire was measured using the method described in subsection 4.4.2. The voltages measured for two different wire lengths are shown in Table 5.1. It is apparent that the relationship between the third harmonic voltage developed and the length (mass) of wire agrees in general with equation 2.50 (which is shown below rearranged)

$$\frac{i^3 R_M^2}{8wc_p r_e} = {}^{m}V_3 \qquad 5.1.$$

i.e. at constant temperature and frequency

$$V_3 \propto m \qquad 5.2.$$

Therefore the ratio of the voltages for two wires heated by the same current should be independent of the size of that current. The result of this operation is shown below in the last column of Table 5.1.

Table 5.1.

Heating current (mA)	V_{3A} (mV)	V_{3B} (mV)	V_{3A}/V_{3B}
170	450	410	1.10
175	475	440	1.08
180	530	475	1.12
185	570	510	1.12
190	610	550	1.11
195	660	590	1.12
200	705	630	1.12
205	755	670	1.13
210	810	720	1.13

The quotient shows indications of an upward trend, however, the accuracy of the third harmonic voltage measurements of $\pm$5mV is not high enough to be sure of this. To check whether these third harmonic voltage measurements were valid, temperature coefficients of resistivity were calculated from them. The result is shown in Fig.5.1. As can be seen, the absolute values of the coefficient of resistivity and the actual shape of the graph are different from those previously obtained by Kraftmakher and Lanina (1965), Kraftmakher and Sushakova (1974) and later on in this chapter (subsection 5.3.3.). The difference was attributed to not using the bridge as a null detector, inaccurate knowledge of the differential amplifier gain, filter attenuation and normal experimental errors.

In view of these disappointing results, this method was not pursued further.

5.3. Equivalent impedance measurement

The effective capacitance of a.c. only heated wires was measured at a range of frequencies in the temperature range 1400K - 1850K using the method described in subsection 4.2.1.

5.3.1. Capacitance correction.

As was mentioned in subsection 4.2.6., it was necessary to correct the measured effective capacitance of the wire by an amount depending almost entirely upon the resistance of the wire. The correction necessary was found by switching out the sample and

Fig.5.1. Temperature coefficient v temperature from third harmonic voltage measurements.

balancing one resistance/capacitance parallel circuit against another. This was done for a range of frequencies, currents, resistances and capacitances and it was found that the correction necessary was a function mainly of the resistance of the wire but also very slightly of the frequency. The frequency effect was virtually negligible, ~1% of the correction capacitance, and so was neglected.

Apart from actually measuring another resistance/capacitance circuit, the procedure used to obtain the measurements was as described in Chapter 4.

The resulting correction curve is shown in Fig.5.2.

5.3.2. Capacitance results

As an example, the corrected and uncorrected capacitances are shown as a function of temperature for a frequency of 82.8Hz in Figs.5.3. and 5.4. It is clear that correction capacitances are significant at higher frequencies and low temperatures : this is because at high frequencies the effective capacitance of the wire is small and at low temperatures the wire resistance is small leading to, as can be seen from the correction curve, Fig.5.2., a larger correction capacitance.

To obtain the correction capacitance necessary, the resistance balance was recorded whenever a capacitance measurement was made. The error

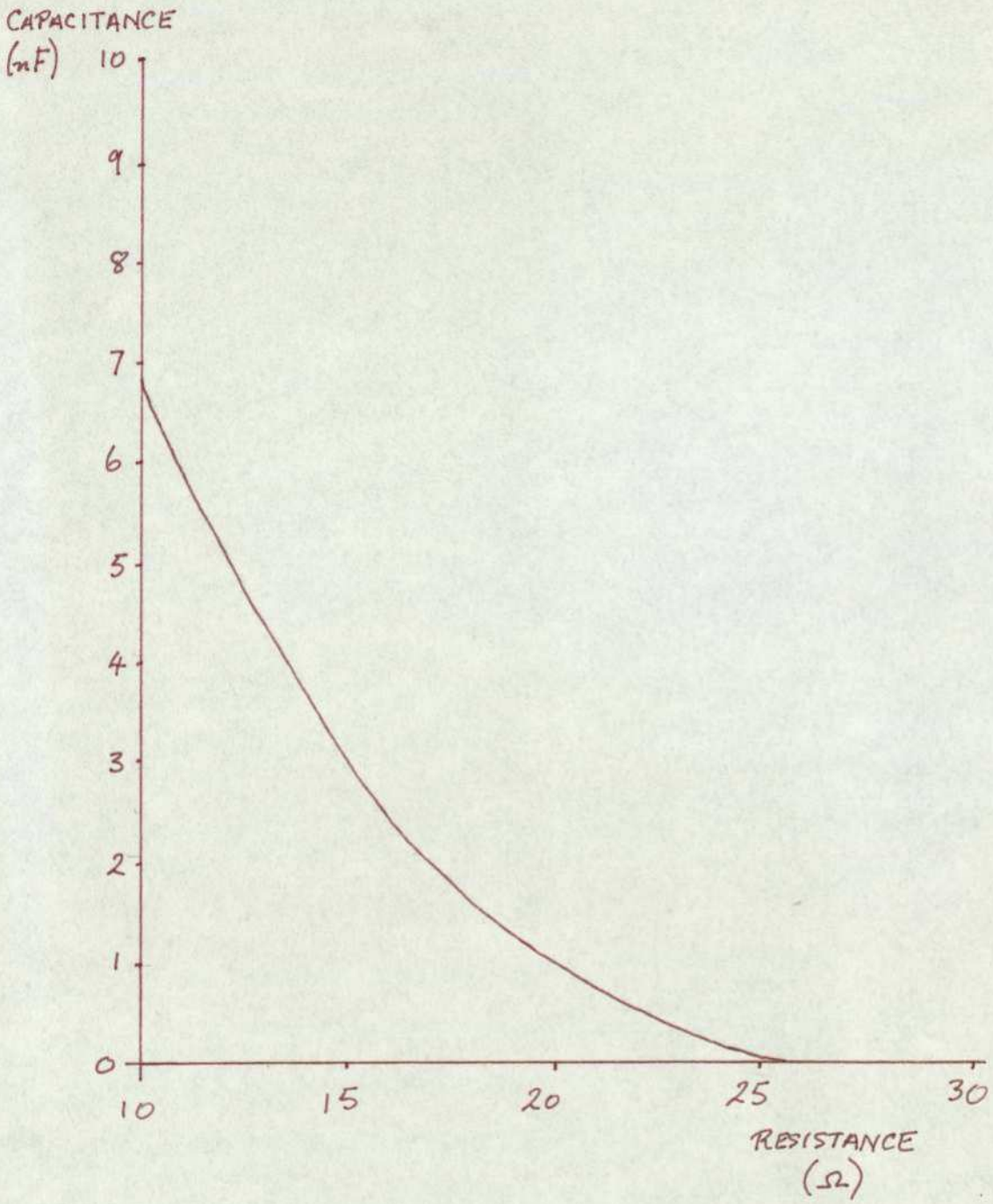

Fig.5.2. Correction capacitance as a function of wire resistance

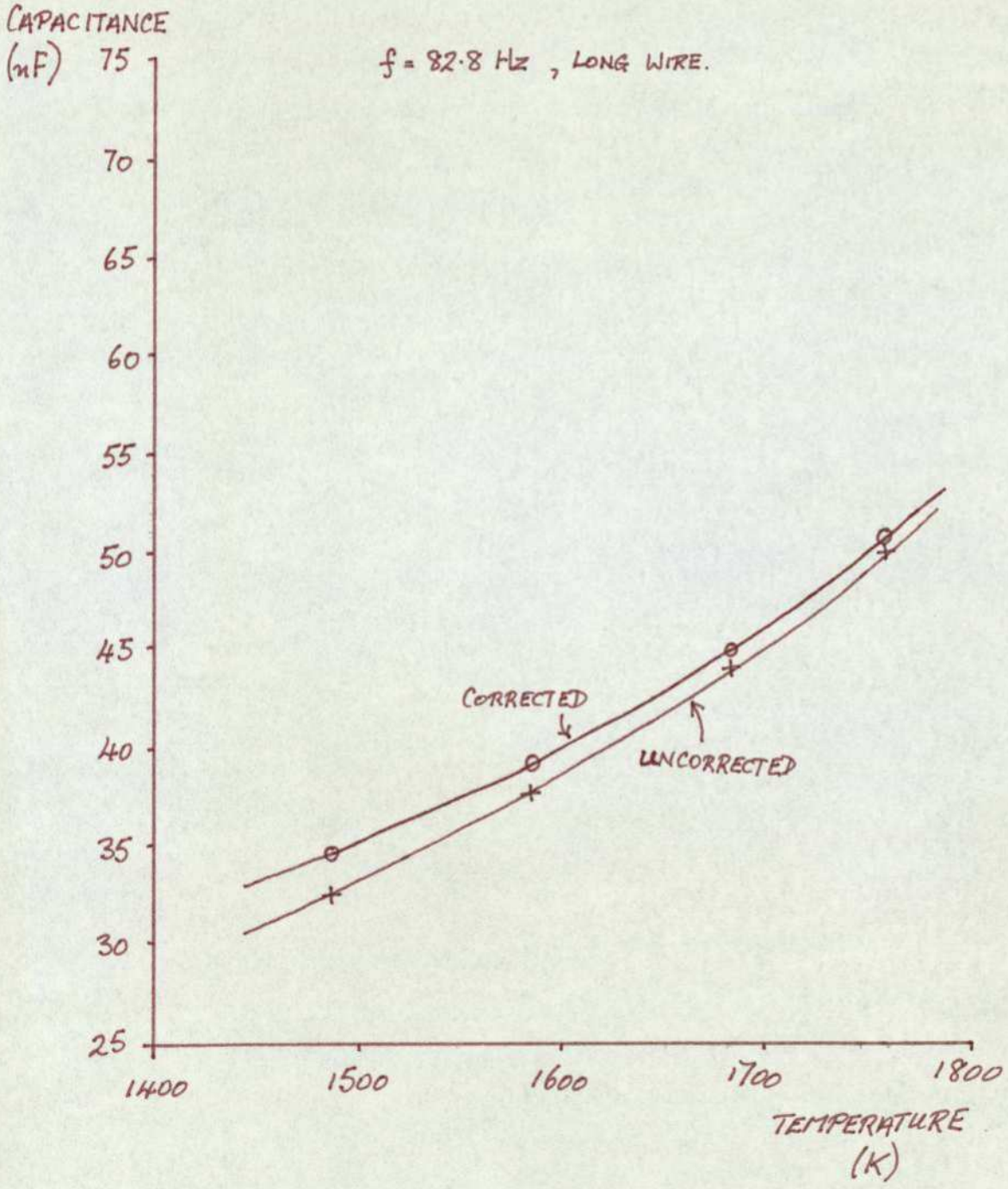

Fig.5.3. Corrected and uncorrected capacitance v temperature. 1. Long wire

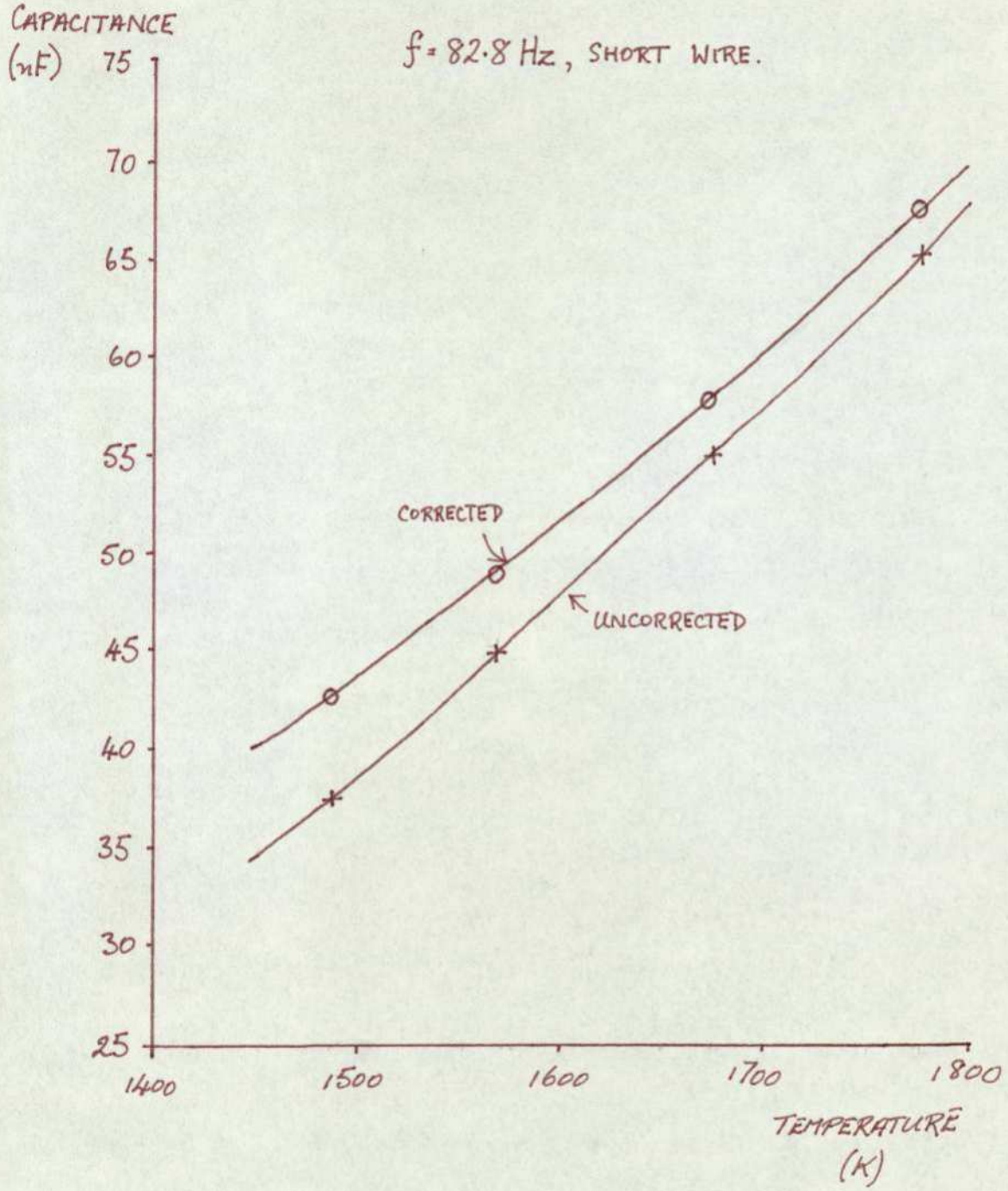

Fig.5.4. Corrected and uncorrected capacitance v temperature. 2. Short wire

in the measured resistance of the wire was small enough compared with the error in the correction curve to introduce no additional significant error when reading off the necessary capacitance correction. A typical resistance curve is shown on Fig.5.5. : the results are for the same wire over the same temperature range at different frequencies.

As an indication of the reproducibility possible with this experiment, two experimental runs on a long wire were performed at a frequency of 130Hz and are shown in Fig.5.6. The reproducibility possible was ~1% compared with the accuracy of capacitance measurement of ~1%.

5.3.3. Temperature coefficient of resistivity results.

As was shown in subsection 2.2.2. the effective capacitance of the wire is related to the temperature coefficient of resistivity by equation 2.20. which is shown below.

$$\alpha = \frac{8 m w^2 r_e c_p C}{i^2} \qquad 5.3.$$

Now, the mass was determined and the frequency measured as described in subsection 4.2.1., the resistance ratio for the relevant current was read off Fig.3.7., the effective capacitance was determined as described in subsection 5.3.2. and the peak value of the heating current was found by

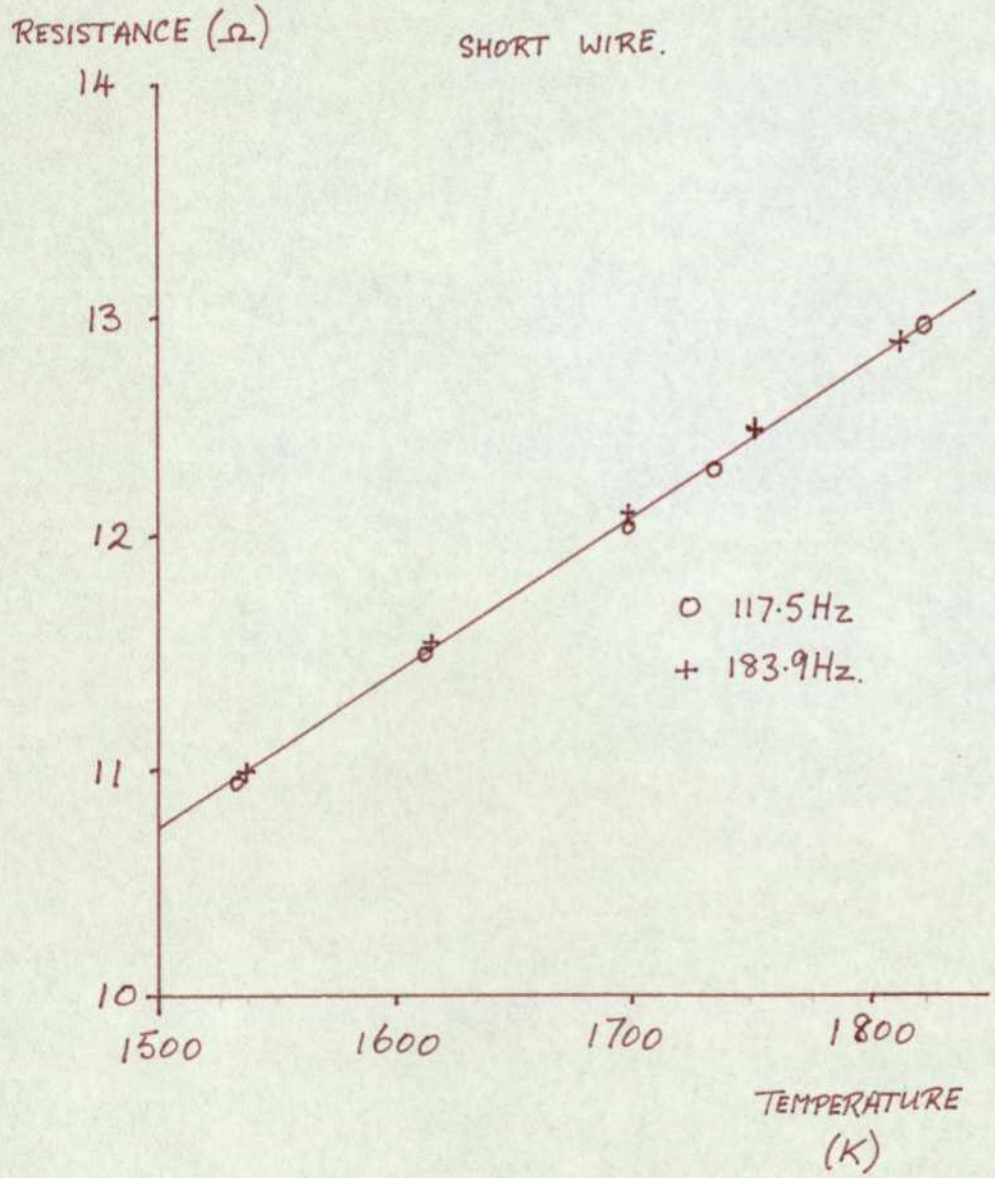

Fig.5.5. Resistance v temperature for a wire at 117.5Hz and 183.9Hz.

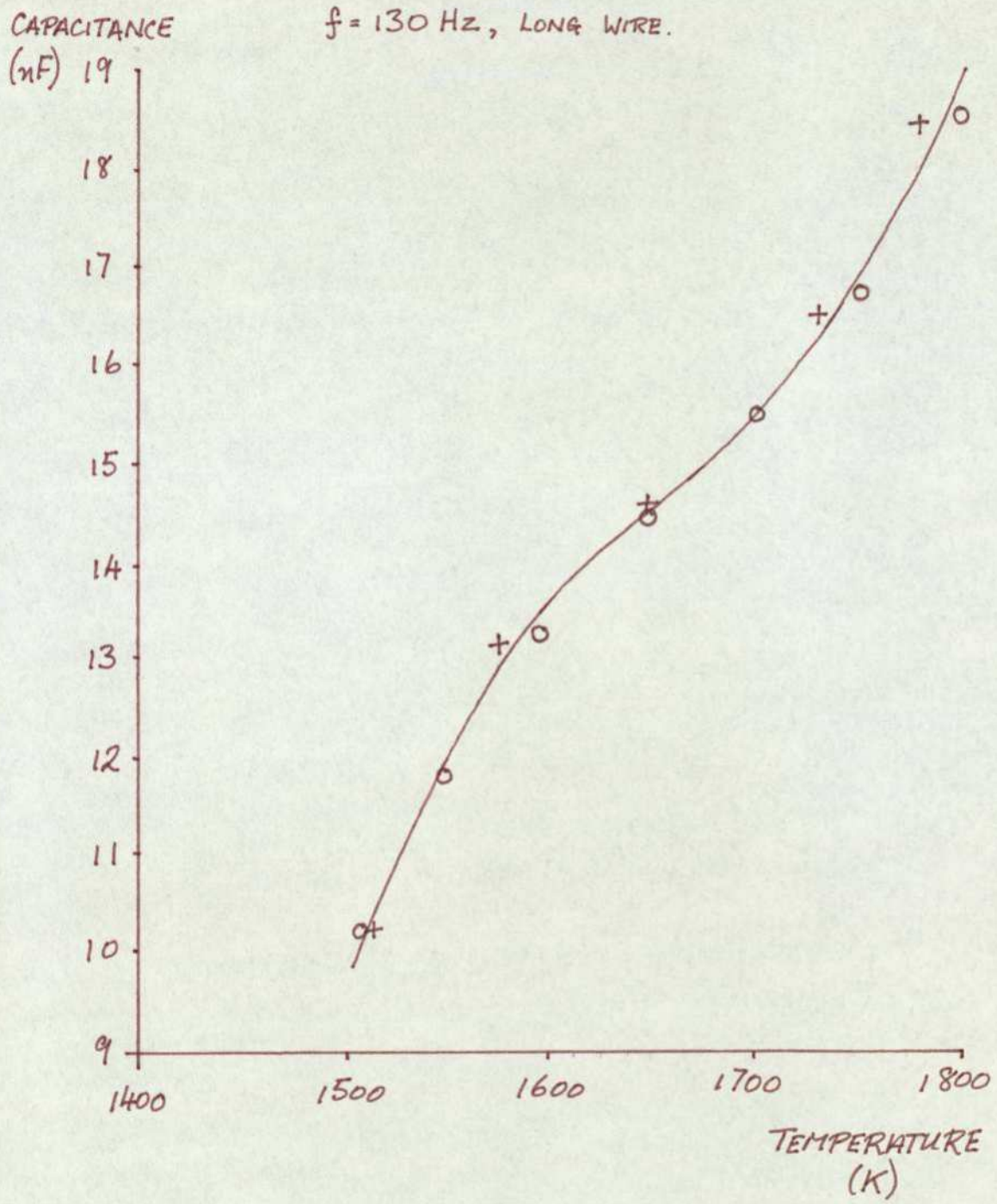

Fig.5.6. Reproducibility of the capacitance v temperature measurements

measuring the voltage drop across a 1Ω standard resistor (see subsection 4.2.1.). The specific heat values used were those obtained by Kraftmakher and Lanina (1965) and Seville (1972) and are shown in Fig.5.7.

The resulting temperature coefficient of resistivity graphs are shown in Figs.5.8. - 5.16. and are the results from four separate wires. Figs.5.17 - 5.19. show the offset values necessary due to the inaccuracy of the phase setting as discussed in Chapter 4.

The low frequency value for the temperature coefficient of resistivity is shown as a dotted curve on these graphs. It is clear that the lower frequency results are consistent with this curve. The exception is the 14.8Hz result, but from Chapter 2 it can be seen that the assumption that the temperature oscillations are in quadrature with the heating current is no longer valid, the angle between these quantities being $\sim 84^{\circ}$ thus causing contamination of the capacitative signal that cannot be removed by the phase sensitive detector.

For comparison, the results of Kraftmakher and Sushakova (1974) for the temperature coefficient of resistivity are shown on Fig.5.20.

Comparison of Figs.5.8.-5.12., 5.14. and 5.17.-5.19. shows a distinct reduction in the high temperature and high frequency value of the temperature

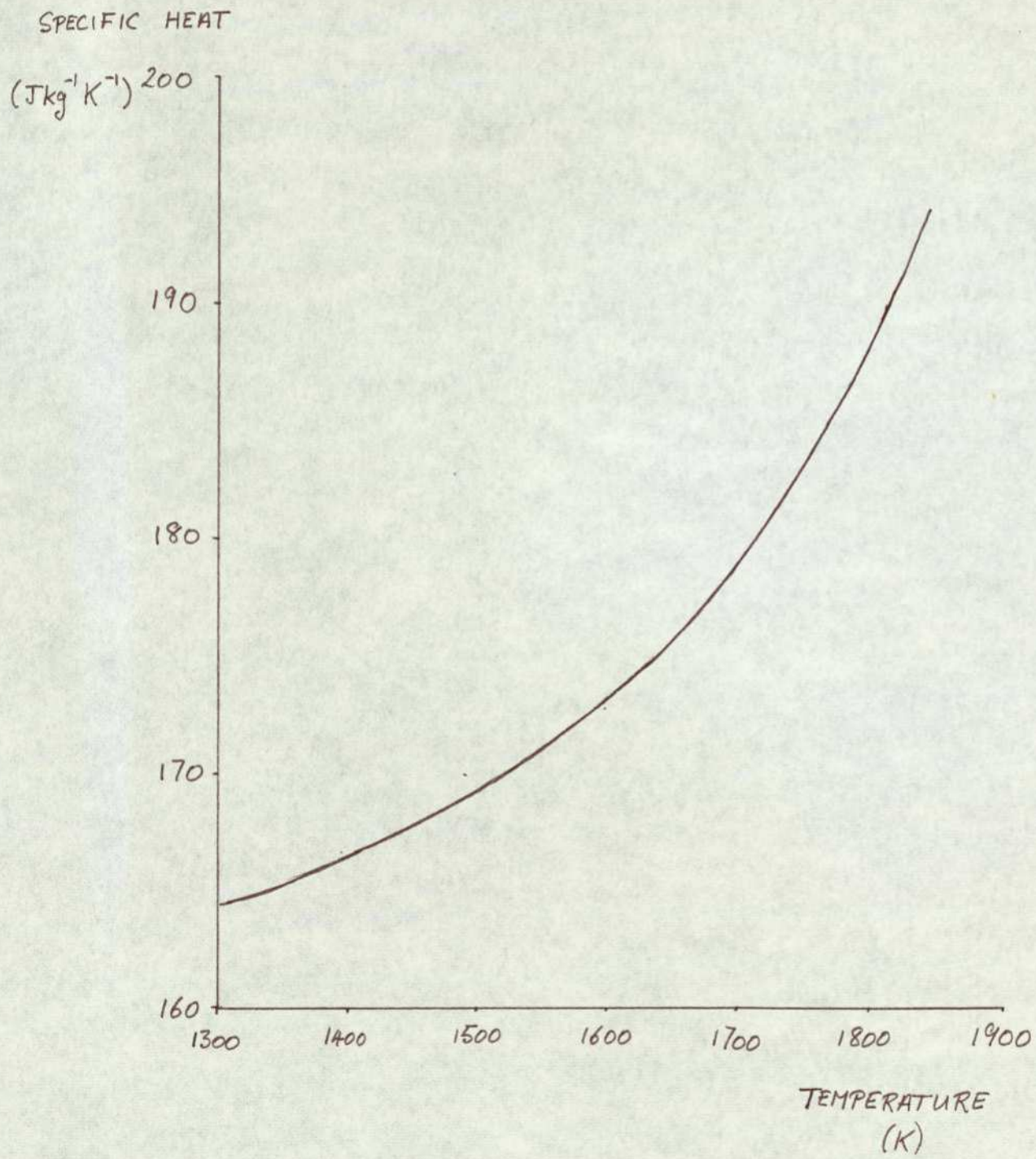

Fig.5.7. Specific heat v temperature for platinum

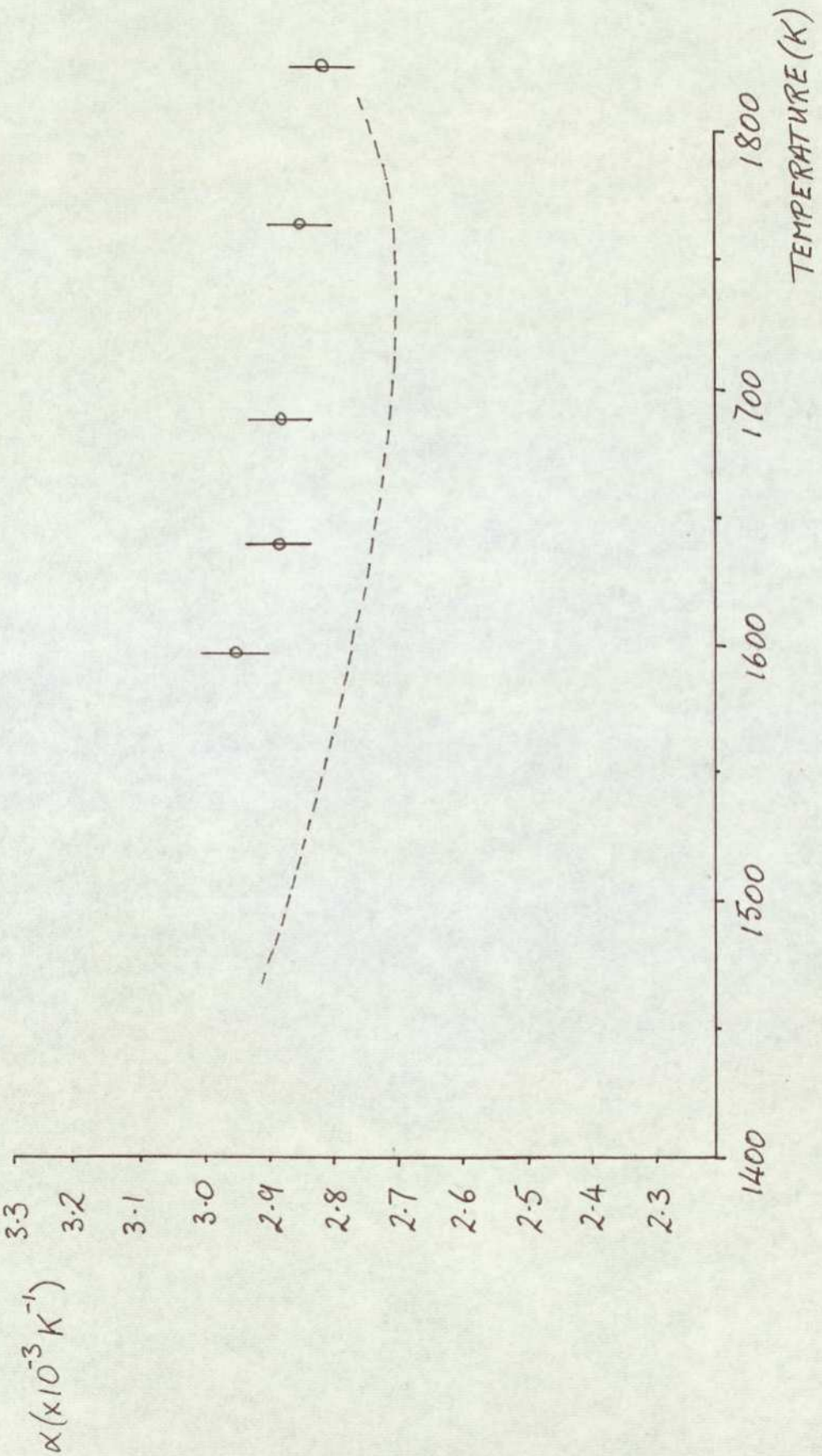

Fig.5.8. Temperature coefficient of resistivity v temperature. f = 14.8Hz.

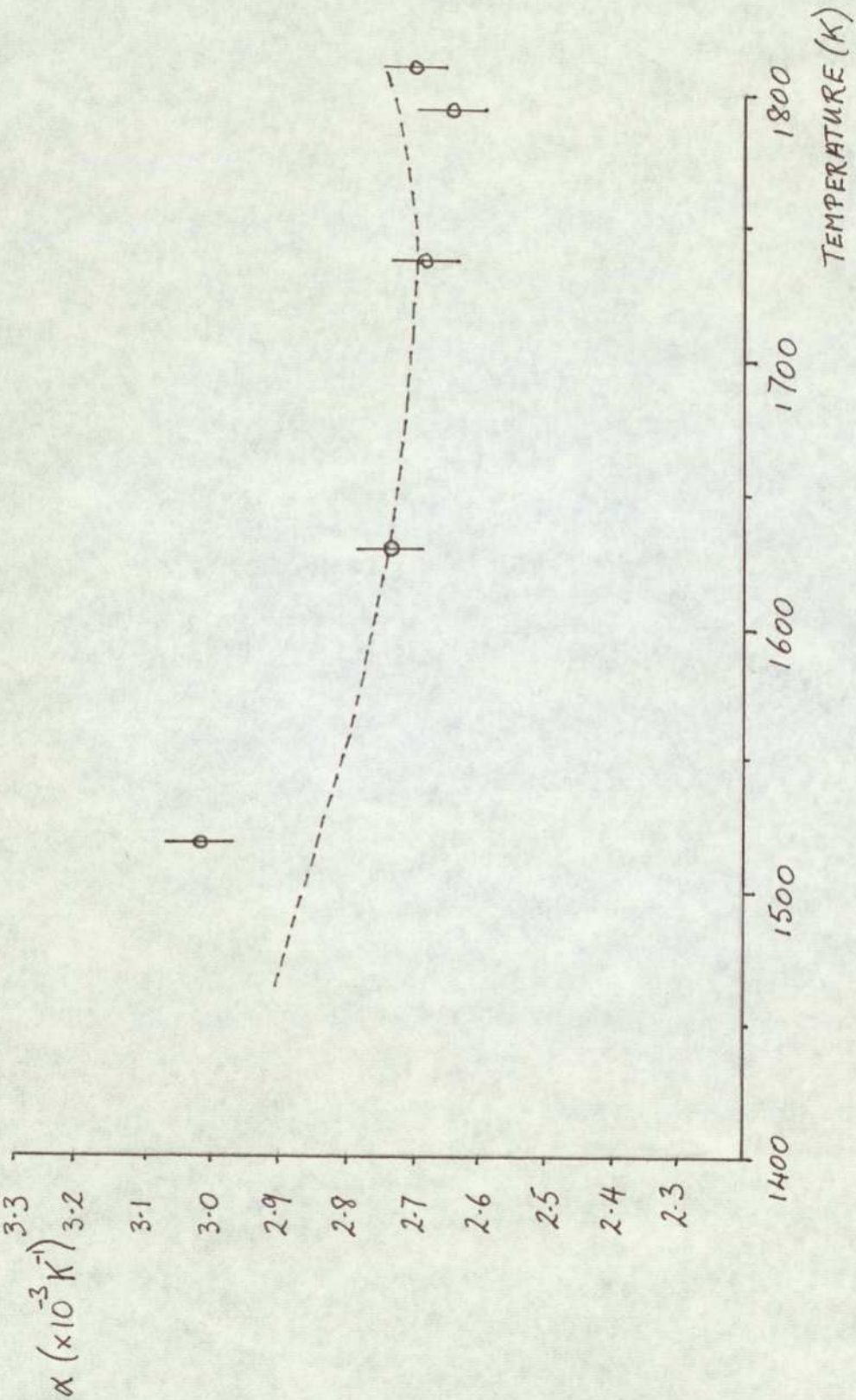

Fig.5.9. Temperature coefficient of resistivity v temperature, f = 26.5Hz.

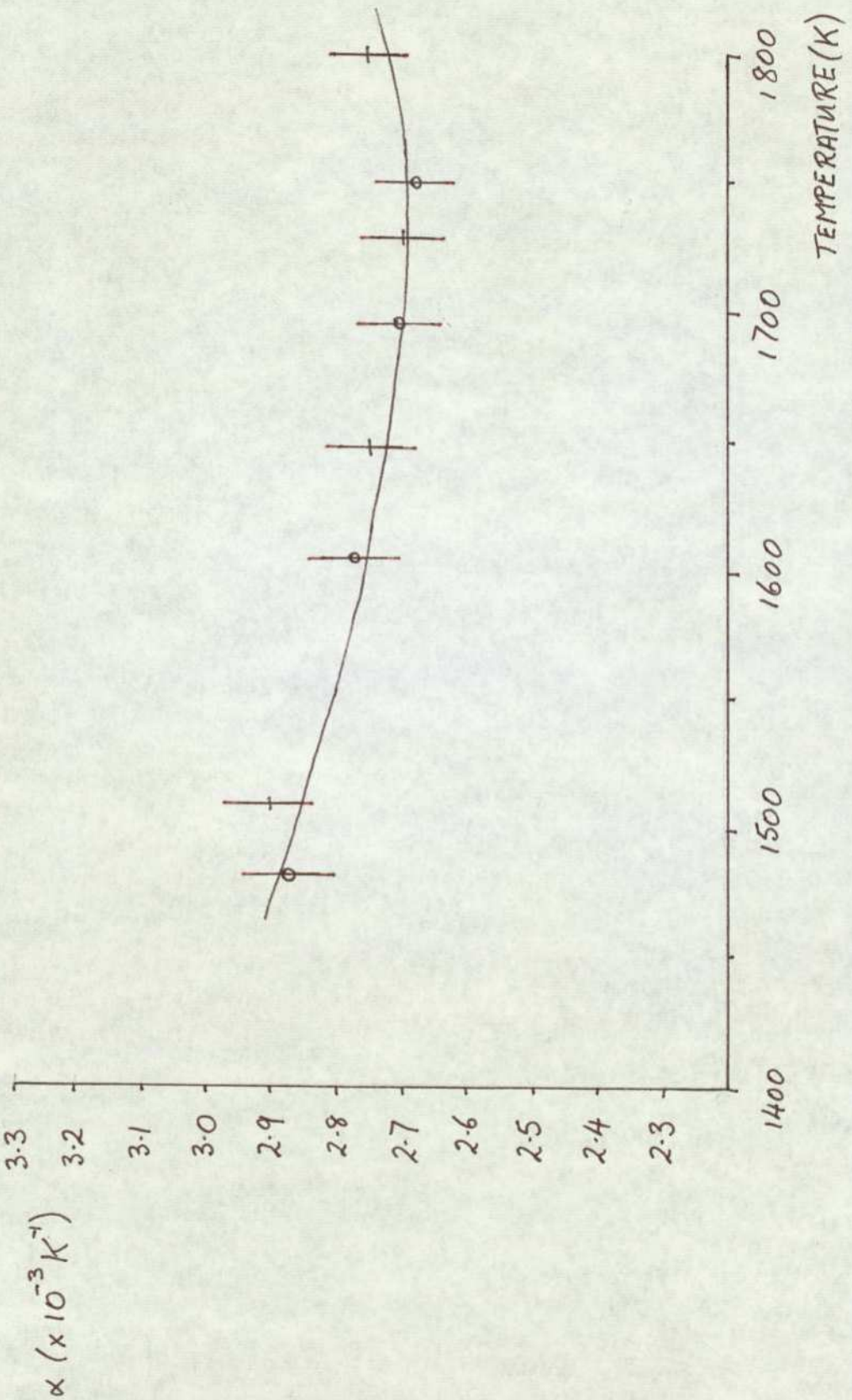

Fig.5.10. Temperature coefficient of resistivity v temperature, f = 41.5Hz.

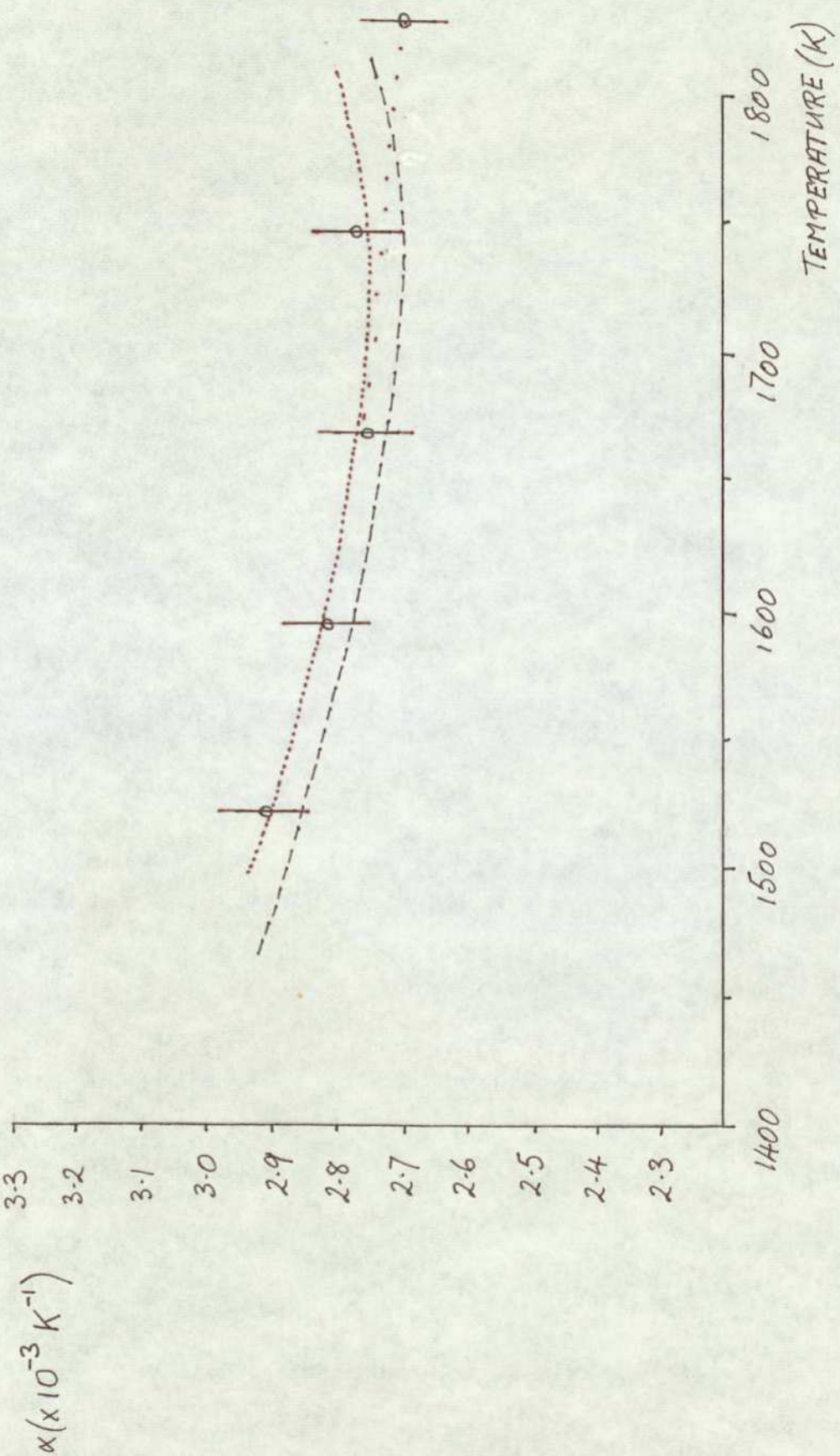

Fig.5.11. Temperature coefficient of resistivity v temperature, f = 62.9Hz.

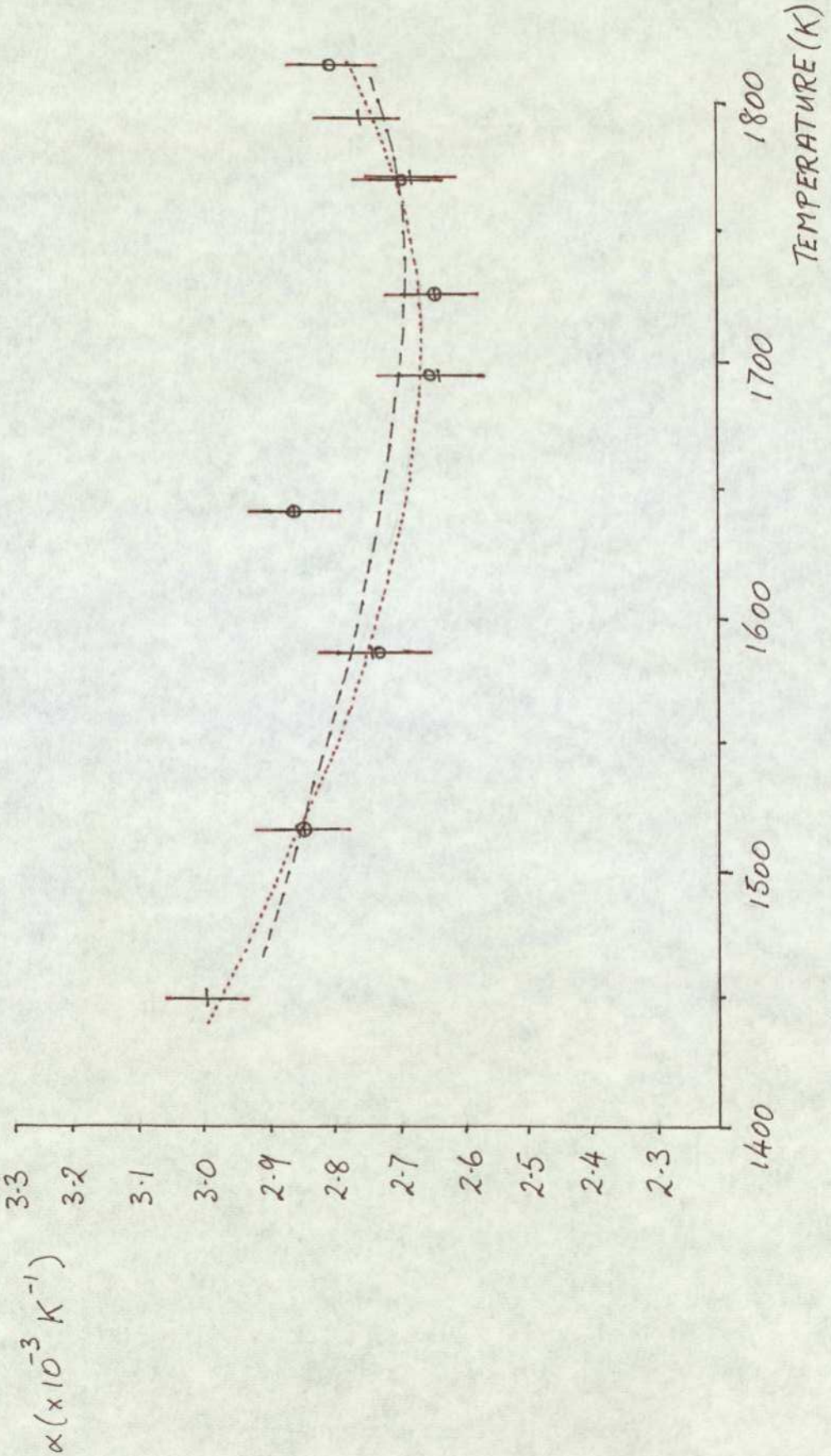

Fig.5.12. Temperature coefficient of resistivity v temperature, f = 82.8Hz.

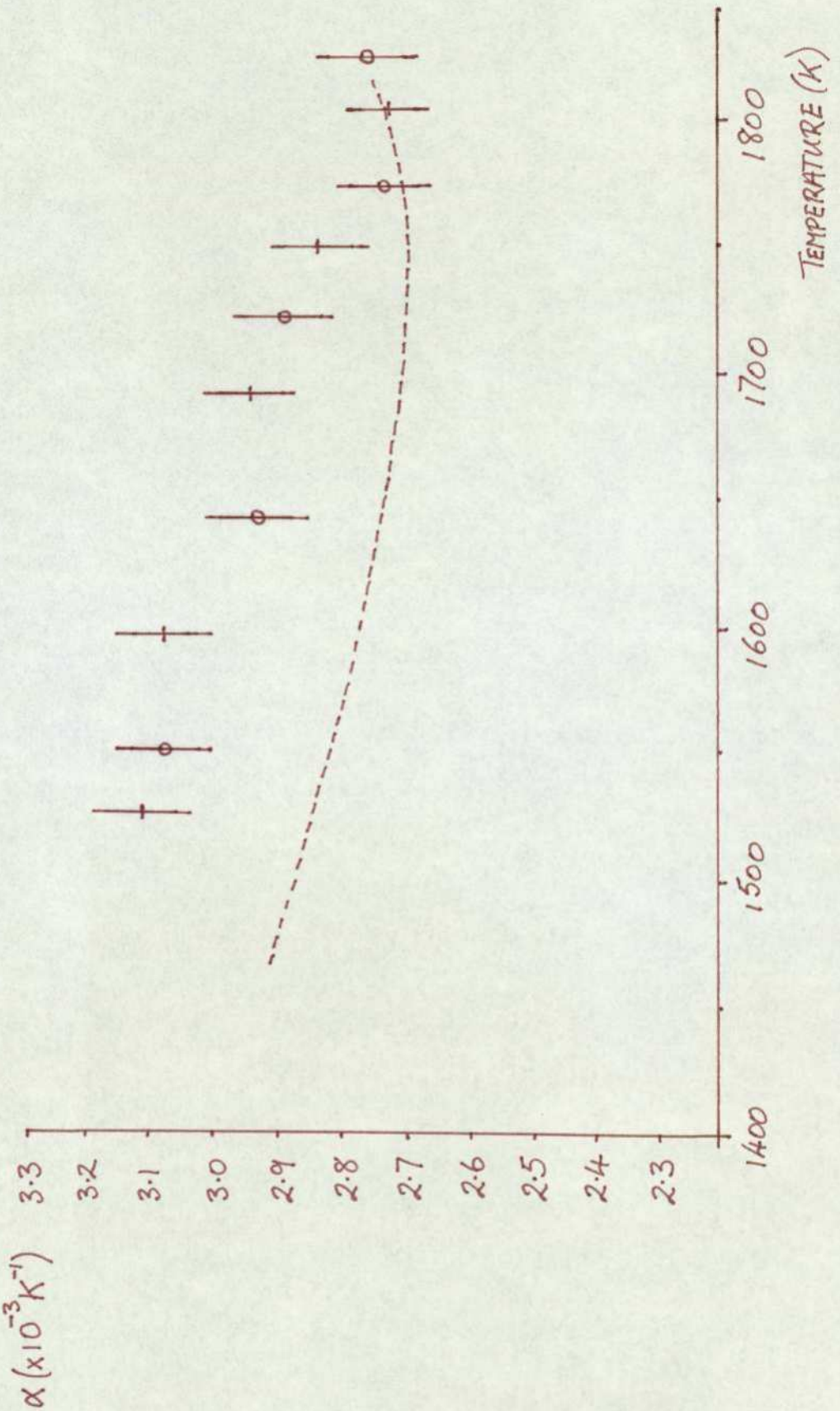

Fig.5.13. Temperature coefficient of resistivity v temperature, f = 117.5Hz.

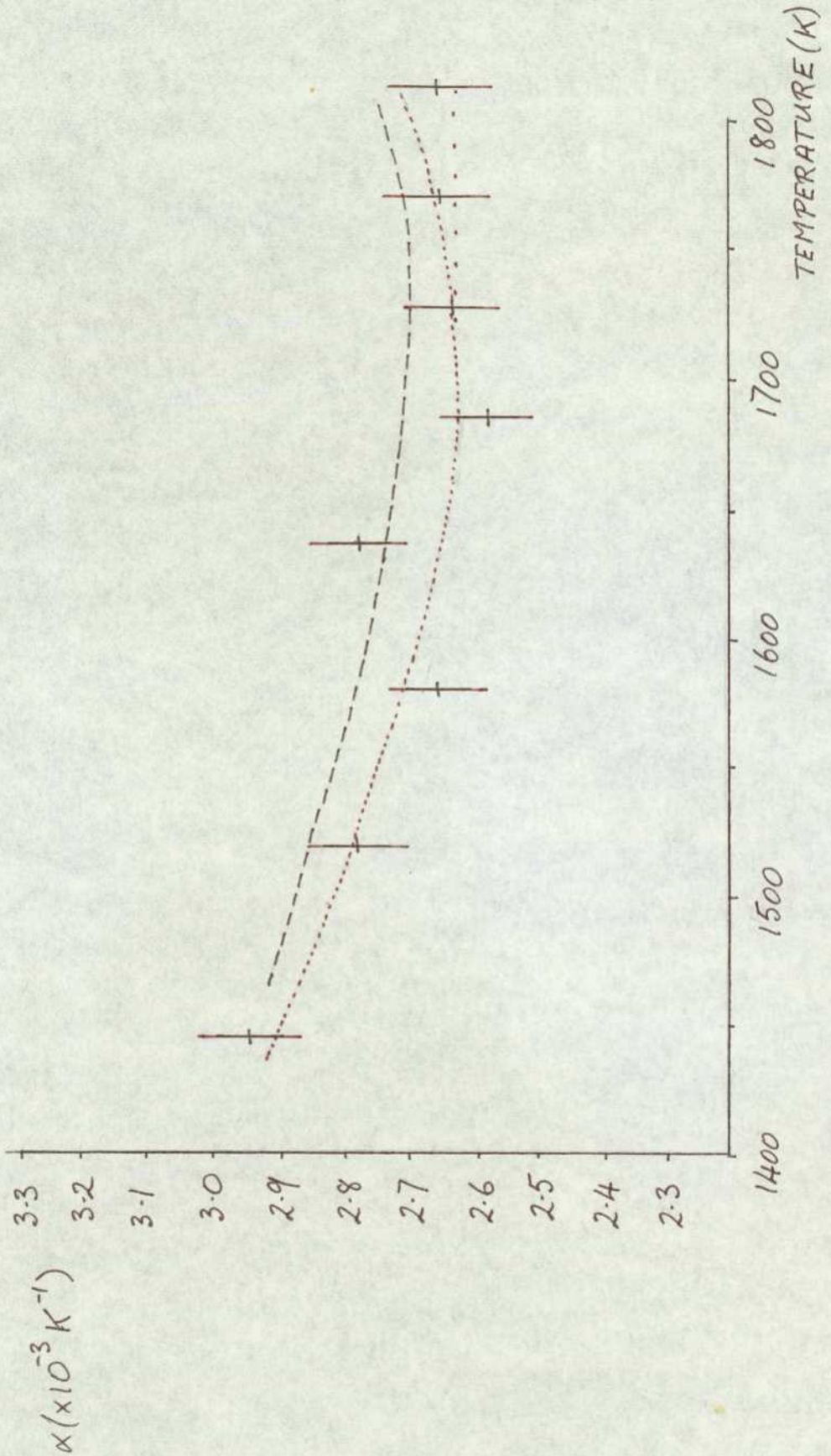

Fig.5.14. Temperature coefficient of resistivity v temperature, f = 134.2Hz.

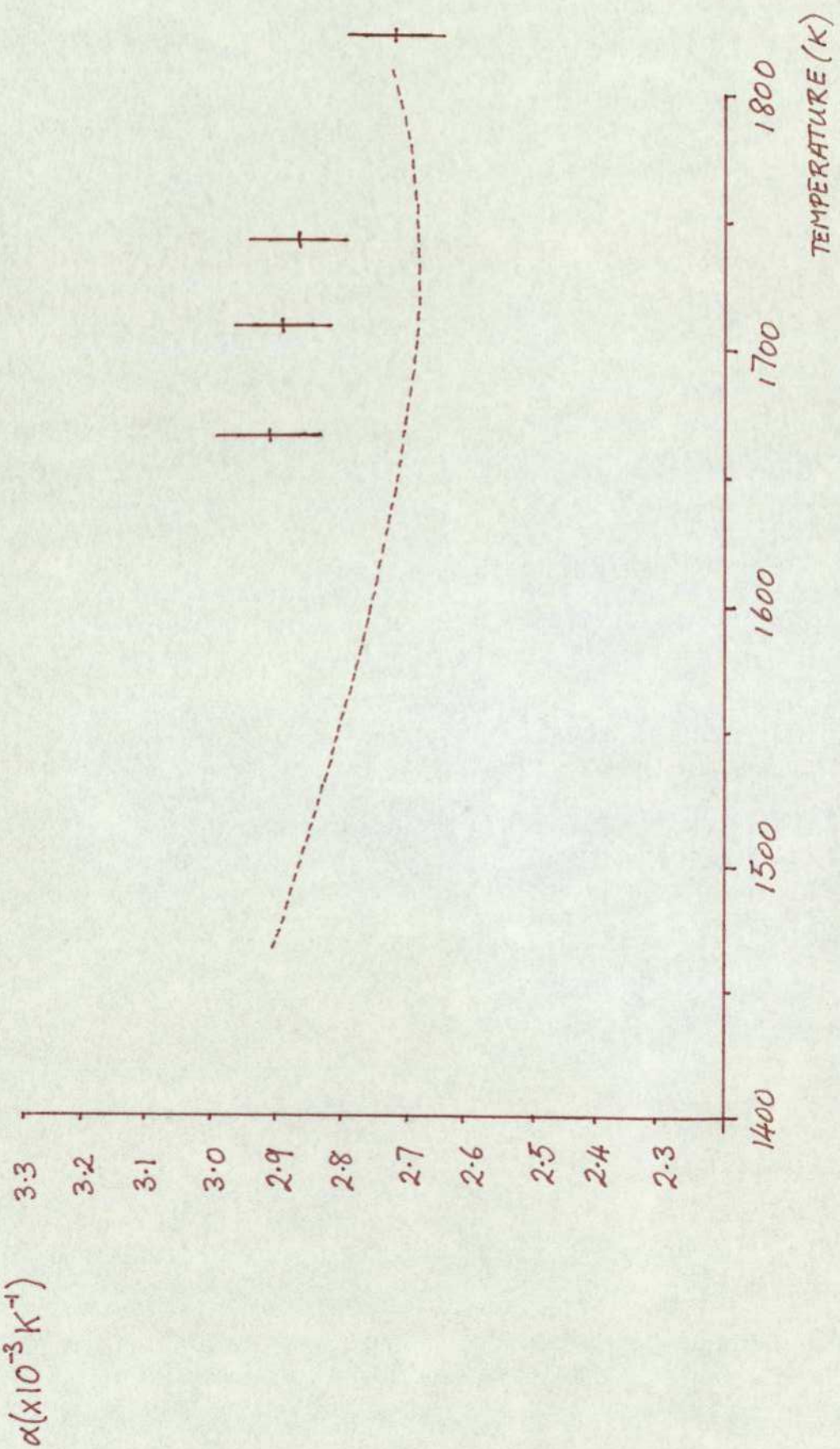

Fig.5.15. Temperature coefficient of resistivity v temperature, f = 167.1Hz.

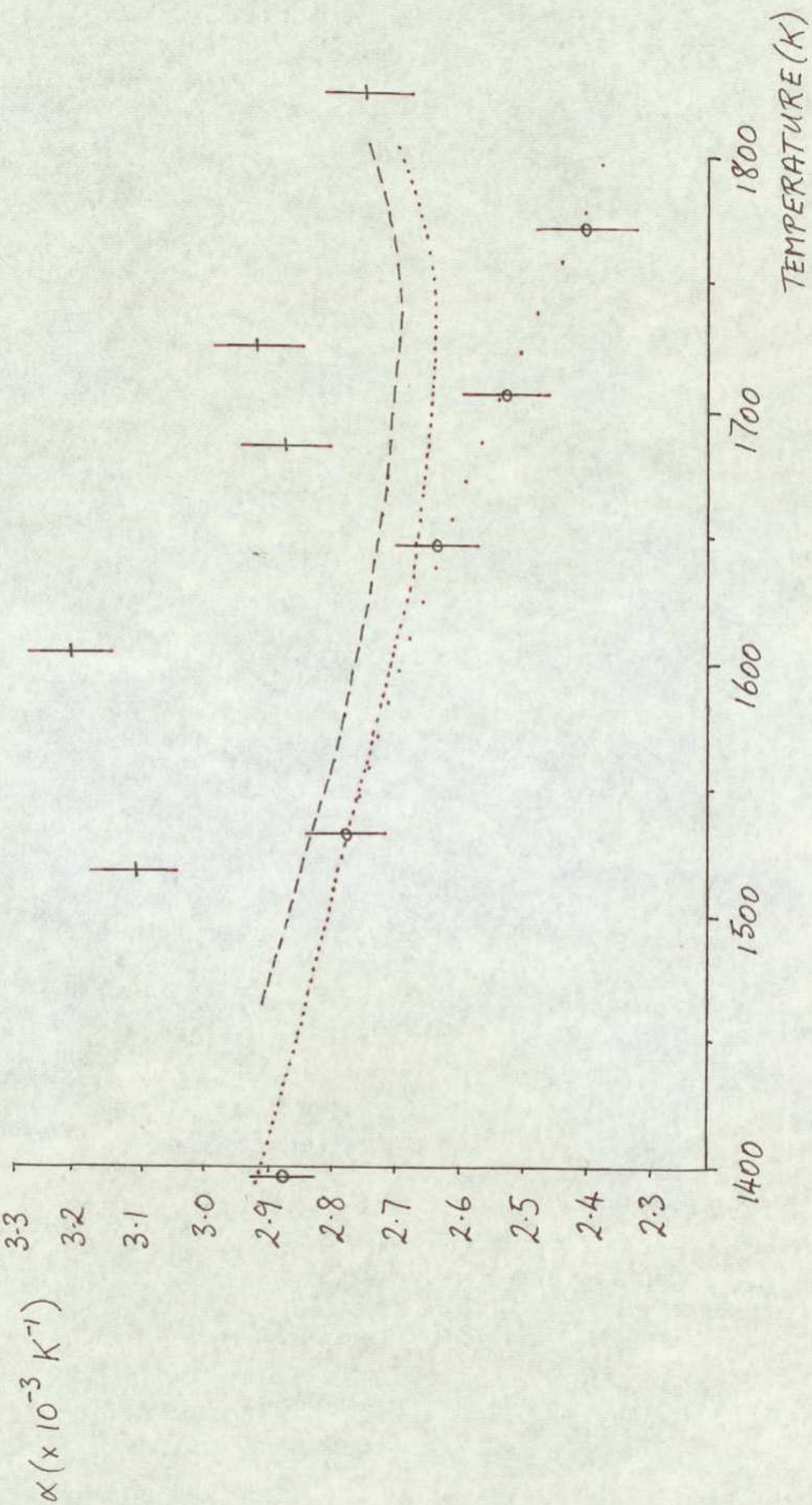

Fig.5.16. Temperature coefficient of resistivity v temperature, f = 183.8Hz.

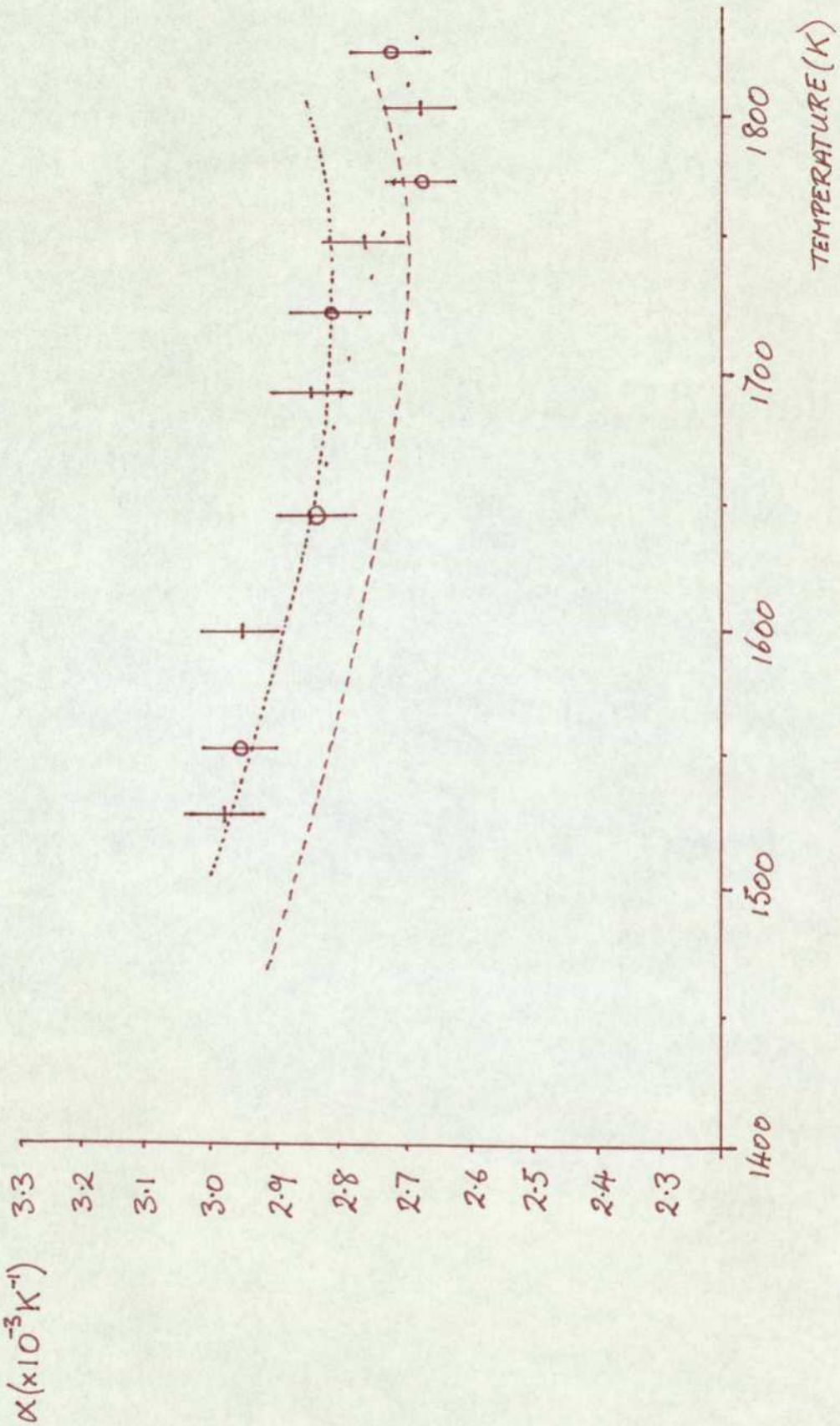

Fig.5.17. Offset temperature coefficient of resistivity v temperature, f = 117.5Hz.

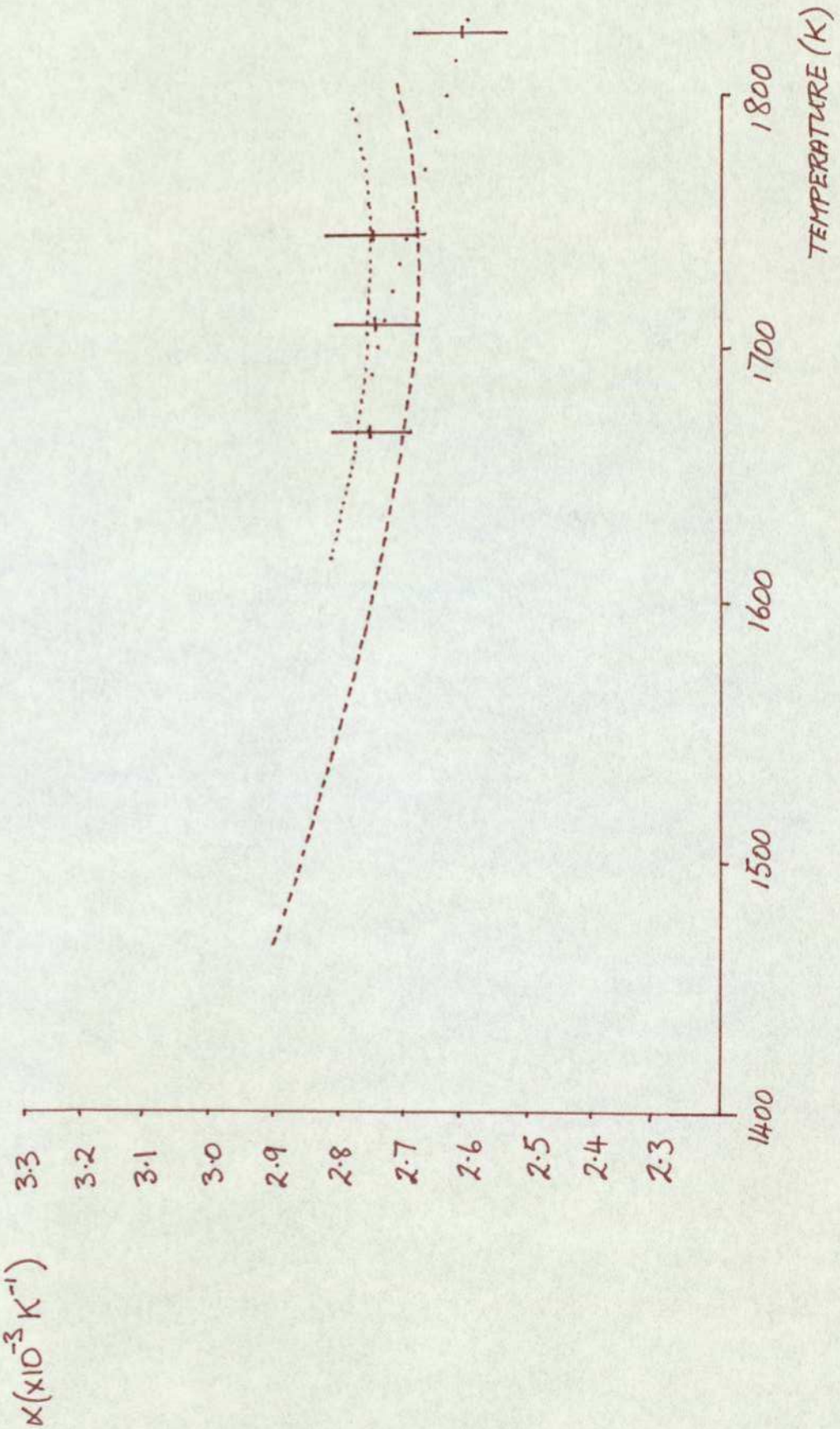

Fig.5.18. Offset temperature coefficient of resistivity v temperature, f = 167.1Hz.

Fig.5.19. Offset temperature coefficient of resistivity v temperature, f = 183.8Hz.

Fig.5.20. Temperature coefficient of resistivity v temperature due to Kraftmakher and Sushakova.

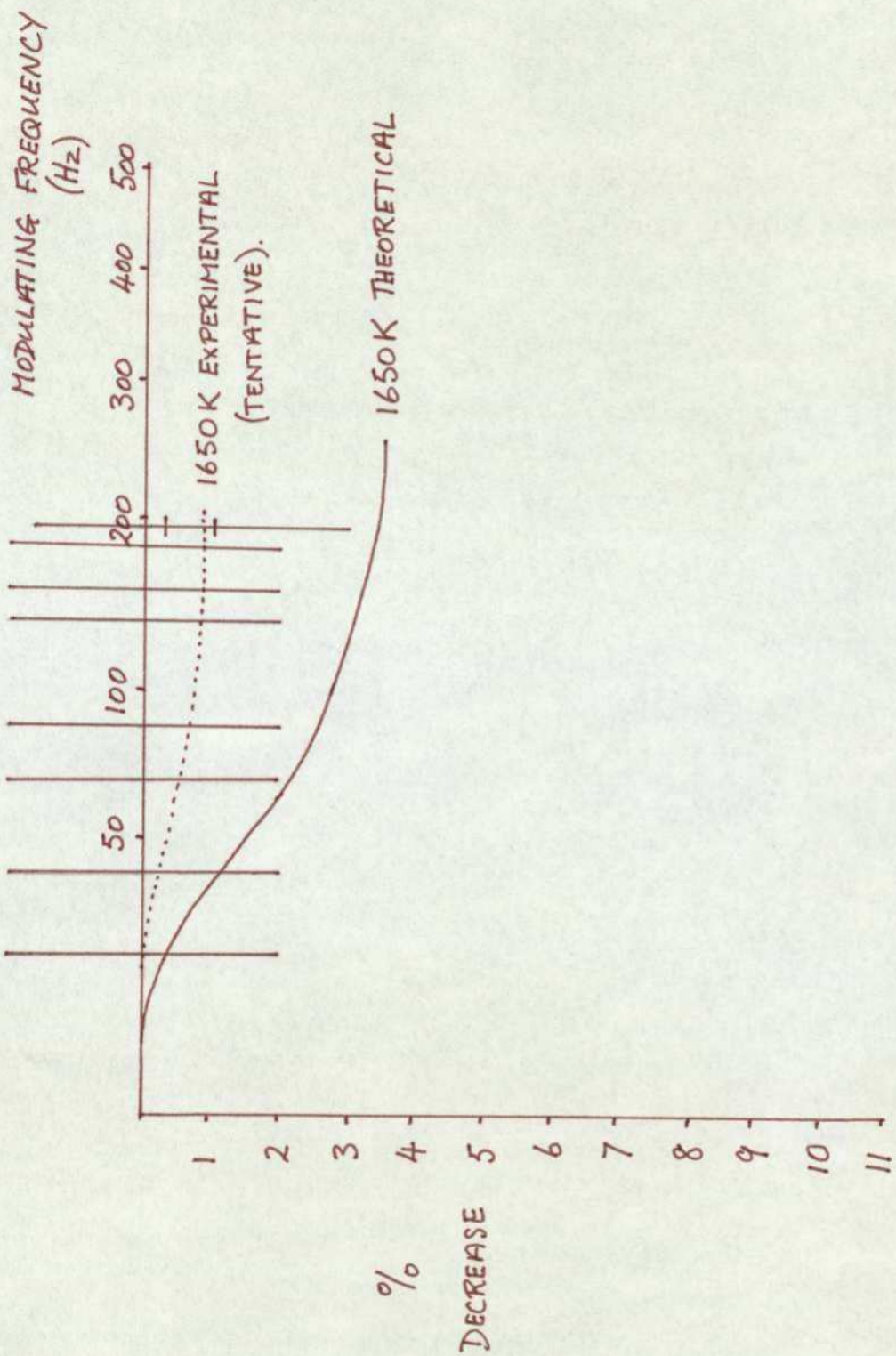

Fig.5.21. Theoretical and experimental decrease in the temperature coefficient of resistivity.1. T = 1650K

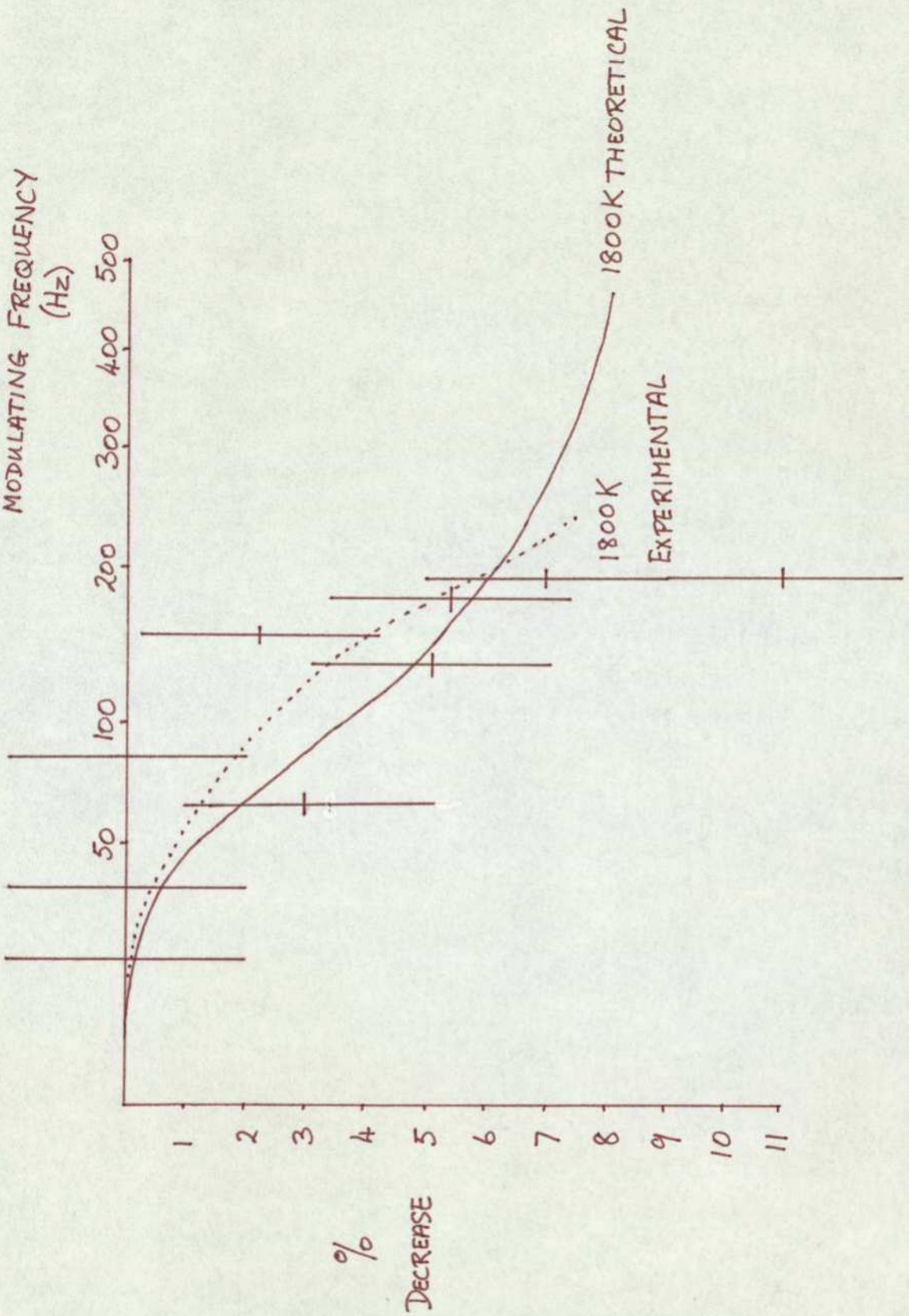

Fig.5.22. Theoretical and experimental decrease in the temperature coefficient of resistivity.2. T = 1800K

coefficient of resistivity at $>$ 100Hz.

Fig.5.21. shows the theoretical and experimental percentage reduction of temperature coefficient of resistivity as a function of frequency at 1650K while Fig.5.22 shows the corresponding results at 1800K.

The theoretical curve is based upon planar source/ sinks of $\sim 5\mu m$ spacing - sub-grain boundaries - after Seville (1975). The similarity of the experimental curve is apparent though the frequency at which the reduction occurs is higher and the rate of reduction is greater than the theoretical result, leading to a vacancy lifetime of ~1ms.

These results are discussed in Chapter 6.

5.4. Estimation of errors

The equation used in calculating the temperature coefficient of resistivity, as mentioned above, is

$$\alpha = \frac{8mw^2 r_e c_p C}{i^2} \qquad 5.4.$$

The approximate size of each quantity on the right hand side of equation 5.4. will now be considered along with an estimate of its error to obtain an estimate for the error in the temperature coefficient of resistivity:

mass, m - typically ~4mg to an accuracy of 0.05mg, so the percentage error is ~1%.

frequency, f - minimum $\sim$40Hz to an accuracy of 0.1Hz, so the percentage error is $<$0.25%.

specific heat, c_p - this was measured from published results (see subsection 5.3.3.) and is dependent upon their accuracy and the accuracy of the temperature calibration. Typically $c_p \sim 170\ Jkg^{-1}K^{-1}$ with an error of $\sim 1 Jkg^{-1}K^{-1}$, so the error is $\sim$0.5%.

resistance ratio, r_e - the small temperature difference (25K) used to calculate the resistance ratio from Kraftmakher and Sushakova (1974)(see subsection 3.5.) preclude any serious error in calculating r_e. Typical resistance ratio value is $\sim$5.50 to an accuracy of not less than 0.01, so the error is $\sim$0.2%.

capacitance, C - the error in measuring this is quantity is $\sim$1% for the lower frequencies, $\sim$2% for the higher.

heating current, i_{RMS} (N.B. $i = \sqrt{2}.\ i_{RMS}$) - typically 500mA to an accuracy of 1mA, so the percentage error is $\sim$0.2%.

The root mean square error in the temperature coefficient of resistivity can be found from

$$\sqrt{\left(\frac{\delta\alpha}{\alpha}\right)^2} = \sqrt{\left(\frac{\delta m}{m}\right)^2 + 2\left(\frac{\delta w}{w}\right)^2 + \left(\frac{\delta c_p}{c_p}\right)^2 + \left(\frac{\delta C}{C}\right)^2 + \left(\frac{\delta r_e}{r_e}\right)^2 + 2\left(\frac{\delta i_{RMS}}{i_{RMS}}\right)^2} \qquad 5.5.$$

Substituting in the estimates of each error from equation 5.5. gives a percentage error of ~ 2.0%.

5.5. Summary

The results obtained using a third harmonic voltage method were briefly presented and shown to be unsatisfactory.

The correction curve necessary to allow the use of effective capacitances measured by an equivalent impedance method was presented. The temperature coefficient of resistivity was calculated from these corrected effective capacitances as a function of temperature at a range of modulating frequencies (20Hz-180Hz). A reduction of up to ~10% at 180OK in the temperature coefficient of resistivity was noted above ~100Hz in reasonable agreement with theoretical results based upon 5μm spaced planar source/sinks.

Finally, the error in the temperature coefficient of resistivity was estimated from the errors in each quantity used in the calculation.

6. DISCUSSION

6.1. Introduction

The measurement of the temperature coefficient of resistivity of platinum in the temperature range 1400K-1800K using an equivalent impedance modulation method over a range of modulating frequencies (20Hz-180Hz) is discussed.

The low frequency (~40Hz) results are compared with those of Kraftmakher and Lanina (1965) and Kraftmakher and Sushakova (1974). The frequency dependence of the temperature coefficient of resistivity is compared with the theoretical predictions of Seville (1975).

The frequency dependence is discussed by considering the possible sources and sinks of vacancies, namely; grain boundaries, sub grain boundaries, sample surface, impurities and dislocations. The implication of the results is that dislocations are primarily the sources and sinks of vacancies at temperatures above about $^{2}/_{3}T_{m}$. In addition the efficiency of the dislocations as sources and sinks increases with increasing temperature.

The final section suggests opportunities for further work using the equivalent impedance modulation method to investigate concentrations and sources and sinks of vacancies in platinum alloys that have been shown to have enhanced strength.

6.2. Low frequency comparison.

The results of Kraftmakher and Lanina (1965) and Kraftmakher and Sushakova (1974) are shown on Fig.6.1. together with the low frequency results from the present work for comparison. It is clear that there is good agreement between Kraftmakher and Lanina (1965) and Kraftmakher and Sushakova (1974), especially at lower temperatures. The present results are consistently higher and the curve is parallel to those previously obtained thereby implying a systematic error. This could be due to impurities in the platinum samples used by Kraftmakher and Lanina (1965) and Kraftmakher and Sushakova (1974) or in the present work.

The work of Kraftmakher and Lanina (1965) does not mention the purity of the samples used. That of Kraftmakher and Sushakova (1974) characterizes the purity of the platinum used by the resistance ratio $R100/R_o = 1.391$, and in comparison, the corresponding resistance ratio from Johnson Matthey Co. Ltd. (1952) for the samples used in the present work was 1.392 (i.e. $A = 3.98 \times 10^{-3} K^{-1}$, $B = -5.85 \times 10^{-7} K^{-2}$). The stated purity was to 1 part in 100,000 and is the highest purity commercially available and the conclusion is that the platinum used by Kraftmakher and Sushakova (1974) is of a lower purity.

The largest difference, at ~1700K, between Kraftmakher and Sushakova (1974) and the present work is ~8%, whilst that at 373K is ~0.2%. If the difference

Fig.6.1. Present α results compared with those of Kraftmakher & Sushakova and Kraftmakher & Lanina.

at 373K is attributed to differences of purity, then a difference of ~ 8% at ~1700K can also be reasonably attributed similarly.

The discrepancy between values of temperature coefficient of resistivity attributed to impurities must also explain the good agreement between the specific heat results of Kraftmakher and Lanina (1965) and Seville (1974) who used platinum of the same stated purity from Johnson Matthey Co. Ltd. as was used to obtain the present results.

The electronic component of the specific heat is ~10%, whilst the lattice component of the temperature coefficient of resistivity (i.e. neglecting vacancies) is ~90% at 1800K - Seville (1975). Therefore any modification of the electronic band structure will have an effect on order of magnitude larger on the temperature coefficient of resistivity compared with that on the specific heat. Because both parameters depend on the density of states immediately above the Fermi Energy, to a first approximation, both will be affected in the same way (but by roughly an order of magnitude difference).

Thus, electronic properties are more sensitive to impurities than a parameter like the specific heat and so it is not surprising for there to be an agreement between specific heat results, whose accuracy is of the order of 2%, when there is a noticeable difference between temperature coefficient of resistivity results

(i.e. one would expect a difference in the specific heat results of ~1%, which would not be resolvable).

6.3. High frequency comparison

6.3.1. Comparison of theory and experiment.

The theoretical and experimental decrease in the temperature coefficient of resistivity as a function of frequency were shown in section 5.3. and their similarity noted. As was stated, the theoretical curves were produced by Seville (1975) and obviously the basis of this prediction is important in order to deduce a physical meaning for the experimental results obtained.

The theoretical results are based upon the experimental work of Heigl and Sizmann (1972) who pulse heated platinum samples up to 1200K for varying lengths of time. The sample was then quenched and the residual resistivity measured and attributed to vacancies. The results were analysed to imply quasi-planar source/sinks of approximately 5μm spacing and a vacancy lifetime of ~1.5ms at 1850K. These kinetics are normally interpreted as dislocations operating in low angle sub-grain boundaries.

These basic kinetics were used by Seville (1975) using the method proposed by Van den Sype (1970a) and assuming a vacancy concentration of .08% to give the theoretical curves for the decrease in the temperature coefficient of resistivity with frequency.

The experimentally obtained variation of temperature coefficient of resistivity with frequency implies a vacancy lifetime at 1800K of ~1ms. This is somewhat smaller than the theoretical estimate but in good general agreement, the shape of the curves are also similar.

An exact agreement between the theoretical and experimental results is not to be expected for a number of reasons:

a) The results of Heigl and Sizmann (1972) were obtained at $< {}^{2}/_{3}$Tm, in the temperature region of low diffusion, whereas the modulation experiment results were all obtained at $> {}^{2}/_{3}$Tm, in the region of high vacancy mobility. The difference between the two regions could be due to an increased number of source/sinks operating or their efficiency increasing. Either way the extrapolation to higher temperatures will have a certain amount of inaccuracy associated with it.

b) The pulse heating technique provides a much larger driving force for the creation of vacancies than was present in the conditions of the modulation experiments above. However, the rapid heating of the sample will not allow the source/sink concentration to reach its equilibrium value at ~1200K, this would tend to nullify the effect of the larger driving force.

c) The residual resistivity was measured after quenching - the problems associated with quenching are well known and these also would add to the experimental errors.

The good agreement of the present experimental results with the theoretical would imply that either these sources of error are small or that they, to a certain extent, cancel out.

Fig.6.2. shows the theoretical and experimental results for the decrease in the temperature coefficient of resistivity at 180Hz over a range of temperatures. These graphs are obtained from Figs.5.21 and 5.22. for a frequency of 180Hz. The agreement of these curves is apparent, an item to note being the different slope of the experimental curve. This would indicate a number of possibilities: the efficiency of the source/sinks increasing with temperature, the vacancy concentration as a function of temperature is different from that predicted or, thirdly, that when the mean temperature is increased, so the amplitude of the sinnsoidal modulation also increases leading to an increased driving force for the production of vacancies.

This last type of possibility is also appropriate in considering the difference in curvature in Figs.5.21 and 5.22, i.e. the amplitude of the temperature modulation dependence upon the frequency of modulation.

6.3.2. Modulating temperature amplitude variations.

A variation in the temperature modulation can come about because there is a single source for both heating the wire and modulating the temperature. Therefore the temperature amplitude could vary due to

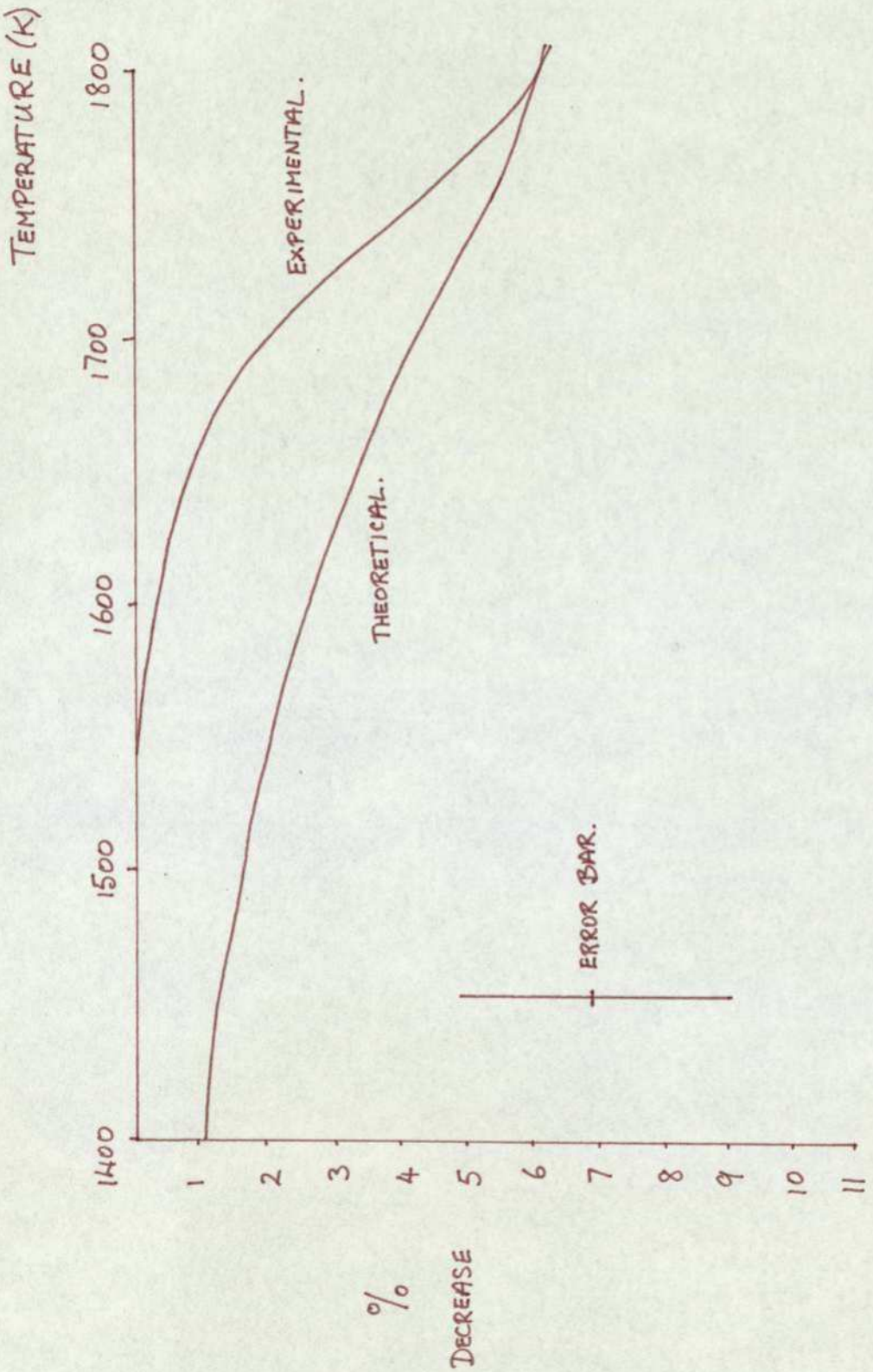

Fig.6.2. Theoretical and experimental decrease in α at f = 180Hz as a function of temperature.

changing the mean temperature and also due to changing the modulating frequency.

The variation in amplitude with mean temperature will be considered first.

From Chapter 2, the expression for the amplitude of the temperature excursion is given by equation 2.11.

$$\theta_2 e^{-j\phi} \approx \frac{\hat{\theta}}{j2w\tau} \qquad 6.1.$$

where $\hat{\theta}$ and τ are given by equations 2.7. and 2.8. respectively

$$\hat{\theta} = \frac{i^2 R_M}{2W_M\gamma - i^2 R_M \beta} \qquad 6.2.$$

and

$$\tau = \frac{2mc_p}{2W_M\gamma - i^2 R_M \beta} \qquad 6.3.$$

where the symbols have the meaning defined in Chapter 2.

Therefore the amplitude of the temperature excursions can be seen to depend upon the heating current as follows :

$$\theta_2 \propto \frac{i^2 R_M}{c_p} \qquad 6.4.$$

where, clearly, R_M and c_p are also functions of i in their own right. However, it is not easy to specify the exact function of i in each case apart from noting that both R_M and c_p increase with increasing i. Therefore experimental values of r_e and i will be used along

with results of c_p from Fig.5.7. to estimate the variation of θ_2 relative to its value at some convenient heating current, say 200 mA.

Table 6.1.

i(mA)	c_p ($Jkg^{-1}K^{-1}$).	r_e	$\theta_2/\theta_2(200)$	Mean Temperature (K)
200	165	5.1	1.0	1530
220	168	5.3	1.2	1610
240	169	5.4	1.3	1675
260	181	5.6	1.7	1735
280	184	5.8	2.0	1800

It can be clearly seen from Table 6.1. that roughly a 20% increase in the mean temperature is accompanied by a 100% increase in the amplitude of the temperature excursions. Therefore the driving chemical potential resulting from the modulating temperature is not constant with increasing mean temperature. From section 6.4. this implies that the efficiency of the vacancy source/sinks will increase with increasing mean temperature. However, it is worth noting that the chemical potential varies as the natural logarithm of the excess vacancy concentration thus reducing the effect of this amplitude variation.

In addition, in section 6.4. in discussing the analysis of Lomer (1958) it is noted that an amplitude of 10K would lead to dislocations 2μm in length operating as source/sinks. The increase in the amplitude with mean temperature to ~20K at ~1800K would imply shorter dislocations, typically of 1μm, operating i.e. not only

have the source/sink efficiencies increased with the temperature excursion amplitude but also the number of vacancy source/sinks operating has increased.

The second case will now be discussed, that is the variation in amplitude of modulating temperature with frequency. From equation 6.1. it is apparent that $\theta_2 \propto w^{-1}$ i.e. with increasing frequency, the amplitude of the modulating temperature varies in inverse proportion. A result is that the driving force for the creation of vacancies is not constant with frequency during the experiment and will fall.

Thus, in the frequency range 45Hz to 180Hz the amplitude of the temperature modulation will fall to a quarter of its original value. Therefore the results of, say, 1530K at 160Hz are obtained with an amplitude of modulation of about an eighth that of those results at 1800K and 40Hz.

It would seem, therefore, that the results were obtained at varying source/sink efficiencies. However, as mentioned above, the effect on the chemical potential will be reduced due to the logarithmic dependence.

6.4. Vacancy source/sinks

The production of vacancies can be understood in terms of a "driving force" which can be a change in temperature (as in this experiment) an applied stress, etc. It is commonly expressed as a chemical potential. This concept will be used later when considering the

sources and sinks of vacancies in some detail.

There are a number of structures that are generally accepted as being sources and sinks of vacancies, namely : the sample surface, grain boundaries, sub-grain boundaries, impurities and dislocations. The possible ways in which these structures can absorb and emit vacancies are detailed below.

6.4.1. Sample surface.

The formation of a vacancy by the sample surface can be considered as the creation of an extra lattice site at the surface, the vacancy diffusing into the bulk of the sample. It is obvious that the equilibration of the vacancy concentration is dependent upon the diffusion coefficient, sample size and, to a lesser extent, sample shape. In fact the larger the ratio of surface area to volume the shorter the time to reach the equilibrium concentration.

As pointed out above (section 6.3.) the vacancy lifetimes implied by the results of the present work are far too short to be compatible with surface source/sinks so this mechanism for vacancy production and destruction will not be considered further.

6.4.2. Grain boundary

A grain boundary can be defined as the junction between adjacent regions in a crystal, the orientation between which being typically greater than $\sim 10^{\circ}$. The

actual boundary is a region of disorder typically 2 atoms wide, the size of the grain being ~0.1→1μm which, due to annealing, tends to increase at higher temperatures. A theoretical study of grain boundaries as sources and sinks of vacancies under an applied stress bas been made by Gleiter (1979) and he finds that because of the disordering of the boundary they act as perfect sources and sinks at all applied stress.

Typically, in this experiment, grains are approximately an order of magnitude smaller than the sample diameter at medium temperatures (~1500K). However, due to annealing, grains can increase in size until they are segments of the wire sample - the sample surface and grain boundary being common. Therefore the same consideration as for section 6.4.1. applied : the obtained vacancy lifetimes are too short to be consistent with grain boundaries. However, by quenching molybdenum and tungsten (B.C.C. metals) Mamalui, Pervakov and Khotkevic (1975) have found that at high temperatures grain boundaries and the sample surface can be sources of vacancies. This may not be too surprising in view of the fact that BCC metals tend to have vacancy concentrations of up to an order of magnitude larger than FCC metals. Therefore it is to be expected that extra or different sources and sinks operate.

6.4.3. Sub-grain boundary.

The basic difference between grain and sub-grain boundaries is one of degree : a sub-grain boundary separates regions in a crystal, the misorientation of

which is $<5^{o}$. In general sub-grains are components of grains and roughly an order of magnitude smaller. Sub-grain boundaries can be regarded as roughly planar arrays of line dislocations (see Fig.6.3.) and in this configuration have a minimum energy and are said to be ideal. Higher energy, non-ideal sub-grain boundaries have a network of dislocations superimposed on the ideal boundary. Gleiter (1979) has found that low energy sub-grain boundaries will only emit vacancies above a certain threshold stress, whilst high energy boundaries emit at all stresses. As mentioned previously, Heigl and Sizmann (1972) concluded that at a temperature of 1200K in platinum the sources of vacancies were sub-grain boundaries. Balluffi et al (1970) concluded that, to a certain extent, sub-grain boundaries are sinks for vacancies during quenching experiments, although the predominant sinks were dislocations.

6.4.4. Dislocations.

Experimental work, particularly on gold, by Ytterhus and Balluffi (1965), Balluffi and Seidman (1965a), Seidman and Balluffi (1965) and Jackson and Koehler (1960) have indicated that the sources and sinks of vacancies are predominantly dislocations. Quenching studies on gold and platinum by Gertsriken and Novikov (1960) indicated that dislocations were likely candidates for vacancy sources. In addition, it is the presence of dislocations in sub-grain boundaries that lead to these structures being vacancy sources and sinks (e.g. Gleiter

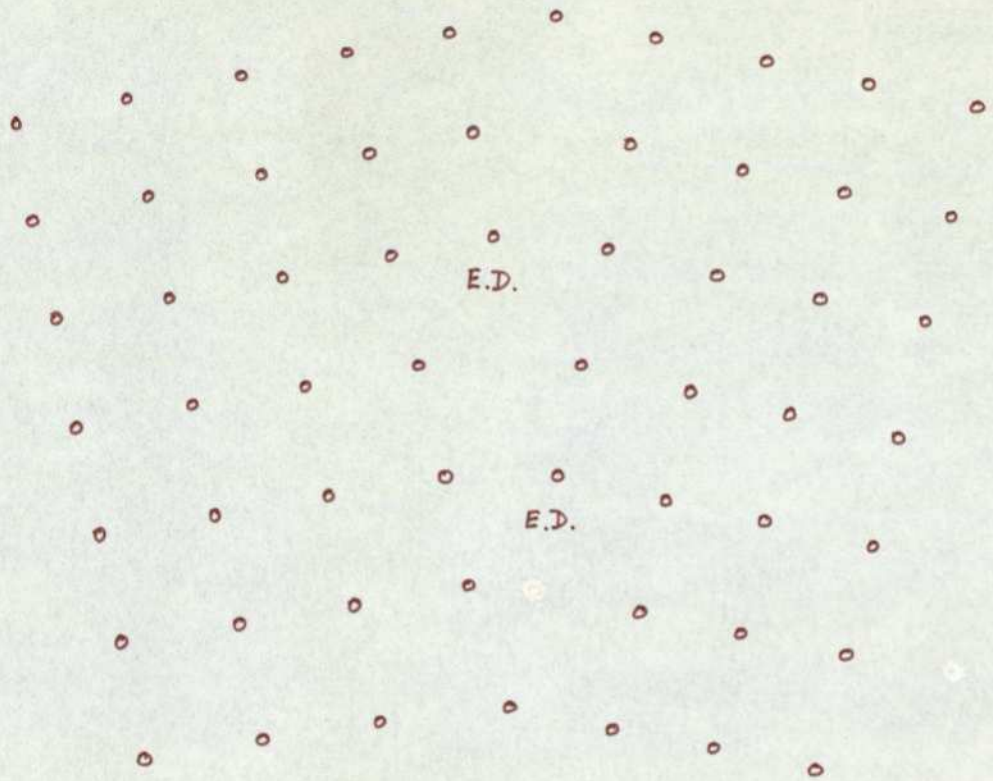

Fig.6.3. Sub-grain boundary made up of line dislocations.

(1979)). Theoretical considerations also point to this conclusion.

As pointed out by Balluffi and Seidman (1965b), dislocation climb is a special case of linear internal crystal growth or dissolution and the climb rate (and hence the efficiency with which they act as source/sinks) depends upon, among other things,the driving chemical potential. In the review of vacancy production/ destruction experiments, they noted that for vacancy driving chemical potentials in the range $\sim 10^{-5}$eV to 0.67eV, the corresponding efficiency of the dislocations (related to the diffusion limited case) was $\sim 10^{-3}$ to 1. The estimated maximum chemical potential operating in the present experiments with a temperature excursion of ~10K is 10^{-3}eV, thus indicating that it is to be expected that dislocations act as vacancy source/sinks.

Lomer (1958) has shown theoretically that dislocations can act as source/sinks with suitable vacancy super/subsaturations, the condition being

$$\ln \left(\frac{c}{c_o}\right) > 40 \frac{b}{l} \qquad 6.5.$$

where b is the Burgers Vector,,

2l the dislocation length,

c_o the equilibrium vacancy concentration

and c the actual vacancy concentration.

Making a linear approximation, a temperature excursion of 10K about a mean of 1500K-2000K would cause

a super/subsaturation of $\sim 5\%$, then the dislocation must be 1μm long to act as a source/sink. Thus theoretically, dislocations are capable of acting as source/sinks in the present experiments.

A rough, theoretical analysis has also been given by Bardeen and Herring (1952), the average distance a vacancy can diffuse being given by

$$L = d\sqrt{f} \qquad 6.6.$$

where L is the diffusion distance per jump,
f the number of jumps made by the vacancy during its lifetime,
and d the jump distance.

Typically $d \sim 3 \times 10^{-8}$cm, $f \sim 10^{9}$, then $L \sim 10^{-3}$cm. A well-annealed wire has a dislocation density of 10^{8}cm^{-2} and this in conjunction with the diffusion distance indicates that a vacancy be destroyed one meeting with a dislocation in a hundred. This does not take into account the attractive force that exists between a vacancy and dislocation, so the number of times a vacancy meets a dislocation before destruction is probably less than a hundred. Seeger and Mehrer (1970) have calculated the jump frequency for platinum to be 2.1×10^{12}Hz, therefore using these values the lifetimes ofvacancies in platinum is of the order of 1ms. This is in agreement, in general, with the accepted vacancy lifetimes and hence this rough treatment shows, again, that dislocations can act as vacancy sinks.

Hence three separate approaches show that it is to be expected, under the conditions of the present work, that dislocations will act as the sources and sinks of vacancies. In view of the importance of dislocations in one form or another as vacancy source/sinks, the means by which they operate shall be reviewed.

Both edge and screw dislocations can emit vacancies, but under different circumstances due to the different character of jogs on edge and screw dislocations. The fundamental difference between edge and screw dislocations is that the Burgers Vector is normal to the dislocation for an edge dislocation and parallel for a screw.

The differences for jogs on each type of dislocation are that those on edge dislocations are screw in character and vice versa. Therefore during dislocation glide, which is in the direction of the Burgers Vector by definition, jogs have no effect on edge dislocations but tend to pin screw dislocations at points along their length. The screw dislocations will bow out increasing the length of the dislocation until increased line tension equals the formation energy of a vacancy, whereupon the jog will be dragged along emitting a row of vacancies or interstitials depending on the sign of the dislocation and its direction of movement. This means of vacancy production only occurs at relatively high applied stresses or temperature excursions.

The second means of dislocation movement is dislocation climb and is defined as movement perpendicular to the Burgers Vector. This means of movement requires the addition or subtraction of atoms from the line of the dislocation causing, in the case of an edge dislocation, movement out of its slip plane. This type of movement occurs only at high temperatures due to the presence of point defects (vacancies or interstitials) and ease of diffusion.

In practice only one or two atoms at a time are added to or subtracted from the edge dislocation, each step being a jog. For instance Fig.6.4. shows three atoms added to an edge dislocation producing two jogs. It is clear that if a fourth atom should be added to the end, the jog will have moved along the dislocation or, alternatively, another section of the dislocation will have climbed. In the process an atom will have been absorbed : either emitting a vacancy or absorbing an interstitial.

The climb of a screw dislocation is far more complicated and has been studied by Thomson and Balluffi (1962). Initially, for positive climb, the aggregation of vacancies onto a screw dislocation cause it to adopt a helical structure. This structure is a mixed dislocation made up of screw and edge components : if the edge component is large enough, subsequent climb will be by edge dislocation climb, thus increasing the radius of the helix.

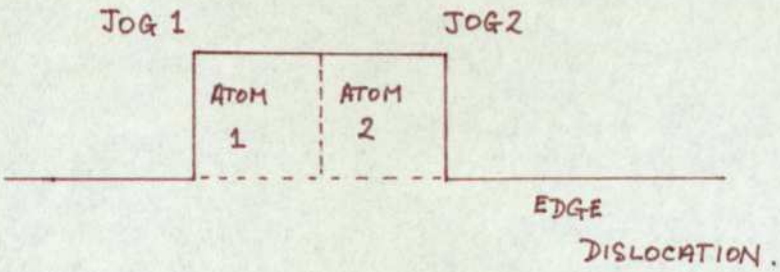

Fig.6.4. An edge dislocation with two jogs.

As mentioned above, it is well known that vacancies (and for that matter interstitials) can only be emitted or absorbed at jogs on dislocations. A kinetic theory for dislocation climb has been developed by Thomson and Balluffi (1962) by considering edge dislocations climb as the growth of extra rows of defects on the extra plane bounded by jogs. They considered only unconstrained climb but concluded that this model could be used when there is pining and line curvature. This theory has been used to analyse positive and negative climb of edge dislocations near and far from vacancy concentrations by Balluffi and Thomson (1962). They found that the climb rate was dependent upon the equilibrium vacancy flux and the lattice supersaturation of vacancies. The effect of climb motion on climb rate was analysed by Balluffi and Seidman (1965a) for the condition of diffusion being the rate limiting factor. Under these conditions they concluded that dislocations are acting as efficient source/sinks, because if the diffusion of vacancies away from the dislocation is slow, an equilibrium concentration will be produced around the jogs. The velocity of the dislocation is then determined solely by the diffusion of the vacancies and not by their emission or absorption at jogs.

For vacancy emission to be rapid enough for diffusion to be the rate limiting factor, two conditions are necessary : firstly the sites at which vacancies can be emitted (i.e. jogs) must be frequent and close together. Secondly, the movement of the vacancy along

the core of the dislocation to a suitable emission site must be rapid. The presence of enhanced diffusion along the core of a dislocation is well known and termed pipe diffusion. For instance Campbell et al (1975) diffused arsenic in a silicon sample which had been treated to have dislocations perpendicular to the diffusion surface. The result was diffusion in the same direction as the dislocations and very little sideways diffusion. Also Mimkes(1975) has applied the complete solution for pipe diffusion in F.C.C. metals to experimental data for different metals. He concluded that for (100) dislocations a vacancy mechanism is responsible for the experimental observations, however, for (110) dislocations this mechanism is inadequate due to the dissociation of these dislocations into partial dislocations. Partial dislocations are two instead of one extra plane inserted in the crystal with the slip plane in the ⟨110⟩ direction thus ensuring the continuity of the stacking order above and below the slip plane (see Fig.6.5.) However, like dislocations are subject to a repulsive force leading to independent movement of each partial and thus producing a stacking fault ribbon. The core region of the partials tend to be weaker and less disorder than in full dislocations, and the diameter of the pipe is of order of the width of the stacking fault ribbon. In fact as Mimkes(1975) pointed out, [100] dislocation pipes have an activation enthalpy for pipe diffusion less than or equal to diffusion in the crystal bulk, [110] dislocation pipes have a higher activation enthalpy indicating

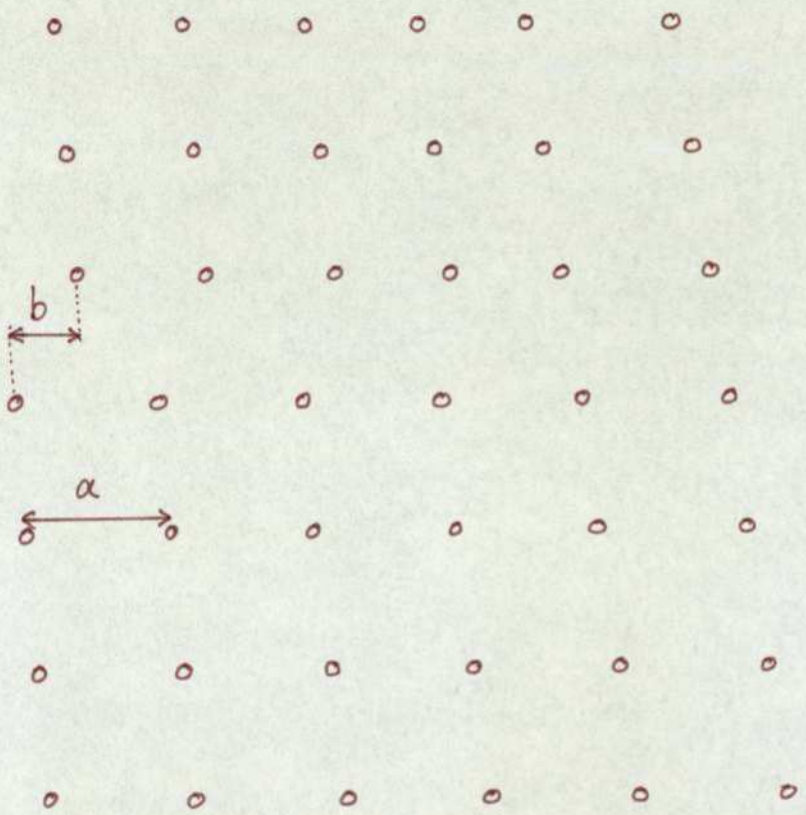

Fig.6.5. Partial dislocation.

a mechanism other than vacancies.

Instead of the rate controlling factor being diffusion from the dislocation, it is possible for the rate controlling factor to be the emission (or absorption) of vacancies at the dislocation (i.e. the jogs are not saturated with vacancies). In fact Friedel (1964) has stated that the saturation of jogs in thermal equilibrium only occurs at high temperatures (typically $> \frac{1}{4}T_m$) and saturation does not occur during climb of dispersed dislocations. This means that the dislocations are not acting as ideally efficient vacancy source/sinks and that the rate controlling factor is no longer diffusion of vacancies to or from the core but the production or destruction process at the jog. On the other hand pulse heating and quenching experiments on platinum to study the formation kinetics have been performed by Sizmann and Wenzl (1963) who concluded that diffusion was the rate controlling process, i.e. the dislocations were ideally efficient. This conclusion is supported by similar studies on gold by Jackson and Koehler (1960). In this type of study it is clear that the driving chemical potential is high and in quenching experiments generally, this potential is high enough for the dislocations to act as efficient source/sinks (Balluffi and Seidman (1965a)). However, under the conditions of the present experiments the ~10K temperature excursion will be unable to produce driving chemical potentials comparable with those produced during quenching. Therefore it is to be expected that the dislocations will act as sources

and sinks of vacancies at reduced efficiency, and that the rate controlling process will be the production/ destruction mechanism for the vacancies.

6.5. Comparison with previous experiments.

The present results may be used to obtain an estimate for the vacancy concentration in platinum by means of comparison with the theoretical predictions with which they are in good agreement. This, then, would imply a vacancy concentration of ~0.1% and in principle this method gives an opportunity of estimating vacancy contributions unambiguously under quasi-equilibrium conditions. In addition, the lifetime of vacancies and some idea of the vacancy kinetics can also be deduced by comparison with theory.

6.5.1. Vacancy Concentration Results

The present technique is fundamentally different from other modulation experiments performed with the express aim of deducing vacancy parameters. The basic philosophy of previous modulation experiments is to measure a physical parameter which it is thought has a measurable vacancy component (usually the specific heat but also the coefficients of resistivity and expansion), then extrapolate low and medium temperature dependence to the high temperature region. The high temperature curvature being attributed solely to the vacancy contribution. This technique is attributed to Kraftmakher and Strelkov (1962).

As mentioned in Chapter 1 there are a number of experimental methods for determining the vacancy concentration.

For comparison, shown below is a review of the experimental determination of the vacancy concentration at the melting point for a variety of metals by a variety of methods.

Table 6.2. shows the vacancy concentration for a range of elements along with the crystal structure and method of determination.

Element	Structure	Melting point (K)	Vacancy Concentration at T_m(%)	Method	Author Number +
Gold	F.C.C.	1336	0.07	X-ray parameter	1
			0.045	Stored energy	2
			0.21	" "	3
			0.4	Specific heat *	4
Copper	F.C.C.	1356	0.02	X-ray parameter	5
			0.5	Specific heat *	6
Titanium	F.C.C.(at high temp)	1943	1.7	Specific heat *	7
Zirconium	F.C.C.(at high temp)		0.7	Specific heat *	8
Niobium	F.C.C.	2698	1.2	Specific heat *	9
			2.7	Enthalpy measurement	10
Molybdenum	B.C.C.	2893	4.3	Specific heat *	11
Tantalum	B.C.C.	3273	0.8	Specific heat *	9
Tungsten	B.C.C.	3660	3.4	Specific heat *	12

Element	Structure	Melting point (K)	Vacancy Concentration at T_m(%)	Method	Author Number +
Platinum	F.C.C.	2045	1	Specific heat *	13
			0.8	Thermal expansion *	14
			0.1	Specific heat +	15
Caesium	B.C.C.	301	0.26	Specific heat	16
Potassium	B.C.C.	336	0.48	Adiabatic calorimetry	17
Sodium	B.C.C.	373	0.76	Adiabatic calorimetry	17
			0.38	Specific heat	18
			0.22	" "	18
			0.1	Thermal expansion	19,20
Lead	F.C.C.	600	0.2	Specific heat	21
			0.015	Thermal expansion	22
Aluminium	F.C.C.	933	0.2	Specific heat	21
			0.1	Thermal expansion	23
			0.09	X-ray parameter	24
			0.03	Thermal expansion	22
			0.06	Enthalpy measurement	25
Silver	F.C.C.	1233	0.017	X-ray parameter	24

+ Author list:

1. Simmons and Balluffi (1962)
2. DeSorbo (1960)
3. Pervakov and Khotkevic (1960)
4. Kraftmakher and Strelkov (1966a)
5. Simmons and Balluffi (1963)
6. Kraftmakher (1967c)
7. Sestopal (1965)
8. Kamel and Kraftmakher (1966)
9. Kraftmakher (1963a)
10. Kirillin et al (1965)
11. Kraftmakher (1964)
12. Kraftmakher and Strelkov (1962)
13. Kraftmakher and Lanina (1965)
14. Kraftmakher (1967b)
15. Seville (1974)
16. Filby and Martin (1965)
17. Carpenter et al (1938)
18. Martin (1967)
19. Sullivan and Weymouth (1964)
20. Feder and Charbnau (1966)
21. Pochapsky (1953)
22. Feder and Nowick (1958)
23. Nenno and Kauffman (1959)
24. Simmons and Balluffi (1960)
25. Guarini and Schiavini (1966)

Results marked * denote modulation experiments in which the extrapolation from low and medium to high temperatures is used to deduce the vacancy concentration.

The result marked + (Seville 1974) is a modulation experiment in which the vacancy concentration is derived by considering the lack of frequency dependence of the specific heat and is considered in some detail later.

The first point to note is that elements for which vacancy concentrations have been derived by a variety of methods show a remarkable spread in the results obtained, e.g. gold and sodium in particular. It is interesting, however, that where a comparison with a modulation experiment is possible, the modulation experiment tends to give a larger value for the vacancy concentration than that obtained by another method. The exception is niobium, where the drop calorimetry method has given a vacancy concentration of nearly three percent. Kraftmakher and Strelkov (1970) have pointed out that the formation enthalpy due to vacancies measured by extrapolation is a small part of the total enthalpy of the sample. Therefore they deduce that the drop calorimetry method is an inaccurate method of determining vacancy concentrations.

The higher vacancy concentrations obtained by the extrapolation technique compared with those results obtained by a variety of other methods tends to experimentally question the validity of this technique. The assumptions of a linear extrapolation to higher temperatures to provide vacancy concentrations is discussed in subsection 6.5.2.

9.5.2. Extrapolation Method Assumptions

There are three main areas where the extrapolation method may not be valid, these are a) the anharmonic forces acting on the atoms of the lattice, b) the variation of the electronic specific heat with

temperature at temperatures above $^2/_3\ T_m$ amd c) the variation of the coefficient of thermal expansion at high temperatures.

Dealing with these three main areas in turn:

a) The linear extrapolation of the specific heat from low temperatures assumes that the anharmonic forces of the lattice increase linearly with temperature, in his review on the subject Hoch (1970) pointed out that there is a cubic temperature term at high enough temperatures. The equation can be fitted to the specific heat results of chromium, molybdenum, tungsten, niobium, rhenium, copper and aluminium to within 1% accuracy.

b) The variation of the electronic specific heat with temperature is a function of the Fermi Surface of the metal under consideration and the density of states within a region kT of the Fermi Surface. As pointed out by Seville (1972), for a metal for which the free electron approximation is good the variation of electronic specific heat with temperature is linear, contributing up to 1% of the total specific heat at the melting point. However, as was considered in Chapter 1, the band structure of the Transition Elements is complicated and the free electron approximation does not hold for them. Fig.6.6. shows the density of states for the F.C.C. phases of chromium, manganese, iron, cobalt, nickel and copper in the two possible configurations s^1d^{n+1} and s^2d^n. It is clear that in cobalt and nickel the Fermi Energy is either on the edge of a sharp decrease in the

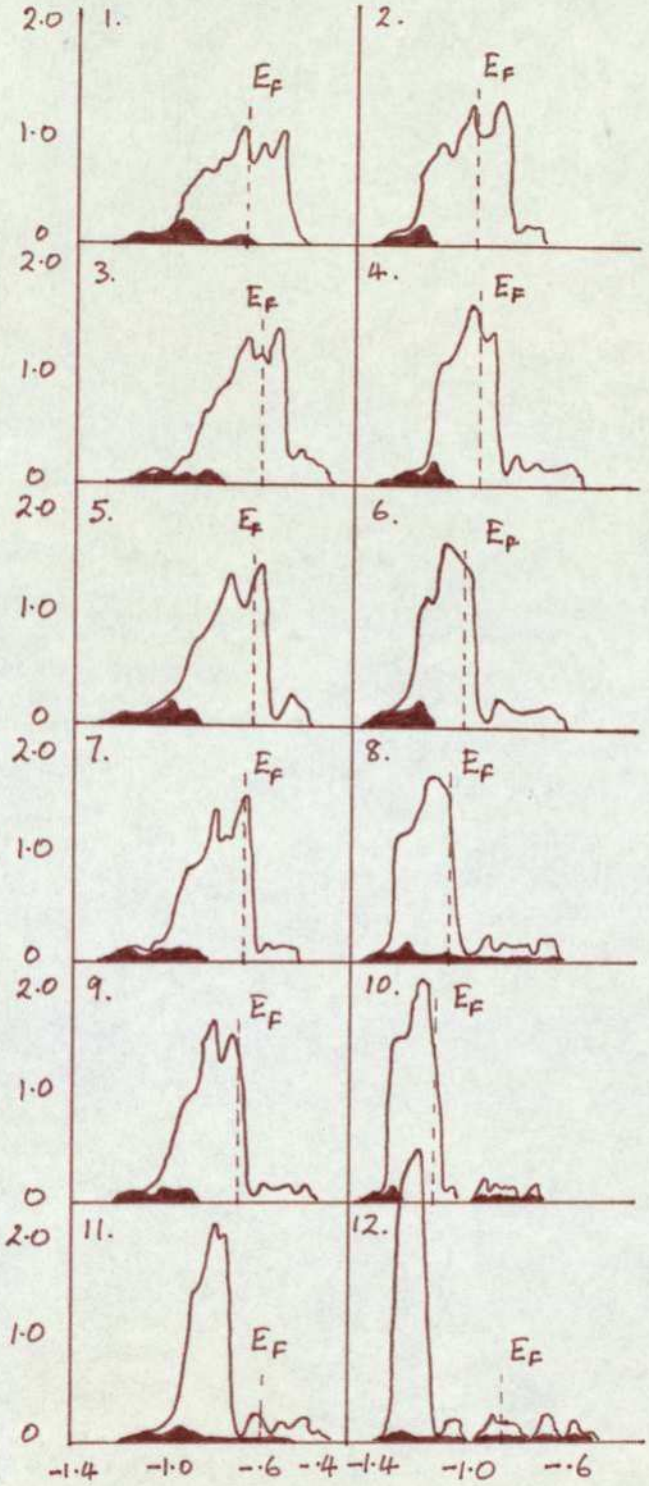

Fig.6.6. Density of states as a function of energy for a series of Transition Elements showing the Fermi energies.

Key to Fig.6.6.

1.	Chromium	$3d^5 4s^1$
2.	Chromium	$3d^4 4s^2$
3.	Manganese	$3d^6 4s^1$
4.	Manganese	$3d^5 4s^2$
5.	Iron	$3d^7 4s^1$
6.	Iron	$3d^6 4s^2$
7.	Cobalt	$3d^8 4s^1$
8.	Cobalt	$3d^7 4s^2$
9.	Nickel	$3d^9 4s^1$
10.	Nickel	$3d^8 4s^2$
11.	Copper	$3d^{10} 4s^1$
12.	Copper	$3d^9 4s^2$

The density of states curves comprise of two parts : the outline areas are the d-like portions, the smaller, filled in areas are the s-like portions.

density of states or else actually on the decrease. It would seem, then, that for these only a restricted number of electrons within a region kT below the Fermi Energy would be capable of contributing to the electronic specific heat. Chromium, manganese and iron, on the other hand, have their Fermi Energy in a relatively flat region of the density of states plot. For these elements it would be possible for all electrons below kT of the Fermi Energy to contribute to the electronic specific heat. Thus these three elements would have a greater electronic specific heat than cobalt and nickel which in turn would have a greater electronic specific heat than copper which, although the density of states plot is flat, has a considerably smaller number of electrons within kT below the Fermi Energy than any of the other five. It is to be expected that those elements with a relatively flat density of states plot will have a linear dependence of electronic specific heat upon temperature even though the free electron approximation is not necessarily good. This is borne out by Hoch (1970) (section a) in the case of chromium and the corresponding elements in the second and third transitions in that the anharmonic lattice forces can account for ~99% of the specific heat curvature implying a linear electronic contribution. For elements like cobalt and nickel especially, where the density of states is a strongly varying function of temperature, the electronic specific heat will not vary linearly with temperature but will be some complex function of temperature.

In particular for these elements, since the Fermi Energy is on the negative going edge of the density of states, the rate of increase of the electronic specific heat will decrease with temperature, possibly countering an upward curvature in the specific heat due to anharmonic lattice vibrations.

The conclusion is that generalisations of the electronic specific heat of individual metals is difficult: depending upon the density of states and shape of the plot in the region of the Fermi Energy as it does. It is therefore rash to extrapolate linearly from low temperatures.

c) Similarly for the high temperature dependence of the coefficient of thermal expansion. This has been dealt with by Seville (1972): the relationship between the specific heat at constant volume, constant pressure and the coefficient of thermal expansion is

$$c_p = c_v + \frac{(3\lambda)^2 VT}{k_T} \qquad 6.7.$$

where c_p is the specific heat at constant pressure, c_v is that at constant volume, λ is the coeffient of thermal expansion, V is the volume, T the absolute temperature and k_T the isothermal compressibility.

It is accepted that V/k_T is independent of temperature (Lowenthal (1962)) and is linearly dependent upon temperature, therefore there is a cubic term in temperature superimposed on the specific heat at constant volume.

Using equation 6.7. and experimental values of the coefficient of thermal expansion extrapolated to high temperature, Seville (1972) has shown that the greater part of the high temperature specific heat curvature can be attributed to thermal expansion.

In conclusion, these three queries show that it is very rash to extrapolate from low and medium temperatures certainly without a detailed study of the anharmonic lattice forces, Fermi Surface/band structure and thermal expansion properties of the metal under consideration. As was mentioned in part b) the electronic specific heat variation could compensate for any anharmonic effects and expansion effects. However, under the conditions that this extrapolation procedure is used any such compansation would be fortuitous.

6.5.3. Vacancy Lifetimes in Platinum.

Seville (1974) performed a modulation experiment on platinum using frequencies in the range 100Hz to 1 kHz and in doing so demonstrated that there was no frequency dependence of the specific heat in this range. He interpreted this result as showing that the contribution of vacancies to the total specific heat to be $<1\%$ in preference to the lifetime of a vacancy being such that the frequency effect was above 1kHz. The former interpretation implies a vacancy concentration of $\sim 0.1\%$ - roughly an order of magnitude less than that obtained by the extrapolation from low temperatures method. The latter interpretation implies a vacancy lifetime of $\sim 40\mu s$ -

lifetimes of this order of magnitude and lower have been observed in quenching experiments : Gertsriken and Novikov (1960) measured a vacancy lifetime for platinum at 1850K of ~4μs, however this low lifetime is almost certainly due to the plastic straining that occurs at very rapid quenching from high temperatures. This view is supported by the work of Jackson (1965) who quenched from low temperatures to reduce the effect of plastic straining, these low temperature results were extrapolated to 1850K to give a vacancy lifetime of ~400μs.

The vacancy lifetime under the conditions of a modulation experiment are likely to be larger than this for these reasons. Firstly because even a low temperature quench will introduce a certain amount of plastic straining, secondly because the chemical potential (driving force) for the production of vacancies is orders of magnitude larger during low temperature quenchs than during modulation experiments and thirdly because of the particular difficulties in extrapolating low temperature results to high temperatures.

In addition the results of Heigl and Sizmann (1972) are again of relevance : they performed pulse heating experiments on platinum, raising the temperature to ~1200K for a range of durations before quenching. The quenched in resistance was then measured to determine the vacancy kinetics. The result suggested a quasi-planar distribution of source/sinks of ~5μm separation. Seville (1974) has used the method proposed by Van den Sype (1965) to calculate the vacancy lifetime based upon

the distribution of source/sinks suggested by Heigl and Sizmann (1972) : the result is a lifetime of ~1.5ms at 1850K. These calculations are also subject to errors due to the fact that the experiment was performed under conditions of large chemical driving potential and, as before, in extrapolating to higher temperatures the extrapolation is from $<^2/_3$Tm to ~Tm i.e. from the low diffusion temperature region to temperatures of high vacancy mobility. There is the possibility that a greater number and more efficient sources and sinks operate to account for thesignificance of diffusion at high temperatures.

These two factors would tend to under estimate the vacancy lifetime again. However, there is a factor that would work in the opposite direction : that is, the concentration of bulk defects, primarily dislocations , that act as sources and sinks would also be dependent upon the time of pulsing. This would effectively reduce the chemical potential and reduce the overall lifetime underestimate.

It would seem, from the discussion above, that a vacancy lifetime of 40μs, although not impossible, is almost certainly too small by at least an order of magnitude. This implies that the lack of frequency dependence of the specific heat up to 1kHz is due to a vacancy concentration of ~0.1%.

6.5.4. Polyvacancy Source/Sinks.

Kraftmakher (1977) supported the view of a short vacancy lifetime and large (1%) vacancy concentrations by

advocating polyvacancies, i.e. clusters, as vacancy source/sinks capable of providing short lifetimes. This is at variance with Polak (1967) who concluded that the ratio of monovacancies to divacancies is consistent with the theoretical distribution, i.e. that the ratio of monovacancies to divacancies is $\sim 40 : 1$. For instance, for gold the ratio of mono to divacancies at a range of temperatures and binding energies has been calculated by Kimura and Maddin (1971).

Table 6.3.

Binding energy (eV)	C_{2v}/C_{1v} 300K	500K	1000K	1200K
0.1	8×10^{-14}	4×10^{-8}	8×10^{-4}	4×10^{-3}
0.2	3.2×10^{-12}	4×10^{-7}	2.5×10^{-7}	1×10^{-2}
0.3	1.6×10^{-10}	4×10^{-6}	4×10^{-6}	2.9×10^{-2}

Therefore, the concentration of polyvacancies is likely to be extremely low. However, even if the polyvacancy concentration was high enough to act as significant source/sinks this mechanism could not possibly account for the enhanced specific heat curve at high temperatures. This is because the formation energy of a monovacancy from a polyvacancy is just the binding energy between them. Fig.6.7. shows the theoretical configurations of a tetravacancy and pentavacancy in an F.C.C. lattice due to Vineyard (1961). The most stable configuration of a tetravacancy is 0.7eV and that of a pentavacancy is 1.5eV. These energies refer to the lowering of the total energy by combining the individual vacancies into a polyvacancy. Therefore to create a monovacancy from the most stable

TETRAVACANCY.

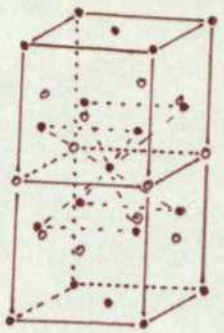

BINDING ENERGY = 0·7eV

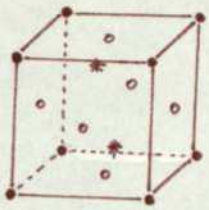

BINDING ENERGY = 0·6eV

PENTAVACANCY.

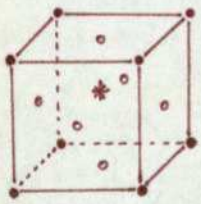

BINDING ENERGY = 1·5eV

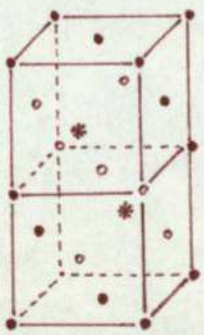

BINDING ENERGY = 0·9eV

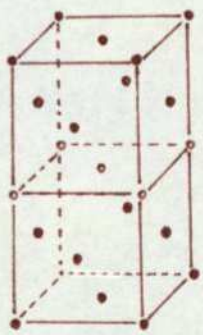

BINDING ENERGY = 0·7eV

KEY:

- • ATOM.
- o VACANCY.
- * RELAXED ATOM.

Fig.6.7. Theoretical tetravacancy and pentavacancy configurations in an F.C.C. lattice.

pentavacancy to leave the most stable form of a tetravacancy will require ~0.8eV. The accepted formation energy of a vacancy in platinum is ~1.5eV and though the results of Vineyard (1961) are for a general F.C.C. crystal, it is clear that the formation energy of a vacancy from this cause would be roughly halved. Therefore, although in principle this mechanism could provide vacancies of short lifetime to explain the lack of frequency effect at 1kHz, it would considerably reduce the vacancy contribution to the specific heat thereby making an explanation of the enhanced high temperature specific heat in terms of vacancy formation highly unlikely.

This is supported by the present results : the agreement with theory indicating a vacancy concentration of ~0.1% and the shape of the frequency v. the percentage decrease in the temperature coefficient of resistivity graph indicating a vacancy lifetime of ~1ms. These results are in direct disagreement with Kraftmakher's (1977) support of high vacancy concentrations and short vacancy lifetimes particularly in platinum. Consequently they imply that the extrapolation of low and medium temperature dependence to high temperatures is not a generally valid procedure, although it could be for individual elements if the high temperature effects discussed in subsection 6.5.2. act to cancel one another out.

6.5.5. Comparison with previous Frequency Dependent Results.

It has just been shown that the present results are, in general terms, in agreement with the idea of low vacancy concentration and long vacancy lifetime. A comparison is also possible, in detailed terms, with other results implying low concentrations and long lifetimes.

Seville (1974) compared results for the specific heat of platinum obtained by two differing modulation methods, the difference being the way in which the temperature excursions were measured : Kraftmakher and Lanina (1965) measured the temperature coefficient of resistivity, Seville (1974) measured the modulation of the emitted light and Zinov'ev et al (1971) used both methods. The results of Kraftmakher and Lanina (1965) and Zinov'ev et al (1971) were obtained at a modulating frequency of 30Hz, those of Seville (1974) over the range 100Hz to 1kHz.

If frequency effects were important at 30Hz in measurements using the temperature coefficient of resistivity, then a discrepancy is to be expected between these two methods. The comparison was made by using the parameter $^{c}p/\alpha_{(w)}$: where c_p is the specific heat and (w) the temperature coefficient of resistivity at frequency f ($w=2\pi f$). In the case of the use of the temperature coefficient of resistivity measurements, the values used were those at $w = 0$ rads^{-1} whereas the values used should have been at $w = 190$ rads^{-1}. By dividing the value

for the specific heat by the value for the temperature coefficient of resistivity used by Kraftmakher and Lanina (1965) and Zinov'ev et al (1971) $^{c}p/\alpha_{(190)}$ is generated. These are compared with the corresponding emitted light results by dividing them by the w=0 rads^{-1} value of the temperature coefficient of resistivity. A difference would indicate a frequency effect at 30Hz.

The comparison graph produced by Seville (1974) is shown in Fig.6.8. and, as is to be expected if there is a relaxation effect at 30Hz, the values of $^{c}p/\alpha_{(190)}$ are higher than those of $^{c}p/\alpha_{(0)}$. The discrepancy between the emitted light methods is large - those of Zinov'ev et al (1971) being far lower than expected. A reason for this could be the periodic heating causing mechanical oscillations in phase with the emitted light - therefore the phase sensitive detector used would not remove this effect. This effect was considered in detail by Seville (1972) but no mention of it is found in the description of their work by Zinov'ev et al (1971). The emitted light results of Zinov'ev et al (1971) are doubtful, then, on the grounds of experimental technique.

However if the error bars for the three remaining results are compared it can be seen that up to the experimental point at the highest temperature shown, the error bars for each overlap. Therefore at no point can it be said that one experimental curve is outside the error bars of the others.

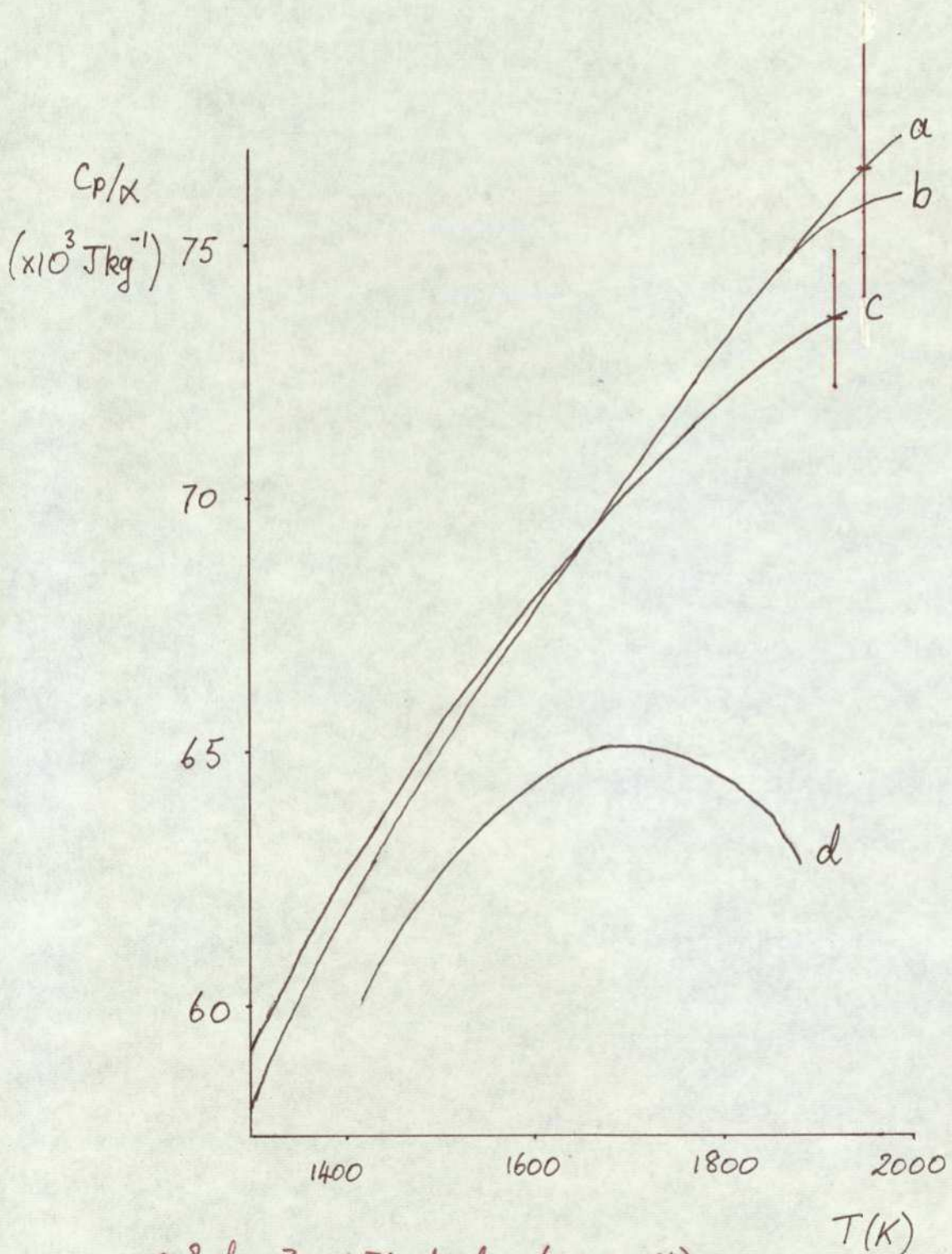

a & d ZINOVIEV et al. (ERROR 4%).
b KRAFTMAKHER & LANINA. (ERROR 2%).
c SEVILLE. (ERROR 2%).

Fig.6.8. Comparison of $^{c}p/\alpha$ for platinum from two experimental techniques

There is consequently, no significant relaxation effect at a modulating frequency of 30Hz and this is in agreement with present results.

6.6. Further Work

This section discusses possible applications of this type of modulation experiment, i.e. that measures the frequency dependence of the temperature coefficient of resistivity (or some other appropriate physical parameter). In particular, the type of material to which this study can be applied will be discussed and also the two classes of modulation experiment that can be used. These are, firstly, low frequency measurements performed in order to compare, for instance, the temperature coefficient of resistivity of alloys with the pure element (this is the type of study discussed by Kraftmakher (1973a,b) in his reviews. Secondly, the novel uses to which frequency dependent measurements can be put in order to understand something of vacancy kinetics in alloys and the pure element.

6.6.1. Range of Applicability.

The range of samples to which this type of modulation method is applicable can be judged by considering some of the reasons why platinum was deemed suitable in section 1.5.

1. No phase transitions over the temperature range of interest (unless the experiment has as its goal the determination of vacancy kinetics just either side

of the transition temperature).

2. Samples obtainable at high purity.

3. Can be manufactured to wire samples of, typically, 50μm diameter.

4. All the physical quantities required are known over the temperature range of interest. (For instance, in the present case the specific heat had to be known up to 1800K).

6.6.2. Low Frequency Experiments.

These experiments are those that are ordinarily made, i.e. modulating frequencies are used such that no vacancy relaxation effects are manifest. The proposal would be to use results obtained from these experiments as a first step in understanding the variation in the mechanical properties between alloys. The result would be, for instance, a set of low frequency temperature coefficient of resistivity as a function of temperature curves, one for each sample of alloy. In the case of rhodium-platinum alloys, there could be some change in the temperature coefficient of resistivity as a function of temperature as the proportion of rhodium is increased. Rhodium is also a face centred cubic transition element with an unusual Fermi Surface but made up of five components (Coleridge (1965,1966)) instead of platinum's three. It is to be expected that rhodium has an unusual temperature coefficient of resistivity graph but the transition from pure platinum to pure rhodium would be of interest.

It is important to realise that to obtain absolute values for the temperature coefficient of resistivity in these alloys their specific heat at the temperature of interest must first be measured.

6.6.3. Frequency Dependence Experiments.

This type of modulation experiment measures the dependence of the parameter being studied on the modulating frequency. The present experiment is one of this type.

Basically, these experiments can be used to study the vacancy kinetics in the sample in question. The power of this technique is in its application to the study of the vacancy kinetics in a series of related samples. In the present case, having obtained information about the vacancy kinetics in platinum, the next logical step would be to extend it to studies of platinum alloys. In particular, comparative studies of 10%, 20% and 40% rhodium-platinum alloys might be made to gain insight into the increase in the high temperature strength (high temperature creep resistance) of these alloys (Selman and Bourne (1972)).

It is relevant at this point to discuss the role of vacancies in high temperature creep and thus indicate the interest in the comparative studies mentioned above.

Creep can be defined as unidirectional plastic deformation and as such is present whenever a sample is

stressed, even if it is only by its own weight. It occurs by the movement of planes of the crystal lattice relative to one another. The mechanism by which this occurs is the movement of dislocations and as was discussed earlier in this chapter (section 6.4.4.) this is by means of the emission or absorption of vacancies. Therefore, at high temperatures where creep is important, the creep resistance of an element or alloy would depend upon the vacancy kinetics. However, since the creep resistance is a maximum for rhodium concentrations of 20%-25% in platinum (Selman and Bourne (1972)), a comparative study of platinum and rhodium-platinum alloys as mentioned above could yield interesting differences in the vacancy kinetics of these alloys.

It is not known how the increased creep resistance of 20% rhodium-platinum would manifest itself in the present type of experiment because the vacancies could show their effect in different ways :

1. A decrease in the equilibrium concentration of vacancies in this alloy. This does not seem likely because it implies that the concentrations at 10% and 40% rhodium-platinum alloys are higher and that there is not, as may be expected, a smooth change from the concentration in pure platinum to that in pure rhodium.

2. Similar vacancy concentrations of all the alloys, but a decrease in vacancy mobility in the 20% rhodium-platinum alloy. This could be due to the pining of vacancies by the stress fields caused by the rhodium

atoms thus impeding their progress. This would lead to a lengthening of the vacancy lifetimes.

3. Again, similar vacancy concentrations in all alloys, but pining of dislocations at rhodium atoms in 20% rhodium-platinum alloys. This restriction of the climb of the dislocations would manifest itself as a decrease in vacancy source/sink efficiency.

Both these last two options are probably operating (it is difficult to envisage one operating but not the other) but would be indistinguishable using the present technique. A decrease in mobility and/or source/sink efficiency would result in a lowering of the modulating frequency at which a frequency effect is measured. There is the possibility that only a proportion of the vacancies might be pined giving rise to more than one relaxation time.

There is also the possibility that the efficiency of the internal source/sinks is so reduced by the impurity alloy that the sample surface becomes the vacancy source/sink. This has been found by Bokshtein et al (1968) in aluminium and lead samples of 99.99% and 99.9% purity respectively and Al + 1.7 at % Cu alloy. However, if this were the case with rhodium-platinum alloys, one would expect an increased creep resistance for a small amount of impurity, caused by dislocation pining. Increasing the impurity concentration would not result in an appreciable increase in creep resistance. However, the nature of the impurity could be of importance.

It is important to note that since the specific heat of the alloys is not known over the temperature range of interest, measurements will have to be made of α/c_p following Seville (1974) to obtain the required information.

Comparative experiments of the type described above will give information of the role of vacancies in the creep and creep resistance of metals.

6.7. Summary

This chapter contains the discussion of the results obtained using a modulation method to determine the temperature coefficient of resistivity at temperatures in the range 1400K - 1800K at various modulation frequencies (20Hz-180Hz).

The low frequency results were compared with those of Kraftmakher and Sushakova (1973) : the shape of both being similar, but the present results are displaced to higher values. This was explained by the use of purer samples in the present study than in that of Kraftmakher and Sushakova (1973).

The high frequency results were compared with theoretical predictions and the conclusion was reached that dislocations act as vacancy source/sinks in platinum and that vacancy lifetimes are of the order of 1ms at 1800K. This value was discussed in relation to vacancy lifetimes obtained by other works and shown to be compatible.

Finally, suggestions were made for further work. These consisted of firstly, low frequency experiments (in conjunction with specific heat results) to gain information about the transition of pure platinum to pure rhodium. Secondly, frequency dependent results of α/c_p could be used to obtain an insight into the enhanced creep resistance of 20% rhodium-platinum and extended to creep resistance studies, in suitable materials, in general.

References

Balluffi, R.W., Lie, K.H., Seidman, D.N. and Siegel, R.W., "Determination of concentrations and formation energies and entropies of vacancy defects from quenching experiments" in "Vacancies and Interstitials in Metals", ed. Seeger et al., North-Holland, Amsterdam, 125, 1970.

Balluffi, R.W. and Seidman, D.N.,J. Appl. Phys., 36, No.9, 2708, 1965a.

Balluffi, R.W. and Seidman, D.N., Bull. Am. Phys. Soc., 10, 697, 1965b.

Balluffi, R.W. and Thomson, R.M., J. Appl. Phys., 33, No.3, 817, 1962.

Bardeen, J. and Herring, C., "Diffusion and the Kirkendall Effect" in "Imperfections in Nearly Perfect Crystals", ed. Schockley et al., John Wiley & Sons, Inc., New York, 275, 1952.

Bokshtein, B.S., Bokshtein, S.Z., Shukhovitskii, A.A., Kishkin, S.I., Kornelyuk, L.G. and Nechaev, Yu.S., Dokl. Akad. Nauk SSSR, 183, 1280, 1968.

Campbell, D.R., Tu, K.N. and Schwenken, R.O., Thin Solid Films, 25, 210, 1975.

Carpenter, L.G., Harle, T.F. and Steward, C.J., Nature, 141, 1015, 1938.

Coleridge, P.T., Phys. Lett., 15, 223, 1965.

Coleridge, P.T., Proc. Roy. Soc. A, 295, 458, 1966.

DeSorbo, W., Phys. Rev., 117, 444, 1960.

Dye, D.H., Ketterson, J.B. and Crabtree, G.W., J. of Low Temp. Phys., 30, No.5/6, 813, 1978.

Feder, R and Charbnau, H.P., Phys. Rev., 149, 464, 1966.

Feder, R. and Nowick, A.S., ibid, 109, 1959, 1958.

Filby, J.D. and Martin, D.L., Proc. Roy. Soc. A, 284, 83, 1965.

Friedel, J., "Dislocations", Oxford : Pergamon Press, 116, 1964.

Fryberg, G.C., J. Chem. Phys. 24, 175, 1965.

Gertsriken, S.D. and Novikov. N.N., Fiz. Metal. Metalloved, 9, 224, 1960.

Gleiter, H., Acta Metall., 27, 187, 1979.

Guarini, G. and Schiavini, G.M., Phil. Mag., 14, 47, 1966.

Heigl, F. and Sizmann, R., Crystal Lattice Defects, 3, 13, 1972.

Hoch, M., "Equilibrium measurements in high melting materials" in "Vacancies and Interstitials in Metals", ed. Seeger et al., North-Holland, Amsterdam, 81, 1970.

Holland, L.R., J. Appl. Phys., 34, No.8, 2350, 1963.

Holland, L.R. and Smith, R.C., ibid, 37, No.12, 4528, 1966.

Huntingdon, H.B., Phys. Rev., 61, 325, 1942.

Huntingdon, H.B. and Seitz, F., ibid, 61, 315, 1942.

Jackson, J.J., "Point defects in quenched platinum" in "Lattice Defects in Quenched Metals", ed. Cotterill et al., Academic Press, 467, 1965.

Jackson, J.J. and Koehler, J.S., Bull. Am. Phys. Soc., 5, 154, 1960.

Jain, S.C. and Krishnan, K.S., Proc. Roy. Soc. A., 222, 167, 1954a.

Jain, S.C. and Krishnan, K.S., ibid, 225, 1, 1954b.

Jain, S.C. and Krishnan, K.S., ibid, 225, 7, 1954c.

Johnson-Matthey and Co. Ltd., "Platinum for Resistance Thermometry", Johnson-Matthey & Co. Ltd., London, 1952.

Kanel, O.M. and Kraftmakher, Ya.A., Fiz. Tverd. Tela, 8, 291, 1966.

Kimura, H. and Maddin, R. "Quench Hardening in Metals", North-Holland, Amsterdam, 12, 1971.

Kirillin, V.A., Sejndlin, A.E., Cechovskoj, V. Ja. and Zukova, I.A., TVT, 3, 395, 1965.

Kovacs, I. and El Sayed, H., J. Mat. Sci., 11, 529, 1976.

Kraftmakher, Ha.A., Zh. Prik. Mekhan.i Tekhn.Fiz., No.5, 176, 1962.

Kraftmakher, Ya. A., Fiz. Tverd. Tela, 5, 950, 1963a.

Kraftmakher, Ya. A., Zh. Prik. Mekhan.i Tekhn. Fiz., No.2, 158, 1963b.

Kraftmakher, Ya. A., Fiz, Tverd. Tela, 6, 503, 1964.

Kraftmakher, Ya. A., Studies in Solid State Physics, 2nd Series, Nauka, Novosibirsk, 219, 1967a.

Kraftmakher, Ya. A., Fiz. Tverd. Tela, 9, 1528, 1967b.

Kraftmakher, Ya. A., ibid, 9, 1850, 1967c.

Kraftmakher, Ya. A., High Temperatures-High Pressures, 5, 433, 1973a.

Kraftmakher, Ya. A., ibid, 5, 645, 1973b.

Kraftmakher, Ya. A., Scripta Metall., 11, 1033, 1977.

Kraftmakher, Ya. A. and Lanina, E.B., Fiz. Tverd. Tela, 7, 123, 1965.

Kraftmakher, Ya. A. and Penegina, T.Yu., Phys. Stat. Sol (a), 42, K151, 1970.

Kraftmakher, Ya. A. and Penegina, T.Yu., Fiz. Tverd. Tela, 13, 2799, 1971.

Kraftmakher, Ya. A. and Penegina, T.Yu., ibid, 16, 132, 1974.

Kraftmakher, Ya. A. and Romashina, T.Yu., Fiz. Tverd. Tela, 7, 2532, 1965.

Kraftmakher, Ya. A. and Romashina, T.Yu., ibid, 8, 1966, 1966.

Kraftmakher, Ya. A. and Strelkov, P.G., ibid, 4, 2271, 1962.

Kraftmakher, Ya. A. and Strelkov, P.G., ibid, 8, 580, 1966a.

Kraftmakher, Ya. A. and Strelkov, P.G., ibid, 8, 1049, 1966b.

Kraftmakher, Ya. A. and Strelkov, P.G., "Equilibrium concentration of vacancies in metals" in "Vacancies and Interstitials in Metals", ed. Seeger et al., North-Holland, Amsterdam, 59, 1970.

Kraftmakher, Ya. A. and Sushakova, G.G., Fiz. Tverd. Tela, 16,138, 1974.

Kraftmakher, Ya. A. and Tonaevskii, V.L., Phys. Stat. Sol. (a), 9, 573, 1972.

Lomer, V.M., "Vacancies and other point defects in metals and alloys", Institute of Physics monograph and report series No. 23, 94, 1958.

Lowenthal, G.C., Aust. J. Phys., 16, No.1, 1962.

Mackintosh, A.R., Bull. Am. Phys. Soc., 11, 215, 1966.

Mamalui, A.A., Pervakov, V.A. and Khotkevic, V.I. Phys. Stat. Sol.(a), 29, K21, 1975.

Martin, D.L., Phys. Rev., 154, 571, 1967.

Mimkes, J., Thin Solid Films, 25, 221, 1975.

Nenno, S. and Kauffman, J.W., Phil. Mag., 4, 1382, 1959.

Nemmonov, S.A., Fiz. Metal. Metalloved., 42, No.4, 723, 1976.

Pervakov, V.A. and Khotkevic , V.I., Dokl. Akad. Nauk, SSSR, 134, 1328, 1960.

Pettifor, D.G., J. Phys. F, 8, No.2, 219, 1978.

Pochapsky, T.E., Acta Met., 1, 747, 1953.

Polak, J., Phys. Stat. Sol. (a), 21, 581, 1967.

Rosenthal, L.A., Rev. Sci. Instr., 32, No.9, 1033, 1961.

Rosenthal, L.A., ibid, 36, No.8, 1179, 1965.

Seeger, A and Mehrer, H., "Analysis of self-diffusion and equilibrium measurements" in "Vacancies and Interstitials in Metals", ed. Seeger et al., North-Holland, Amsterdam, 1, 1970.

Seeger, A., Crystal Lattice Defects, 4, 221, 1973.

Seidman, D.N. and Balluffi, R.W., Phys. Rev., 139, A1824, 1965.

Selman, G.L. and Bourne, A.A., Plat. Met. Rev., 20, No.3, 86, 1976.

Seville, A.H., Ph.D. Thesis, University of Edinburgh, 1972.

Seville, A.H., Phys. Stat. Sol. (a), 21, 649, 1974.

Seville, A.H., Plat. Met. Rev., 19, No.3, 96, 1975.

Shestopal, V.O., Fiz. Tverd. Tela, 7, 3461, 1965.

Siegel, R.W., J. Nucl. Mat., 69-70, 117, 1978.

Simmons, R.O. and Balluffi, R.W., Phys. Rev., 117, 62, 1960.

Simmons, R.O. and Balluffi, R.W., ibid, 125, 862, 1962.

Simmons, R.O. and Balluffi, R.W., ibid, 129, 1533, 1963.

Sizmann, R. and Wenzl, H., Z. Naturforschg., 18a, 673, 1963.

Smith, R.C. and Holland, L.R., J. Appl. Phys., 37, No.13, 4866, 1966.

Sullivan, G.A. and Weymouth, J.W., Phys. Rev., 136A, 1141, 1964.

Thomson, R.M. and Balluffi, R.W., J. Appl. Phys., 33, No.3, 803, 1962.

Van den Sype, J., Ph.D. Thesis, University of Pennsylvania, 1965.

Van den Sype, J., Phys. Stat. Sol.(a), 39, 659, 1970a.

Van den Sype, J., Scripta Metll., 4, 251, 1970b.

Vineyard, G.H., Discussions Faraday Soc., No.31, 7, 1961.

Ytterhus, J.A. and Balluffi, R.W., Phil. Mag., 11, No.112, 707, 1965.

Zinov'ev, V.E., Korshunov, I.G. and Gel'd, P.V., Fiz. Tverd. Tela, 13, 3459, 1971.